MODELLING THE DRIVERS OF LAND AVAILABILITY FOR AFFORESTATION AND BECCS

A thesis submitted to the School of Environmental Sciences
of the University of East Anglia in partial fulfilment
of the requirements for the degree of Doctor of Philosophy

THOMAS S. BALL - 100261319

OCTOBER 2022

ABSTRACT

This thesis contains an exploration of the drivers of human land use for agriculture in the context of land intense climate change mitigation strategies (afforestation and BECCS). To do this, a model of the global food system was developed (C-LLAMA). The model linearly projects country level diet, yield, and production data to 2050, taking in to account waste and losses, and finally producing an output of agricultural land use for crops and pasture. A business as usual 'anchor' scenario was produced, in which all parameters and inputs are projected normally, which results in a global agricultural land footprint of 5.2 Gha. In subsequent chapters, the model is used to explore the sensitivity of agricultural land use to three key drivers: dietary trends, food waste and losses, and crop yields. Prescribing a trajectory toward the EAT-Lancet planetary health diet in all countries leads to a slight increase in global land use of 100 Mha when compared with the anchor scenario. Reducing food waste and losses, and increasing crop yields both unsurprisingly reduced global land use. The final chapter contains an examination of various potential threats to the sustainable delivery of bioenergy in four mitigation scenarios. The chapter explores the climate, governance, environmental performance, and food demand changes in regions that produce energy crops in this scenarios. It is found that large portions of energy crop production occur in the tropics, in regions of moderate or poor governance, or with significant (>30%) increases in food demand by 2050.

ACKNOWLEDGEMENTS

First and foremost, my wholehearted thanks to Nem, for being an amazing mentor and guide, both personally and scientifically, throughout this entire process. For motivating me through difficult times, and for encouraging me to take a step back at times when things were overwhelming. Nobody could have prepared me for just how much a PhD is akin to a marathon, mentally and emotionally, especially in light of the isolation and uncertainty caused by the pandemic. I could not have done it without Nem's support.

Secondly, my sincere thanks to my wider supervisory team: Andrew, Tim, and Tom, for their guidance, insight, and invaluable contributions to the discussions of this work. Tim and Tom, I have thoroughly enjoyed my many trips to Exeter. The warm welcomes and hospitality from you both and the wider research community there made me feel right at home.

My thanks to the members of the FAB-GGR project for welcoming me into the group, for their feedback on my work, and for providing me with valuable professional experiences.

Thanks to my family for never missing an opportunity to tell me that they're proud of me and for providing all the love and support one could ever need. Special thanks to Em for putting up with my never-ending incompetence and queries about figures and mathematical formalism. Thank you to Rosie for being the sweetest and gentlest soul in some of the most difficult times I have known; I will miss you immensely.

Thank you to all my friends, old and new. I have met some amazing people since moving to Norwich. Thank you for making my time here an enjoyable one; I have countless wonderful memories of this city and it's people already, and many more are to come.

Finally, my deepest gratitude to Elie, for providing me with seemingly limitless support, patience, and love through the good times and the bad. I cannot thank you enough.

ACRONYMS

Table 1: List of acronyms commonly used in this thesis (alphabetical order).

AFOLU	Agriculture, Forestry, and Other Land Use
BECCS	Biomass Energy with Carbon Capture and Storage
CCS	Carbon Capture and Storage
CDR	Carbon Dioxide Removal
DACCS	Direct Air Capture with Carbon Storage
FAO	Food and Agriculture Organisation of the United Nations
GDP	Gross Domestic Product
GHG	Greenhouse Gas
IAM	Integrated Assessment Model
IPCC	Intergovernmental Panel on Climate Change
NET	Negative Emissions Technology
RCP	Representative Concentration Pathway
SDG	Sustainable Development Goal
SRC	Short Rotation Coppice
SSP	Shared Socio-economic Pathway

Contents

1

Introduction

1.1 Anthropogenic climate change

It is well established that human activity since the industrial revolution is directly responsible for the release of greenhouse gases into the atmosphere, which enhance the natural greenhouse effect, cause the retention of additional solar energy by the atmosphere, and hence a lead to a rise in global average temperature. Rising temperatures drive changes in almost all of Earth's natural systems, the influences of which are already being felt. Changes in weather patterns, temperature, sea level rises, ocean acidification, to name a few, are responsible for emerging threats to terrestrial and marine ecosystems (Turner *et al.*, 2020; Malhi *et al.*, 2020) and to human activity; food production, freshwater availability, and cultural heritage are all under threat (Sesana *et al.*, 2021; Mankin *et al.*, 2019; Ray *et al.*, 2019; Bhattacharya, 2019). This is anthropogenic climate change. In addition to emerging threats, the long term impacts of climate change are unknown. Climate change impacts could trigger 'tipping points'; continued human emissions and appropriation of natural resources could push any one (or several) of a number of natural Earth systems beyond a point of no return (Lenton *et al.*, 2019). Action must be taken to reverse the effects of human induced greenhouse gas emissions and climate change before irreversible effects begin to accumulate.

1.2 MITIGATION SCENARIOS

The 2015 Paris Agreement (United Nations Treaty Series, 2015) set the international target of limiting the mean global temperature increase above the pre-industrial level to well below 2 °C by the year 2100, with an aspiration to further limit warming to 1.5 °C. Limiting warming to 1.5 °C corresponds to a limit on radiative forcing: relative energy received from the Sun that is 'trapped' in the atmosphere as a result of increased greenhouse gas concentrations. Representative concentration pathways (RCPs), are future trajectories of greenhouse gas concentrations up to 2100, with characteristic end-of-the-century radiative forcing values (van Vuuren *et al.*, 2011). Each of these pathways corresponds with a warming target: a mean global temperature above the pre-industrial level. Two of these trajectories, RCP2.6 and RCP1.9, correspond with end-of-the-century mean global temperatures above the pre-industrial of 2 °C (van Vuuren *et al.*, 2011) and 1.5 °C (Millar *et al.*, 2017) respectively. Modelling approaches are used to produce future scenarios that explore the possibility of achieving these RCP targets: *how* can we follow the RCP1.9 greenhouse gas trajectory, and by doing so limit warming to 1.5 °C?

Climate scenarios consistent with the representative concentration pathways are produced using integrated assessment models (IAMs). These are a complex, economically driven modelling approach that engage with a wide range of biophysical and socio-economic factors, particularly those that can lead to the emission (or reduction) of atmospheric greenhouse gases. Their primary outputs are scenarios of future energy provision, land use, and greenhouse gas emissions. Amongst their inputs, alongside the RCP trajectories, are shared socio-economic pathways (SSPs), which were developed as a framework for modelling climate related scenarios (O'Neill *et al.*, 2014). There are five of these reference pathways (SSP1 to SSP5), each characterised by their level of global challenges to climate change mitigation, with the SSP1 representing the least challenges, and SSP5 the most (Fricko *et al.*, 2017). SSP2 is the middle of the road pathway, in which many factors are at their central position and represent a 'continuation of the historical experience' (Fricko *et al.*, 2017). Many IAM scenarios adhere to a combination of an RCP and an SSP, with denominations such as 'SSP1-RCP1.9'. However, there can still be significant variation between scenarios even when constrained by the same pathways: two scenarios might reach the same end point in different ways, especially when produced by different IAMs.

There are two dimensions to anthropogenic emissions: ongoing emissions, and cumulative emissions. Human activity is the cause of continual carbon dioxide emissions, primarily through the combustion of fossil fuels for the provision of energy but also secondarily through activity such as agriculture and land use change. These emissions can ostensibly be reduced to just a fraction of their current amounts, by transitioning to alternative energy sources such as biomass, wind, and solar power, by electrifying road infrastructure, and by improving land management and agricultural practices. However, these emissions have been prevalent in some quantity since the beginning of the industrial revolution, and while Earth's natural land and ocean systems act as a buffer, absorbing some of these emissions, continued emissions has lead to their accumulation. Therefore, in almost all climate change mitigation scenarios, not only do current emissions need to be minimised, but some amount of overshoot into 'net negative emissions' is required to reverse historical cumulative emissions (Rogelj *et al.*, 2018a). The process of removing carbon dioxide from the atmosphere will be referred to as carbon dioxide removal (CDR) moving forward, the mechanisms for which will be discussed in upcoming sections.

Scenarios that achieve 1.5 °C by 2100 almost all require at least some amount of CDR, and those that don't would necessitate unrealistically rapid decarbonisation of energy production globally before 2030; the lower emissions are in 2030, the greater the chance of limiting 2100 warming to 1.5 °C (Rogelj *et al.*, 2018a). In a given scenario, the greater the reduction in current emissions the less CDR is required to offset them. The IPCC estimate that for a two-thirds chance at limiting warming to 1.5 °C, the remaining 'carbon budget' (that is, total cumulative emissions that are 'allowed') is approximately 420 Gt of CO_2 (Rogelj *et al.*, 2018a). That leaves approximately 10 years at the current rate of emissions of approximately 42.2 $GtCO_2\ yr^{-1}$ (2020 estimate, Friedlingstein *et al.* (2020)). Additionally, there are other greenhouse gases and other factors that may affect radiative forcing, with an estimated forcing difference of up to 0.26 Wm^{-2} (Mengis & Matthews, 2020), which is not an insignificant impact given the target of 1.9 Wm^{-2}; this may reduce the remaining cumulative carbon budget even further.

1.3 CARBON DIOXIDE REMOVAL

It is well established that limiting warming to 1.5 °C will require at least some amount of carbon dioxide removal to offset continuing global emissions (Keller *et al.*, 2018). The exact requirement is unknown, but likely to be on the order of 100 $GtCO_2$ to well over 1200 $GtCO_2$ over the course of the century (Kreuter & Lederer, 2021; Vaughan *et al.*, 2018). There are a number of methods for removing carbon dioxide, some of which are favoured significantly more than others in IAM scenarios, and none of which have seen real-world deployment at any relevant scale (Forster *et al.*, 2020; Brack & King, 2021).

The simplest method of CDR is through growing trees or other vegetation, which draws carbon dioxide from the atmosphere through photosynthesis, which the plants or trees then uses as 'food' to grow, effectively storing the carbon within the living biomass. Some of this carbon is also transferred to the ground as leaf litter or other litterfall where it enters the soil. The IPCC special report on climate change and land use defines reforestation as the large scale planting of trees on land that has previously contained forest. Afforestation is the conversion of land to forest that has not 'historically contained forest': the planting of trees on land under another use (such as agriculture) (van Diemen *et al.*, 2019). The definition of these terms is somewhat blurry, no timescale is given for how long land must be free of forest before reforestation becomes afforestation. Typically when discussing CDR, reforestation and afforestation are used somewhat interchangeably, and afforestation is commonly used to refer to both (Waller *et al.*, 2021). The rate at which afforestation is able to remove carbon dioxide from the atmosphere is heavily dependant on climate, land productivity and plant physiology. Additionally, the rate of carbon accumulation tends to plateau as forests mature (Cook-Patton *et al.*, 2020). Afforestation as a CDR method is used moderately in IAM scenarios; it is relatively cheap and has almost no upkeep costs once deployed, although ultimately its total storage potential is constrained by the area of trees planted (Fuss *et al.*, 2018).

Afforestation forms part of broader suite of land-based emissions related activity: agriculture, forestry, and other land use (AFOLU). AFOLU describes a range of activities, some of which (like afforestation) have the potential for net negative emissions, but also includes positive emissions, for example from land use change from grassland to energy crops (Pradhan *et al.*, 2019). AFOLU emissions account for approximately a quarter of current GHG emissions, but net negative carbon dioxide emissions in this sector are possible (Pradhan *et al.*, 2019; Henderson *et al.*, 2021). AFOLU emissions reach net zero emissions by around the mid century and provide between 10-520 $GtCO_2$ net negative emissions in mitigation scenarios; afforestation and reforestation form the majority of this CDR (Rogelj *et al.*, 2018a).

A key component of CDR is carbon capture and storage (CCS). CCS is a broad term that refers to a method with a variety of applications, including as a standalone technology, heavy industry that cannot be decarbonised in other ways, fossil fuel energy, or bioenergy. Carbon dioxide is captured in one of several ways, then the carbon is transferred via either pipeline or transport infrastructure to long term storage, typically in saline aquifers underground (Bui *et al.*, 2018). Current estimates of the global storage potential suggest that it exceeds capacity requirements by estimates of CCS deployment, however suitable reservoirs are not distributed evenly across the planet, so transport infrastructure for biomass or post-capture carbon is a significant consideration (Consoli & Wildgust, 2017). The technology behind CCS is largely well understood; the challenges to it's use are societal rather than technological (Wennersten *et al.*, 2015). The application of CCS as a standalone technology involves directly capturing air from the atmosphere; in combination with CCS this method is referred to as direct air capture with carbon storage (DACCS). DACCS typically involves an array of air intakes inside which are chemical sorbents that scrub carbon dioxide from the air. DACCS requires almost no land (relative to some other CDR methods), but is dependant on considerable energy input, with it's only 'output' being the carbon captured (Creutzig *et al.*, 2019).

Another application for the capture of carbon is for heavy industries with limited other decarbonisation options, for example the cement, paper, chemical, and steel industries. These are essential industries, so to facilitate their continued operation in the context of 1.5 °C warming, currently their best option is to decarbonise using CCS (van Sluisveld *et al.*, 2021). A third application of CCS is in the flue gases released by combustion of fuel for energy generation. This can be applied to fossil fuel power plants (in future constructions or retroactively), which can offset large portions of the carbon dioxide that would otherwise be emitted by burning fossil fuels (Haszeldine, 2009). While this may initially appear to be an attractive option, this energy supply chain simply cancels out some of the emissions generated by removing fossil fuels from the ground, rather than a net removal of carbon dioxide from the atmosphere.

The most pertinent application of CCS in the context of climate change mitigation scenarios (the reasons for which will be discussed shortly), is the capture of carbon dioxide in the flue gases produced during the combustion of biomass for energy. The carbon dioxide removed from the atmosphere by vegetation as it grows is almost all released upon it's combustion, meaning that in a perfect world biomass energy is effectively carbon neutral. Combining biomass energy with CCS foregoes the re-release of the captured carbon, the result being an energy system with a net-negative effect on atmospheric carbon. This combination is referred to as biomass energy with carbon dioxide and storage (BECCS).

BECCS and afforestation are heavily favoured over other CDR methods in mitigation scenarios produced by IAMs (Rogelj *et al.*, 2018a). BECCS provides co-benefits, solving two problems at once: the reduction of current emissions through decarbonisation of energy provision, as well as carbon dioxide removal to account for accumulated historical emissions. It appears almost 'too good to be true' in the economically optimised world of IAMs, and hence the majority of mitigation scenarios consistent with 1.5 °C make heavy use of BECCS (along with of bioenergy without CCS); up to 1300 $GtCO_2$ stored using BECCS by 2100 (Low & Schäfer, 2020; Vaughan *et al.*, 2018).

Biomass energy requires biomass of some kind to use as feedstock for combustion. Biomass feedstock can come from a range of sources: from agricultural residues, forestry and its associated residues, or dedicated crops grown specifically for energy (Gough *et al.*, 2018). While residues can account for up to 50% of biomass feedstock in some scenarios (Vaughan *et al.*, 2018), the deployment of bioenergy and BECCS on the scales projected in mitigation scenarios consistent with 1.5 °C warming will require significant use of dedicated energy crops. The primary candidates for these crops are fast growing grasses such as miscanthus x giganteus: a tall, woody grass with a C4 metabolic pathway (meaning it is highly resource efficient), or short rotation coppicing (SRC) of tree species such as willow or poplar. The use of either is dependant on climate and land productivity; miscanthus in particular is not a 'fussy' organism and is capable of growing on relatively unproductive land such as field margins (Haberzettl *et al.*, 2021).

The projected increase in the demand for land for afforestation and dedicated energy crops, both for bioenergy in the energy system and for BECCS, begins to raise questions about the global land area available for these land intensive mitigation strategies.

1.3.1 Other CDR and mitigation methods

It is important to note that there are other strategies for reducing atmospheric carbon, but none are land intensive, rather they are a supplement to keystone options like BECCS and afforestation. The first of these is the use of biochar. Produced by the pyrolysis of organic matter to form a substance like charcoal, biochar can then be added to soils where it improves conditions for plant root growth and soil carbon accumulation (Joseph *et al.*, 2021). A similar method is enhanced weathering, which is an enhancement of the chemical weathering of rocks, which is a natural process. Presently, natural weathering absorbs about 1.1 $GtCO_2$ yr^{-1} from the atmosphere, most of which becomes bicarbonate in the ocean (Strefler *et al.*, 2018). Fine rock can be integrated into soil, where it's high surface area speeds up the weathering process and can improve crop yields (Beerling *et al.*, 2020; Strefler *et al.*, 2018). Both biochar and enhanced weathering may contribute significantly to carbon dioxide removal efforts, but are typically applied to cropland (which can include energy crops) (Jia *et al.*, 2019). They are sometimes included as part of AFOLU figures. They won't be considered as part of the work of this thesis since they require no additional land.

There are a set of CDR methods that involve the oceans, including alkanisation similar to that of enhanced weathering. While the body of literature surrounding these methods is growing rapidly in light of the 1.5 °C target, they remain largely uncertain and their feasibility at the necessary scales is unknown and hence they aren't currently included in the portfolio of CDR options in mitigation scenarios (Rogelj *et al.*, 2018a).

Finally there are solar radiation management (SRM) options. SRM does not involve the removal of atmospheric carbon, so does not constitute CDR. Instead, SRM directly affects radiative forcing or surface albedo, reducing the absorption of solar energy by the atmosphere. Methods for this include stratospheric aerosol injection or cloud brightening (which increase cloud density or reflectivity respectively) (Nicholson *et al.*, 2018). The long term impacts of these methods are not yet understood and could potentially have serious negative ecological and climatic consequences (Tang & Kemp, 2021). These methods also require constant upkeep: they only effective while they are in place, and are not presently included in mitigation scenarios developed following the instigation of a 1.5 °C warming target (Rogelj *et al.*, 2018a), hence will not be considered for this thesis.

1.4 GLOBAL LAND USE

The global land use system is incredibly complex, there are a wide range of factors affecting the amount of land that might be available for land intensive CDR and mitigation strategies such as BECCS, afforestation, and bioenergy. Figure 1.1 shows the state of global land use in 2019. Approximately half of all habitable land is currently used for agriculture, with the remaining half being covered in forests and shrub. While global hunger is likely to see a net decrease over the course of the century, in the immediate future and well into the middle term, hunger is likely to increase (Berndes & Cowie, 2021). With the sustainable development goals (SDGs) in mind, particularly SDG 2, which is to 'end hunger, achieve food security and improved nutrition and promote sustainable agriculture' (United Nations, 2019a), the widespread land requirements of BECCS deployment may well conflict with the rising demands of the food system. However options for offsetting some of the land use pressure from BECCS and AFOLU as mitigation strategies may yet lie within the

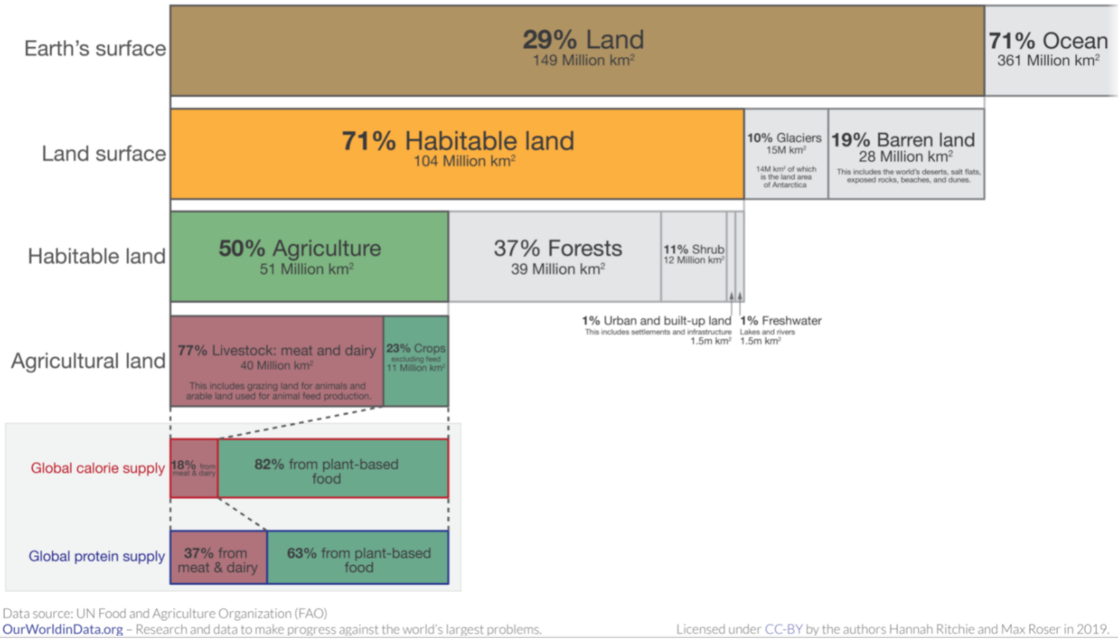

Figure 1.1: Global land cover by forests and agriculture in 2019, from https://ourworldindata.org/land-use [Accessed 31-03-2022]. One square kilometre is 100 ha, so the 51 million km^2 used for agriculture is equivalent to 5.1 Gha.

food system: in this section several avenues are identified for improving the land use footprint and overall sustainability of food production (Springmann *et al.*, 2018).

1.4.1 Population growth

Population is the most basic driver of food demand: in the context of the sustainable development goals, a growing population translates directly to growing food demand and hence increasing demand for agricultural land. The overall global trend in population is currently one of accelerating growth, especially in middle income countries, although the growth is expect to slow around middle of the century; in the UN medium population scenario (which is a component of SSP2 and is a 'middle of the road' - expected trajectory), the global population is projected to increase throughout the majority of the first half of the 21st century, beginning to slow around the year 2050 and stagnating almost entirely by 2100 (United Nations, 2019b). Much of this increase occurs in Sub-Saharan Africa and Southern Asia, which currently face

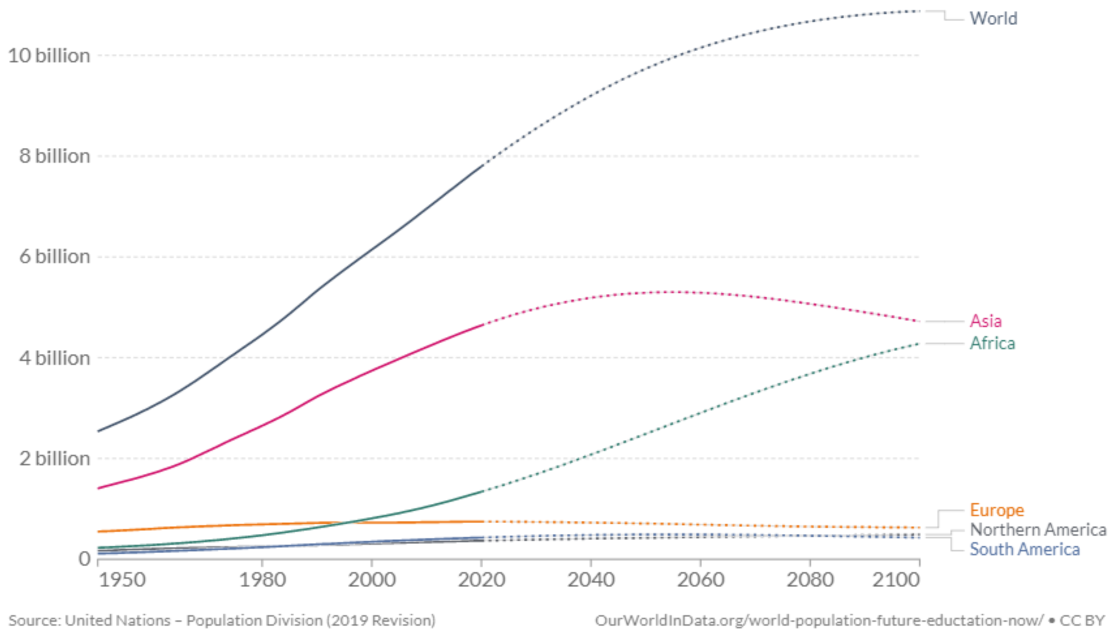

Figure 1.2: Global population trajectories from 1950 to 2100, with future values taken from the UN medium variant population scenario (OurWorldInData.org - World Population Growth, Max Roser, Hannah Ritchie and Esteban Ortiz-Ospina).

high levels (upwards of 50% of the populations of some sub regions) of food insecurity (Cooper *et al.*, 2021). For the purpose of this thesis, population trajectories will be assumed to be a constant - this is fairly common practice in literature surrounding climate change mitigation scenarios: while the sustainability impacts of limiting population growth in mitigation scenarios are acknowledged, the policy mechanisms for doing so are often ignored (Dodson *et al.*, 2020).

1.4.2 DIETARY TRENDS

Animal products require not only the land on which to raise livestock, but also land to feed livestock. The food demand for livestock is met through fodder crops or by grazing on pastoral land. The extreme land efficiency case is one in which the footprint of an animal is only that required to grow the crops that feed it: animals may be confined in minimal housing, and all their feed provided to them via fodder crops. The opposite extreme is that of extensive grazing, in which the animal gains all of it's feed energy from foraging. In either case, energy losses are incurred as plant-based energy is converted to 'animal-based' energy, meaning that, in general, animal products are inherently less land efficient (per calorie) than the majority of vegetal products (Poore & Nemecek, 2018; Springmann *et al.*, 2018; Alexander *et al.*, 2016). Beef, for example, has a feed conversion efficiency of approximately 3%, meaning that every 100 kcal of energy consumed by the cow translates to only 3 kcal of 'useful product' (Shepon *et al.*, 2016). Poultry meat and eggs are the most efficient commonly consumed animal products, with conversion efficiencies of 13% and 17% respectively (Shepon *et al.*, 2016). As a result, grazing land along with fodder crops account for 77% of agricultural land use, around 4Gha, whilst animal products provide only 17% of food energy to the human population (see Figure 1.1). Reducing the consumption of animal products, especially in high income regions of the world, has the potential to improve the land use efficiency of the food system, and reduce other environmental impacts such as deforestation and greenhouse gas emissions (Weindl *et al.*, 2017; Röös *et al.*, 2017).

1.4.3 FOOD WASTE AND LOSSES

An estimated third of all food produced yearly is wasted or lost between production and consumption (Alexander *et al.*, 2017; Gustavsson *et al.*, 2011). There are three primary avenues for food waste or loss on the journey from farm to consumer: processing, distribution, and post-production. Losses tend to be much higher earlier on the food supply chain for countries of low or lower-middle income, and later for countries of upper-middle or high income (Gustavsson *et al.*, 2011). Food *losses* are usually not 'avoidable' where they occur in their economic context. Typically they are due to poor transport and storage infrastructure, or lack of appropriate processing technology; these require some level of investment to alleviate and hence they typically occur in lower income countries (Kumar & Kalita, 2017; Lipinski *et al.*, 2013). Food *waste* on the other hand, is the avoidable discarding of food that was otherwise perfectly good to eat, in the household, in retail due to poor purchasing management, or by processing inefficiencies due to (unnecessarily) high commercial standards, e.g. trimming potato fries to be perfectly square (Dhir *et al.*, 2020; Kavanaugh & Quinlan, 2020; Porat *et al.*, 2018).

Food waste and losses artificially ‘inflate’ food demand - increasing the production requirement to feed the same number of people, hence increasing land use to produce food in addition to increasing other environmental impacts of the food system. Clearly this is an avenue for improving the land use efficiency of the food system, while some losses are unavoidable, there is the potential for significant reduction through education and policy (in the case of post-production waste), or through investment in infrastructure improvements and technology (in the case of processing and distribution losses) (Cattaneo *et al.*, 2021).

1.4.4 INTENSIFICATION

In recent decades, global agricultural production has increased dramatically to meet the rising demand for food (Godfray *et al.*, 2010). Much of this productivity increase can be attributed to improvements in yield: the amount of produced mass per area (in a given year), through improvements in technology and agricultural practices such as irrigation and fertilisation (van Zeist *et al.*, 2020). It is not unreasonable to expect this pattern of increasing yields to continue. In many regions of the world, particularly low income and middle income regions, crop yields are lower than their potential physiological maximum for the climate of the region, so there is plenty of room for crop yield improvement (Mueller *et al.*, 2012). However the closure of these yield gaps will require significant improvement to land management practices (Mueller *et al.*, 2012). Moreover, mitigation scenarios are overly optimistic about yield improvements for food crops and pasture, with crop yields exceeding linearly projected yields and modelled maximum ‘attainable’ yields in a large portion of scenarios and crop types (van Zeist *et al.*, 2020). In reality, the yields of several major crops are beginning to show signs of growth stagnation in many regions of the world. Not limited to high income regions with plentiful access to agricultural technology; yields of staple food crops (rice, wheat, and maize) have been observed to be stagnating in Nigeria, India, France, and the USA amongst many others (Madhukar *et al.*, 2020; Ramankutty *et al.*, 2018; Ray *et al.*, 2012). Additionally, the emergent threat of climate change impacts, including rising temperature, are likely to drive further yield stagnation due to both biophysical and agronomic impacts (Iizumi *et al.*, 2017).

It is possible to 'intensify' the production of animal products, as mentioned in Section 1.4.2, at one extreme end of the spectrum of animal production systems are housed animals that subsist entirely on fodder crops. These fodder-fed systems are likely to play a critical role in future production of animal products if the food system is to remain within sustainable boundaries (Davis & D'Odorico, 2015). Although more sustainable livestock management practices such as silvopasture are presenting themselves as an option for the sustainable intensification of animal product production (Jose & Dollinger, 2019), the livestock sector is responsible for the majority share of impacts on soil degradation and general greenhouse gas emissions within the food system (De Oliveira Silva *et al.*, 2021; Herrero *et al.*, 2016). Despite the option of intensification, animal products are almost always less land efficient, so from the perspective of improving land use efficiency, the best option is to reduce their consumption, especially that of ruminant meat and dairy products (Weindl *et al.*, 2017; Shepon *et al.*, 2016).

1.4.5 Protected areas and conservation

Protected areas are those in which agricultural development could damage or destroy sites of cultural or biophysical importance. Examples of this might include monuments of historical or religious significance, or national parks, which are culturally as well as economically significant on a somewhat larger scale. They are generally included in IAM modelling as 'forbidden' regions, or are of small enough area that they are not resolved in spatial models. The United Nations maintains a list of protected areas (UN Environment World Conservation Monitoring Centre, 2018). Areas within this list include “national protected areas recognised by the government, areas designated under regional and international conventions, privately protected areas and indigenous peoples’ and community conserved territories and areas". These areas are grouped into the following categories: strict nature reserves, wilderness areas, national parks, natural monuments, habitat or species management areas, protected landscape or seascapes, managed resource protected areas. These areas can be considered to be completely out of bounds for energy crop production, and although typically they account for a very small proportion of available land there is a growing body of literature suggesting that in the looming shadow of climate change impacts, they may be insufficient for biodiversity preservation (Elsen *et al.*, 2020).

1.4.6 MODELLING TOOLS FOR LAND USE

IAMs are generally driven by economic equilibrium; the models attempt to achieve this by finding the most cost effective solution within the constraints of the scenario for each ‘agent’. The agents are different economic sectors, of which the agricultural sector and by extension, land-use allocation, are one. Because of this, their land-use components typically prioritise land allocation in one of two ways, profit maximisation or cost minimisation. For example, GCAM focuses on profit maximisation (in the case of agriculture) while IMAGE and MAgPIE(ReMIND) are based around cost minimisation (Popp *et al.*, 2014). The representative concentration pathways were developed using these models, but are also used as input for analyses of other aspects, such as land use. Whilst IAMs are well suited to broad scale analyses of future scenarios, especially with policy-making in mind, they are somewhat nebulous in their approach. Their outputs can be difficult to interpret in such a way that it becomes clear, in the case of land-use allocation, how different drivers affect the availability and location of land for bioenergy, BECCS, and afforestation (Havlık *et al.*, 2014; Popp *et al.*, 2014; Calvin *et al.*, 2013; Fujimori *et al.*, 2012; van Vuuren *et al.*, 2011).

Another type of model that are crucial in the development of future BECCS scenarios and associated land-usages are dynamic global vegetation models (DGVMs), such as the Joint UK Land Environment Simulator (JULES) or the Lund-Potsdam-Jena DGVM (LPJ) (Clark *et al.*, 2011; Sitch *et al.*, 2003). These models simulate the interactions between vegetation, energy and the water and carbon cycles. Whilst unable to directly model available land, in the context of BECCS these models are used to simulate aspects of bioenergy crop from pre-prescribed land allocation data, such as carbon captured and energy yields. They have also been used to model various effects on the environment, such as the hydrological cycle (Elliott *et al.*, 2014). Some integrated assessment models include a DGVM as part of their framework, for example the inclusion of LPJmL in IMAGE.

At the other end of the spectrum from IAMs are simple, balance, accounting, and flux models. The Flux Assessment of Linked Agricultural Food production, Energy potentials & Land-use change (FALAFEL) model is one such example, in which the primary input driver is a trajectory of the global food energy consumption per capita, per day, up to 2050 (Powell, 2015). FALAFEL is at it's heart a food system model; at each time step (yearly), calculations of the flux of various aspects of the model between 'boxes' are made, finally calculating production demands for crop and livestock, which are then converted into a projected land use. FALAFEL operates at a global aggregation, which allows it to bypass considerations of the geographic, economic, and cultural differences between food systems, but also precludes it from exploring the impacts due to changes these differences.

Similar approaches to FALAFEL are taken by the Biomass Balance Model (BioBaM) (Kalt *et al.*, 2021), and a model presented by Bijl *et al.* (2017), which calculates food demand (but not land use). Both BioBaM and the Bijl model operate at the regional level, with 11 and 26 regions respectively, allowing them explore regional differences in food demand and production. BioBaM calculates biomass demand and production scenarios, then discounts scenarios in which the two are not able to be balanced. The Bijl model does not calculate a land use, rather stopping at the demand stage, however it is worth mentioning since it's structure is similar to that of FALAFEL up that point. All of these models make greater simplifications of real-world processes than spatially explicit or dynamic equilibrium models do, and thusfar they have seen only limited use in projections of future land availability for BECCS, afforestation, and bioenergy. However, they are more transparent than IAMs in their inputs and outputs; the influence of each input on each output can be clearly understood. Drawing aspects of these models together into a model that operates at a regional level but produces land use as an output (rather than as an input like BioBaM) could provide a useful framework for exploring food related drivers of land available for land intensive mitigation.

1.5 LAND-USE FOR MITIGATION STRATEGIES

The widespread deployment of energy crop production will require an unprecedented quantity of land to support it; there are a range of estimates, varying significantly based on assumed yields and the type of land used (Vaughan *et al.*, 2018; Burns & Nicholson, 2017). In mitigation scenarios, the change in forest area from present to 2100 ranged from -20 Mha to 720 Mha, and bioenergy energy crop cover from 320 Mha to 660 Mha (median values across a range of models, RCP4.5, RCP2.6, and RCP1.9 scenarios), with many scenarios having higher peaks mid-century (Jia *et al.*, 2019). Bioenergy potentials (for BECCS or otherwise) within IAM scenarios that achieve 1.5 °C are based on the assumption that almost all dedicated energy crops can be grown on abandoned cropland or marginal land (Næss *et al.*, 2021), or through expansion into natural grasslands (Vaughan *et al.*, 2018; Dias *et al.*, 2021). In reality, the amount of abandoned land that is actually available for energy crop production may be limited. Næss *et al.* (2021) identified only 83 Mha of abandoned cropland (2015), slightly under half of which (48%) of which is unsuitable for energy crop production (at the rates assumed in IAM scenarios, unless the areas are irrigated) due to a lack of water availability, or biodiversity concerns.

1.5.1 LAND-USE CHANGE AND FORESTS

Land stores carbon within vegetation above and below ground, organic compounds within soil and inorganically, in carbonate compounds. Changing land use inevitably causes the release of some of this carbon through mechanical disruption and vegetation storage losses. The intensity of carbon release varies greatly dependant on types of land between which the transition is occurring. Deforestation is the transition of land use type away from natural forest, which presently accounts for between 6-17% of anthropogenic carbon emissions (Baccini *et al.*, 2012). Cumulatively, deforestation is responsible for approximately 25% of all historical emissions, as well as contributing heavily to biodiversity losses and land degradation (Kindermann *et al.*, 2008). Agricultural expansion is one of the primary drivers of deforestation, particularly in the tropics (Milford *et al.*, 2019; Pendrill *et al.*, 2019).

Around 870 Gt of carbon is presently stored in the world's forests, 380 Gt of which is stored in soil, whilst the remainder is stored in trees, deadwood and litterfall (Pan *et al.*, 2011). Forests are a large store of carbon, but have different storage densities dependant on their environment. Tropical and boreal forests store similar densities of carbon, at around 240 t ha^{-1} of carbon. Temperate forests are less carbon dense, at around 155 t ha^{-1} carbon (Pan *et al.*, 2011). If the land use changes made to facilitate energy crop production 'leak' carbon back into the atmosphere, the efficacy of BECCS as a CDR method, or bioenergy as a carbon neutral energy sourced will be significantly reduced, so deforestation is typically avoided or severely limited in mitigation scenarios (Harper *et al.*, 2018). It is crucial that governance frameworks, incentives, and accounting mechanisms surrounding BECCS deployment are properly implemented such that they don't inadvertently incentivise the appropriation of natural forests and other carbon rich ecosystems for bioenergy (Torvanger, 2019).

Harper *et al.* (2018) explore the trade-offs between carbon released and re-captured as land transitions to BECCS feedstock production in different modelled scenarios, finding that in around 40% of areas, afforestation, or re-forestation would result in a greater net carbon reduction from the atmosphere than transitioning the area to energy crop production for BECCS. In an assessment of the emissions efficiency of transitioning between land uses in mitigation strategies, a wide range of carbon emission efficiencies were identified when transitioning agricultural land to energy crop or forest, or changing agricultural systems. In some cases it is more carbon-efficient to avoid transitioning pasture to energy crop, instead using the land for more intense pasture, or for food crop (Searchinger *et al.*, 2018).

1.5.2 ENVIRONMENTAL GOVERNANCE AND POLITICAL STABILITY

Limiting 2100 warming to 1.5 °C through the widespread deployment of BECCS and afforestation is highly likely to require solid environmental policies and intergovernmental collaboration (Burns & Nicholson, 2017). Yet in mitigation scenarios, IAMs derive a significant portion of BECCS and afforestation potentials from failed states or countries of historically weak environmental governance (Brack & King, 2021); up to a third of energy crop production occurs in developing regions, and another third in China, Brazil, and Russia (Vaughan *et al.*, 2018). Despite the acknowledgement that BECCS and afforestation are likely to play a crucial role in efforts to mitigate climate change in the coming decades, the necessary national and international policy measures remain highly uncertain (Radunsky, 2018).

The magnitude of the effect that governance failure may have on the efficacy of

BECCS and afforestation is unknown, but given historically weak environmental performance in many regions, their adherence to prospective constraints cannot be assumed (Brack & King, 2021). It is essential that deforestation doesn't occur to facilitate BECCS, and that forests remains in place once established, which may not transpire if governance frameworks are not sufficient to incentivise these practices. Such failure could pose significant risks not only to the efficacy of CDR, but also to biodiversity (Brack & King, 2021). Thus far there have been no efforts to quantify the 'risk' of reliance on regions of poor environmental governance, or even the portion of energy crop production that may be at risk; Mace *et al.* (2021) suggest that to reduce the risks posed by unsustainable BECCS implementation, initial reliance on CDR should be minimised until proper governance frameworks are in place.

1.6 THESIS DESCRIPTION

The work in this thesis was carried out primarily in the context of the 2018 IPCC special report on warming of 1.5 °C (Rogelj *et al.*, 2018a), and their 2019 special report on climate change and land use (Arneth *et al.*, 2019). These reports propose with high confidence that meeting a climate target of 1.5 °C will likely require an unprecedented expansion of land based mitigation: BECCS and AFOLU (including afforestation). In April of 2022, the IPCC working group 3 released their contribution to the sixth assessment cycle, which discusses climate change mitigation options. The new report presents a portfolio of mitigation options with minor deviations from the previous; the role of BECCS and afforestation are reduced, with the difference in captured carbon dioxide being taken up largely by DACCS, especially in the near term (IPCC, 2022). This reduced reliance may alleviate some of the threats to sustainable development and land use by these mitigation strategies; nevertheless BECCS and AFOLU remain in place as keystone mitigation options, with their scenario ranges for net negative emissions being 30-780 $GtCO_2$ and 20-400 $GtCO_2$ respectively.

Integrated assessment models are powerful tools for exploring the mitigation scenario space, they provide a substantial basis for further investigation and deployment of climate change mitigation strategies in future scenarios. In the case of mitigation scenarios consistent with a 2100 warming limit of 1.5 °C, those mitigation strategies are BECCS and afforestation, both of which see widespread use across the board in mitigation scenarios, and both of which are require extensive land use change to support their deployment (Brack & King, 2021; Roe *et al.*, 2019). However, IAMs are incredibly complex models, and their widespread use of BECCS and afforestation to meet climate targets is based on a vast array of assumptions, many of which are subject to high levels of uncertainty or contested claims of feasibility, including their land use (Hansson *et al.*, 2021; Low & Schäfer, 2020; Vaughan *et al.*, 2018).

The overall objective of this thesis is to step away from the complexities of integrated assessment modelling; to explore some of the drivers of global land that could be made available for BECCS and afforestation through the development and use of a simplistic and traceable model of the global food system and it's land footprint, and to examine some of the assumptions surrounding the assumed land available for BECCS and afforestation in mitigation scenarios.

Chapter 2 represents approximately two years of model development of the Country-Level Land Availability Model for Agriculture (C-LLAMA), and details the processes and mechanisms therein. The contents of Chapter 2 were published in Geoscientific Model Development in February of 2022 (Ball *et al.*, 2022). C-LLAMA is based on the 'Flux Assessment of Linked Agricultural Food production, Energy potentials & Land use change' (FALAFEL) model (Powell, 2015; Powell & Lenton, 2012), which has previously been used to investigate the land use impacts of diet and food waste and losses. However unlike FALAFEL, C-LLAMA operates at a country level, which allows it to represent inherent differences in food systems, especially those between countries of differing industrialisation. In this Chapter an anchor scenario is outlined, which is used as the baseline C-LLAMA scenario for comparison, as a means to explore the sensitivity of agricultural land use in subsequent chapters to the various drivers outlined in this introduction.

In Chapters 3 to 5, the C-LLAMA model is used to explore the land use implications of pulling various 'levers' related to the drivers of agricultural land use that have been outlined in this Chapter. In **Chapter 3**, the drivers and subsequent impacts on the food supply chain (including land use) of dietary trends are discussed. The land use impacts of changing diets are explored using C-LLAMA, including a scenario in which all animal product consumption is eliminated by 2050. Rather than simply trying to find the best dietary composition for the sake of land use, the work in this Chapter was carried out in the context of the sustainable development goals, specifically SDG 2 (end hunger and improve nutrition). With SDG 2 in mind, the EAT-Lancet 'planetary health' diet was selected: a globally applicable diet that aims to provide sufficient nutrition whilst remaining within planetary boundaries (The Eat-Lancet Commission, 2019). The land use impacts of transitioning to the EAT-Lancet diet are explored by prescribing the diet to each region in turn.

Chapter 4 follows the same principles as Chapter 3. The general causes and potential resolutions are discussed for early to mid (distribution and processing) and late stage (household, retail, and commerce) food waste and losses. Two simple C-LLAMA scenarios are constructed and compared, in which food waste and losses early and late in the food supply chain are reduced globally. Then, the land use impacts of reducing waste and losses are explored at a regional level, using estimates for 'best case' observed values for various stages of waste and loss.

The first part of **Chapter 5** discusses the mechanisms through which crop yields and land use for animal production may be improved, followed by a simple examination of closing 'yield gaps' (Mueller *et al.*, 2012) at a regional level. The second part of Chapter 5 is a comparison of the regional results from the first part with those of the previous two chapters (3 and 4), identifying the relative regional sensitivity to the three key drivers of land agricultural land use.

Chapter 6 is an investigation of the land use and production of energy crops in mitigation scenarios consistent with 2 °C or 1.5 °C. The range of energy crop production, along with the rate of expansion in all SSP scenarios is discussed. Following this is an exploration of various factors that may impact the availability, suitability, and risk of energy crop production based on their location in these scenarios. Exploratory attempts are made to quantify the portion of energy crop that is produced in tropical regions, and regions of differing levels of environmental and general governance quality.

2

Country-Level Land Availability Model for Agriculture (C-LLAMA) 1.0

This chapter represents two years of work developing the C-LLAMA model. This model description was then submitted to Geoscientific Model Development in July of 2021, then published in February 2022 (Ball et al., 2022). T. Ball was responsible for the development of the model, and preparation of the manuscript and figures therein. All authors contributed suggestions to editing.

Abstract

We present C-LLAMA 1.0 (Country-level Land Availability Model for Agriculture), a statistical-empirical model of the global food and agriculture system. C-LLAMA uses simplistic and highly traceable methods to provide an open and transparent

approach to modelling the sensitivity of future agricultural land-use to drivers such as diet, crop yields and food-system efficiency. C-LLAMA uses publicly available FAOSTAT food supply, food production, and crop yield data to make linear projections of diet, food system and agricultural efficiencies, and land-use at a national level, aiming to capture aspects of food systems in both developing and developed nations. In this paper we describe the structure and processes within the model, outline an anchor scenario, and perform sensitivity analyses of key components. The models land-use output behaves as anticipated during sensitivity tests and under a scenario with a prescribed reduction in animal product consumption, in which land-use for agriculture is reduced by 1.8 Gha in 2050 when compared with the anchor scenario.

2.1 Introduction

Land-use plays a critical role in achieving Paris Agreement temperature goals. Favoured climate change mitigation strategies such as biomass energy with carbon capture and storage (BECCS) and afforestation rely heavily on widespread land-use change to achieve the necessary scales to be effective (Gough *et al.*, 2018; Roe *et al.*, 2019; Rogelj *et al.*, 2018a; Vaughan *et al.*, 2018). However, a range of interlinked factors may jeopardise the sustainable deployment of these mitigation strategies; these include carbon leakage, ecosystem services and biodiversity, and the need for land to support human livelihood and food supply (Arneth *et al.*, 2019). With growing global populations and wealth there are also increasing demands for food quantity and diversity, placing additional pressure on the agricultural system and corresponding land use to meet the demand (Alexander *et al.*, 2016).

Integrated assessment models (IAMs) make comprehensive projections of future scenarios by coupling economics and land-use with simple carbon cycle and climate models. These models are driven by macro-economics, using a combination of dynamic and static input factors to project future scenarios and are the basis of the Paris Agreement warming targets (United Nations Treaty Series, 2015). Most IAMs deal with land use, although there are some exceptions. IAMs are well suited to holistic modelling of future scenarios, especially with the objective of informing policy. They are able to draw together a wide variety of physical, social, and economic processes to produce informed estimates of future scenarios; their mechanisms are well documented and many are open source (Havlık *et al.*, 2014; Popp *et al.*, 2014; Calvin *et al.*, 2013; Fujimori *et al.*, 2012; van Vuuren *et al.*, 2011). However, from their complexity arises an element of nebulousness, they are not able to undertake more detailed analysis of more specific aspects independent of the whole. Despite the broad applicability of IAMs, there remains a need for models of reduced complexity; they are able to undertake more specific analyses of components that more complex models like IAMs are unable to represent individually. There are significant strengths and weakness to both approaches and they are best used in conjunction with one another, somewhat analogous to reduced-complexity climate models and their general-circulation counterparts (R. J. Nicholls *et al.*, 2020; Sarofim *et al.*, 2021).

FALAFEL (Flux Assessment of Linked Agricultural Food production, Energy potentials & Land-use change) is a global-level model, using linear projections of global food supply, agricultural efficiencies, and yields to produce trajectories for land-use, carbon capture and energy to 2050 (Powell, 2015; Powell & Lenton, 2012). C-LLAMA (Country-Level Land Availability Model for Agriculture) is the successor to FALAFEL; it is based on the same principles and processes as FALAFEL but disaggregated to the country level. It produces a land-use trajectory to 2050 for each food commodity and commodity group within a country. Where a global model cannot represent the differences between the food systems in a highly developed country and a developing one, C-LLAMA is able to. This is the primary advantage of moving to a country-level model: it allows for the exploration of the drivers of land-availability in the across a variety of food systems. C-LLAMA is built in Python (Van Rossum & Drake Jr, 1995), unlike FALAFEL which is built in Microsoft Excel. The purpose of the model is to be transparent and easily traceable, as such the model code is open-source and uses only publicly available data as it's inputs.

C-LLAMA is situated at the opposite end of the modelling spectrum to IAMs; taking a bottom-up approach to modelling future land availability; beginning with food supply, then projecting food demand and production forward. In a similar approach to that of FALAFEL, Bijl *et al.* (2017) consider the relationships between income and dietary patterns to model long-term food demand, but halt at the crop demand stage. C-LLAMA has no economic considerations but models the full range of the food-system from the consumer to the production of crops and animal products. Where FALAFEL and Bijl et al. model the food-system at a global and regional level, C-LLAMA operates at a national level.

2.2 Model overview

C-LLAMA is a statistical-empirical model that uses data from the FAOSTAT database as its primary input (FAO, 2021a). These datasets contain food supply and production data, with the food-balance sheets used containing data from 1961 to 2013, and all other datasets (such as land-use and production) running from 1961 to 2017. All data is at a country-level. C-LLAMA models the same timespan as FALAFEL: from 2017 to 2050. Many of the processes in the model are the same as those in the FALAFEL but operate at a country level as opposed to being globally aggregated. An overview of the structure of C-LLAMA is given in Figure 2.1. A list of all modules responsible for model processes in C-LLAMA, grouped into model sections, can be found in Table A.1.

The model operates across five continents: Africa, the Americas, Asia, Europe and Oceania, C-LLAMA then splits these into further subcontinental regions (for example, the Americas are split into N. America, S. America, Central America and the Caribbean), most of which contain several countries or states. The model is structured into the following four spatial aggregations: global, continent, region, and country, aligning with the United Nations Statistics Division (UNSD). The structuring

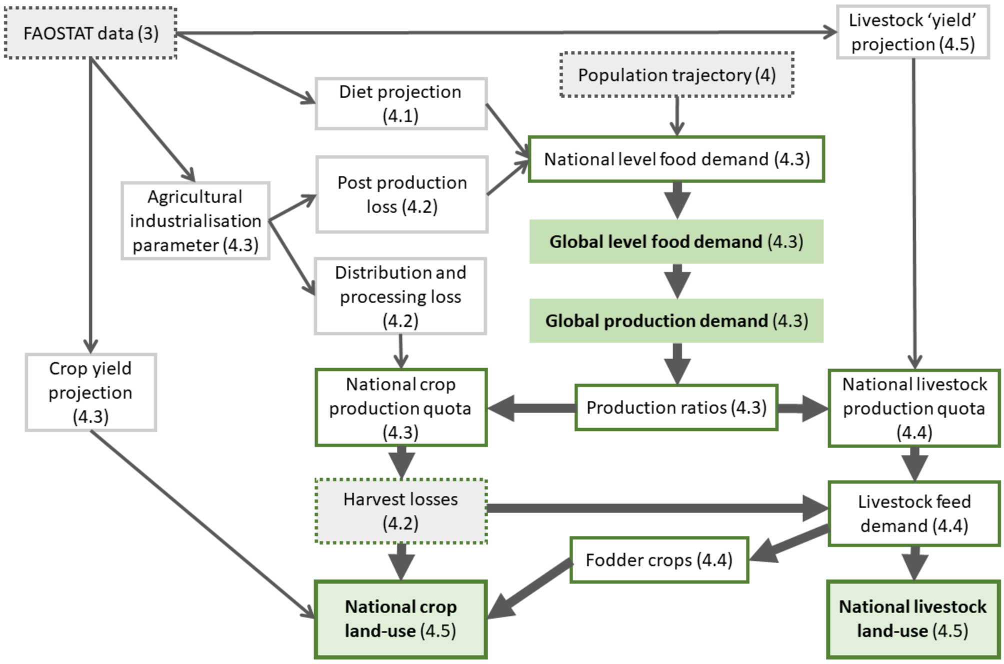

Figure 2.1: Overview of C-LLAMA Model structure and flow, with relevant section numbers within the paper indicated in parentheses. Boxes with a dotted border are external datasets while a solid border represents values calculated in C-LLAMA. Thick arrows represent a flow of mass or energy, thin arrows represent the contributing trajectories or factors. Boxes outlined in green are core processes. Boxes shaded in green are globally summed quantities. National crop land-use and livestock land-use are shaded and outlined in green, to highlight them as the primary output of the model. Not all model processes and connections are depicted, this diagram gives a general overview of C-LLAMA.

of the model into these spatial aggregations allows modifications to be targeted at specific levels. All model processes operate at the country level, with the exception of total global level food demand and global production demand, which are globally aggregated. Food production is then allocated at the country-level.

Global food production and demand is dominated by a small handful of countries. For example: Brazil, the USA and Argentina together accounted for 52% of production by mass of crops used for food in 2017. Of the 162 countries in the FAOSTAT data (that produced food in 2017), the 100 most food-productive countries account for 99.7% of the total production mass. The remaining 62 countries account for only 0.3% of the total food production. Countries whose food production mass in 2017 equates to less than 0.01% of the 2017 global total and whose agricultural land-area is less than 34,000 hectares are excluded from the model processes. Figures illustrating this can be found in appendix A. This is done in C-LLAMA for two reasons. The first is to reduce unnecessary model run-time and development complexity. The second reason is that many of these countries have reduced data quality and availability due to their size. Often the data is discontinuous, most commonly due to changes in reporting or assessment. This can lead to unrealistic behaviour when making projections of the data as C-LLAMA does.

There are a small number of countries not included in the model processes because no food balance data for them is available from the FAOSTAT database. The reason for this in most cases is a recent history of political instability or conflict, which suggests that motivating land-based climate mitigation action in these regions may be difficult (The World Bank, 2020). Notable for their large land areas, Libya, Sudan, Somalia, and the Democratic Republic of the Congo in Africa (DRC), and Papua New Guinea in Oceania are not included in the dataset, a total land area of 500 Mha. Despite their large land areas, Libya, the DRC, and Papua New Guinea have a small amount of agricultural land for their size at less than 10%, and as low as 2% in the case of Papua New Guinea. Sudan has 40% agricultural land coverage and Somalia has 70%.

2.3 Model components

Population

C-LLAMA uses population trajectories from the shared socio-economic pathways (SSP) database, available as 5-yearly population values for each country. SSP2 is a middle of the road scenario with corresponding population projection based on medium values for fertility, mortality, education and migration (KC and Lutz, 2017).

The SSP2 population projection is used as a default but any population projection data can be applied. The population data is interpolated linearly to produce a yearly population trajectory to 2050.

2.3.1 FOOD SUPPLY

We define food supply for a given country to be the mean number of kilocalories available per capita per day in a given year. This includes any post-production food waste; some food reaches consumers but is never eaten, either commercially or as domestic waste. The proportion of food wasted in this way is as high as 30% in most developed countries (Alexander et al., 2017).

FAOSTAT food balance sheets contain food supply data disaggregated into different food commodities (Food and Agriculture Organization of the United Nations, 1997). C-LLAMA uses this data to produce a projected food demand for each country. First, a regression line is calculated for the total food supply for a given country in the period 1961 to 2013, which is then used to calculate a projected food supply value for the year 2050. A linear projection is made for each country from their current total food supply to the projected 2050 total food supply, using the following equation:

$$F(n) = F_0 + \frac{n - n_0}{n_{\text{target}} - n_0}(F_{\text{target}} - F_0), \tag{2.1}$$

where F_n is the total food supply in year n, F_{target} is the projected 2050 total food supply per capita, F_0 is the mean of the most recent five years of historical food supply data. n_0 and n_{target} are the start and end years of the projection, 2013 and 2050. Secondly, a linear regression is used to make a projection for the calorie supply from each of the food groups animal products, vegetal products, and aquatic products. Regression lines with a p-value greater than 0.05 are discounted (this threshold value can be changed), instead fixing the projection at the mean value of the most recent five years of data. These projections are then converted into fractions. The proportion of food supply (P) made up by group i in year n, is given by

$$P_i(n) = \frac{a_i n + b_i}{\sum_{g \in G}(a_g n + b_g)}, \tag{2.2}$$

where a and b are the gradient and intercept of the regression line for that group and G is the set of groups: animal, vegetal and aquatic products.

Third, another linear regression is used to project the relative proportions of individual food commodities within the three food groups. Key food commodities are represented individually, for example wheat, maize and rice in the vegetal product group, and bovine meat and poultry meat in the animal product group. Other commodities are represented in groups, for example 'cereals – other' contains all cereals that are not singled out as key commodities, while the 'luxuries' group contains all tea and coffee. Aquatic products are not the focus of the model as they have minimal to no land requirements during their production; thus they are placed in a single group. Hence, in C-LLAMA, aquatic products simply offset some of the calorific demand from the other food groups. Where possible, C-LLAMA uses vegetal product groups defined in FAOSTAT data. A full list of food commodities and groupings can be found in Appendix Tables A.2 and A.3. The commodities within a group are then converted into ratios, so the proportional calorific contribution of commodity j to its umbrella food group i in year n is

$$P_j(n) = \frac{a_j n + b_j}{\sum_{c \in C}(a_c n + b_c)}, \tag{2.3}$$

where a and b are the gradient and intercept respectively of the regression line for that commodity and C is the set of commodities within the group, for example if j is wheat then C would be all vegetal products. The structure of the projected food supply is then as follows: the total calorie projection is apportioned to each of the food groups by their projected ratios, which are in turn apportioned to the projected commodity ratios. Hence by combining equations 1, 2 and 3, the number of calories contributed to the mean daily food supply per capita by commodity j (of group i) is

$$E_j(n) = F(n) * P_i(n) * P_j(n), \tag{2.4}$$

where all symbols have their previously defined meanings. This approach facilitates the tuning of dietary scenarios by modifying the growth rate of the animal product group or dairy commodities to simulate increases in vegetarianism or veganism.

2.3.2 FOOD SYSTEM EFFICIENCY

FOOD SYSTEM EFFICIENCY PARAMETER

There is significant variation in food system efficiency, both at different stages and between developed and developing food systems. To reflect this in C-LLAMA, a parameter was developed to assign areas an appropriate degree of efficiency at each stage of the food system and in the model processes. The requirements of the system are the following:

1. Allow the food system efficiency of states to improve as the model progresses.
2. Limit improvement to a realistic maximum.
3. Be representative of most real-world cases. Outliers are inevitable but significant contributors of food demand or food production to the global food system should be captured well.

A highly developed nation in which the majority of farming practices are heavily industrialised with high levels of efficiency should have a score of greater than 1.0 whilst a less developed country in which the majority of people are fed through subsistence farming should score lower than 0.5. A metric such as GDP per capita is not suitable, because a state with extreme income equality could score highly when in actuality the majority of inhabitants rely on subsistence agriculture. Other metrics such as irrigation, fertiliser use and agricultural machinery density were all considered. However, each of these metrics can be skewed by climate, crop types and traditional practices. As such these are also not always reflective of the relative agricultural efficiency of an area.

A parameter was developed based on the yearly mean of daily food energy consumption per capita. This is a self-moderating quantity: unlike GDP there is a maximum realistic value that this can take regardless of economic disparity, so the mean cannot be skewed by extreme cases. The equation for the food system efficiency parameter X for a country a in year n is

$$X_{a,n} = \frac{F_{a,n}}{0.7 * F_{\text{target}}} - \frac{0.5}{0.7}, \tag{2.5}$$

where F is the country's total food supply in year n. F_{target} is an idealised food supply, defined as 2500 kcal per capita per day with an additional 30% lost to post-production food waste (see Table 1). This is representative of the food supply in the majority of highly developed regions (N. America, Europe, and Australia and New Zealand) (Kearney, 2010; United Nations Environment Programme, 2021). . Using the ratio of food supply to an idealised food supply generates values in the approximate range 0.5 to 1.2 for the year 2013. The values 0.5 and 0.7 scale the metric to produce values for X_n in the range 0.0 and 1.0.

This parameter is then projected forward with a simple linear projection to 2050 for use in the model processes. In the very few cases where the projection prescribes a decline in food system efficiency, the parameter is halted at the most recent historic value. In the majority of cases this parameter reasonably depicts the position of a country along a scale between complete subsistence agriculture to an industrialised nation with developed infrastructure. However, due to the complexity of the real-world food system, there are a small number of expected outliers, notably Japan and the Republic of South Korea, both of which score in the range 0.4 to 0.6, much lower than expected given their level of industrialisation. This can be explained by a combination of two factors: a slightly lower post-production food waste of around 15% (Liu *et al.*, 2016) and typically a lower daily calorific intake than other similarly industrialised nations; a result of cultural and dietary trends (Tsugane & Sawada, 2014).

The parameter is used in the model processes to inform processes relating to agricultural efficiency, including food energy losses at three stages: processing, distribution, and post-production losses. The ratios of livestock feed energy obtained from forage and non-forage are also derived using this parameter, along with the portion of food waste that is used as livestock feed. Minimum and maximum values are chosen for each, representing either the totally subsistence or total industrialised case, and the metric is used to scale the value for a country between the two. The equation for a factor μ is:

$$\mu_a(n) = \mu_{\text{sub}} + X_a(n)\left(\mu_{\text{ind}} - \mu_{\text{sub}}\right), \tag{2.6}$$

where X is the value of the food system efficiency parameter for the country a in given year n and sub and μ_{ind} are the subsistence or industrialisation boundaries of the factor respectively. The upper and lower boundaries for each of these parameters can be modified as a means of scenario adjustment. The behaviour of the boundaries as the model progresses can also be modified; they can be fixed at the initial values, or an overall efficiency increase can be prescribed, in which case the limits will also change over time.

INEFFICIENCY IN THE FOOD SYSTEM

In C-LLAMA, losses in the food system are grouped in four ways: losses at the harvest stage, losses in the processing stage, distribution losses and post-production losses.

Losses at the harvest stage occur before any processing or distribution and are either non-recoverable or recoverable. Causes of non-recoverable losses include insect and animal pests, weeds, and disease. Developing regions see greater losses during production than developed regions due to the availability of disease and pest prevention measures (Oerke & Dehne, 2004; Savary *et al.*, 2012). Losses due to these factors are accounted for in crop-yield data so no loss factor is applied at this stage.

The methodology for handling recoverable harvest losses: 'harvest residues', is more complicated since these are crop dependant. Not all harvested material is edible for humans, for example the husks and casings or 'chaff' produced when harvesting grains. The formalisation of this concept is the harvest index, defined as the ratio of the mass of useful product to the mass of above ground biomass (Singh & Stoskopf, 1971). Despite being an inefficiency in the food system, many waste products produced at the harvest stage can be used for other purposes to reduce this inefficiency. Chaff for example, while inedible to humans, is suitable feed for most livestock. Harvest residue indices and harvest residue recovery rates are used to inform a ratio of produced residue to recovered residue (Krausmann *et al.*, 2008; Wirsenius *et al.*, 2010). Harvest residue indices and recovery rates can be found in Appendix Tables A.4 and A.5.

Processing losses occur as the raw crops are processed to a form suitable for their intended purposes, for example the removal of kernels from olives. Some of these losses are potentially recoverable for use as animal feed, bioenergy feedstock or in other industries (Van Dyk *et al.*, 2013). Fodder crops generally incur less loss than crops destined for human consumption at the processing stage as they require little to no processing (Gustavsson *et al.*, 2011; Kitinoja, 2013).

Distribution losses are incurred through transportation or storage. This stage is a major contributor to food system inefficiency in developing countries; due to poor road infrastructure, pests and lack of suitable refrigeration or other storage, losses at this stage can be as high as 50% and as low as 5% in developing and developed areas

Loss factor	Industrialised ($X = 1.0$)	Subsistence ($X = 0.0$)
Processing	6%	10%
Distribution	5%	50%
Post-production	30%	5%
Post-production waste to feed	5%	40%
Other waste to feed	40%	15%

Table 2.1: Boundary values for factors informed by the food system efficiency parameter.

respectively (Lipinski *et al.*, 2013; Parfitt *et al.*, 2010).

Post-production food waste refers to food lost at the consumer level, including food thrown away after purchase in the home, or in commercial environments such as restaurants. Unlike most other food system loss factors, the heaviest post-production losses are seen in the developed world (Parfitt *et al.*, 2010; Stancu *et al.*, 2016). Since post-production waste is inherently included in food supply data, the post-production factor shown in table 1 is used only to estimate the amount of post-production waste potentially available for use as livestock feed.

2.3.3 FOOD PRODUCTION

PRODUCTION

Following the application of the loss factors determined in the food system efficiency section to the food supply projections described in section 3.1, each country is left with a food energy requirement for each food commodity r, calculated using the following equation:

$$r_{j,a}(n) = \frac{E_{j,a}(n)}{\prod_{l \in L}\left(1 - \mu_{l,a}(n)\right)}, \tag{2.7}$$

where r is the energy demand from a country a for commodity j, μ is a loss factor and L is the set of processing and distribution losses. E is the calorific contribution to the countries food supply from commodity j, described in section 3.1. The food energy lost due to efficiency loss factors is retained for potential re-use as livestock feed. Food demand is then summed globally for each key commodity or commodity group is, so the global production requirement R for the commodity j is

$$R_j(n) = \sum_{a \in A} r_{j,a}(n), \tag{2.8}$$

where r is the food energy demand for commodity j from a country a, and A is the set of all countries.

C-LLAMA does not have a formal representation of trade, instead trade is implicit in the allocation of food production; global proportions of production for each crop commodity are calculated using the most recent five years of production data then allocated accordingly. For example, the USA was responsible for 42% of global wheat production between 2012 and 2017, thus 42% of all wheat production in C-LLAMA is allocated to the USA. To account for the significant industrial use of primary crops in Brazil and the USA, the historical production value is reduced by a factor to provide an estimate for only food use of those crops. These factors are 0.34 and 0.289 for sugar cane in Brazil and corn in the USA (Bordonal *et al.*, 2018; De Miranda & Fonseca, 2019; Mohanty & Swain, 2019). Following this process, each nation is left with a production allocation for each key commodity and commodity group, the equation for which is

$$q_{j,a}(n) = \frac{M_{j,a}}{\sum_{a \in A} M_{j,a}} * R_j(n), \tag{2.9}$$

where q is the allocated production energy of commodity j in the country a, M is the mean of the most recent five years (2012 to 2017) of historical production mass of commodity j in country a and A is the set of all countries.

CROP YIELD

A large proportion of yield variation can be explained by climate variability, with the remainder being a result of farming practices and industrialisation (Mueller *et al.*, 2012; Ray *et al.*, 2015). C-LLAMA takes largely the same approach as FALAFEL; historical yields for each crop and group are projected linearly to 2050, but this is done for each country. Yield has the potential for large transient variation on a year by year basis, often a result of climate events, pests or management (Ray *et al.*, 2015; Frieler *et al.*, 2017). Consequently, there is the possibility of yields increasing at an unrealistically high rate through this kind of projection. To address this, in C-LLAMA yields are capped at the historical maximum value for a region, preventing any region from exceeding an observed value whilst allowing each country within a region to catch up to a localised observed maximum. Linear projections with a p-value greater than 0.05 (this threshold can be changed) or a decreasing yield are discarded. In either of these cases, the mean yield from the previous ten years of data is used instead.

For all key crops the raw yield data, in tonnes per hectare per year, was used to make the projection. In the case of grouped crops, the groups yield was calculated by taking mean of all crops contained in the group, weighted by national production mass. The group 'sugar crops' consists almost entirely of sugar beet since sugar cane is represented as an individual crop. For palm oil, vegetable oils and other oil crops, an effective oil yield was calculated for each using their respective oil factors which can be found in the FAOSTAT database (FAO, 2021a).

2.3.4 LIVESTOCK

Animal product demand is one of the highest contributors to agricultural land demand and greenhouse gas emissions globally, with estimated emissions between 5.6 and 7.5 Gt CO2 yr-1 equivalent between 1995 and 2005; as such livestock are a crucial component of the C-LLAMA model (Herrero *et al.*, 2016; Pikaar *et al.*, 2018;

Van Zanten *et al.*, 2018). As with vegetal food commodities, livestock commodities are partially grouped, with major commodities: bovine meat, pig meat, mutton/goat meat and poultry meat remaining separate. The remaining meat products contribute comparably little to the global demand for animal products and are grouped into an 'other meat' category. Eggs, dairy and fish are each in their own groups. For each country, an animal commodity demand is produced per year in the diet and food supply section of the model. As is well established, livestock are inherently less resource efficient than vegetal products as a means of providing calories for human consumption. The feed consumed by livestock does not go directly to become fresh animal product, instead much of it supports the survival of the animal. This is commonly quantified as a feed efficiency (FE) or livestock conversion efficiency (LCE, the inverse of feed efficiency), expressed as the quantity of fresh animal product to feed energy mass or equivalent energy. This number varies drastically between animal product types: bovine meat has an energy FE of approximately 3%, whereas poultry meat is much higher at 21% (Shepon *et al.*, 2016). Note that these FEs are produced from data acquired in the USA. Currently the values used in C-LLAMA are taken from FALAFEL; a cohesive energy-equivalent FE dataset was not found at a regional or country level. FEs certainly do vary regionally, largely due to the different role of livestock in different food systems. A cow in a subsistence agriculture environment is more likely to be allowed to live to substantial age, providing dairy and driving machinery. This contrasts with a cow in industrialised agriculture, where it might be reared solely for meat and slaughtered in early adulthood (Wirsenius *et al.*, 2010). A proportion of livestock feed demand is met through forage (μ_{forage}) and the remainder is met through feed and residues ($\mu_{\text{non-forage}}$, equivalent to $1 - \mu_{\text{forage}}$), calculated using the food system efficiency parameter to assign a value between the subsistence case and the industrialised case, using the same method as in Eq. (6). The quantity of feed demand energy from non-forage D for animal product j in country a and year n is

$$D_{j,a}(n) = Q_{j,a}(n) * \mu_{\text{non-forage}\,j,a}(n) * \frac{1}{\text{FE}_j} \tag{2.10}$$

where FE_j is the livestock dependant feed efficiency and Q is the production allocation. The extreme cases for each animal product are centred around the FALAFEL numbers, with the developing limit being 20% lower and the developed limit being 20% higher. The proportion also varies dependant on the animal product, for example chickens and pigs typically obtain a higher proportion of their food energy from feed than ruminants (Tufarelli *et al.*, 2018). An individual animal will likely be fed through a combination of forage and feed, but for the purpose of the model the assumption is made that the land footprint of non-foraging animals comes only from the land required for fodder crops. The portion of livestock feed demand met through forage is therefore $\frac{1}{\text{FE}_j} * Q$ minus D for each animal product j. This approach is coarse compared with modelling livestock as entities with individual mixed feed demands, however the feed energy requirements are comparable.

WASTE AND RESIDUES AS FEED

In some situations, livestock can utilise waste from the agricultural system, processing losses, post-production food waste and harvest residues. For each livestock commodity a potential feed ratio for each of these waste streams is estimated: the maximum proportion of each waste type that could contribute to the livestock diet (z). These ratios can be found in Appendix Table A.6. Waste produced by processing, distribution and post-production are calculated at the country of consumption, while harvest residues are calculated at the crop production stage. Post-production waste is assumed to only be available to animals in the area in which it was produced and is informed by a post-production waste to feed factor (μ_{post}), scaled by the food system efficiency parameter using Eq. (6) between 40% and 5% for the subsistence and industrialised cases respectively. Note that in the case of post-production waste the subsistence extreme is 'more efficient' than the industrialised case. The remaining total available waste energy is multiplied by an 'other waste to feed factor' (μ_{other}), again informed by the food system efficiency parameter using Eq. (6), with the subsistence and industrialised limits being 15% and 40% respectively. Other waste is that of harvest residues and processing waste, but not distribution waste since this is 'lost' or spoiled. These numbers are taken from the low and high efficiency scenarios in FALAFEL. Waste energy is 'fed' to livestock, up to the potential feed ratio limit, allocated by the potential feed ratios (z). The energy used is then subtracted from the livestock feed energy demand, the remainder of which is accounted for with fodder crops. The remaining feed energy demand to be met through fodder crops (D') is

$$\begin{aligned} D'_{j,a}(n) = D_{j,a}(n) * \left[1 - \sum_{\omega \in \Omega} z_{j,\omega}\right] \\ + \sum_{\omega \in \Omega} \left[S\left(D_{j,a}(n) * z_{j,\omega} - \left[w_{\omega}(n) * \mu_{\omega} * \frac{z_{j,\omega}}{\sum_{c \in C} \left(z_{c,\omega} \right)} \right] \right) \right] \end{aligned} \tag{2.11}$$

$$S(x) = \begin{cases} x & \text{for } x > 0 \\ x & \text{for } x <= 0 \end{cases} \tag{2.12}$$

where D is the total feed energy demand, z is the maximum portion of feed energy that livestock j can obtain from waste stream ω, w is the available waste energy and μ is the waste to feed factor. C is the set of all livestock commodities andω is the set of all waste streams: post-production, processing, and harvest residues. μ is μ_{post} for post-production waste and μ_{other} for all other waste streams.

FODDER

Following the reduction of livestock feed demand through waste to feed and foraging, the remaining feed energy demand is met with fodder crops. The historical fodder mix, the ratio of each crop making up fodder in a country, is calculated using the most recent five years of 'feed' energy data in the FAOSTAT food balance sheets. The cereals contributing the most to the fodder mix globally are maize, wheat, sorghum, barley and rice. In addition, soybeans, potatoes, cassava, pulses and fruits also contribute in the top ten. Each of these products are represented individually while all other products used as feed are grouped as ‘other feed’. Around 8% of the total feed mass each year comes from non-crop products. The majority of this 8% is milk and the remainder is largely comprised of aquatic products such as fishmeal and aquatic plants, often added to livestock feed to supplement nutrition (Holman & Malau-Aduli, 2013; Oliveira Vieira *et al.*, 2015). These products are removed from the fodder mix, as these products require minimal additional land. The remaining livestock feed demand is split according to the derived fodder mix, so the contribution to the total fodder requirement (r) in country a from fodder product k is

$$r_{k,a}(n) = \frac{f_{k,a}}{\sum_{s\in S} f_{s,a}} * \left(1 - \frac{f_{\text{milk},a} + f_{\text{aq},a}}{\sum_{s\in S} f_{s,a}}\right) * \sum_{c\in C} \left(D'_{c,a}\right) \tag{2.13}$$

where f is the five year mean of feed data for fodder product k from the FAOSTAT food balance sheets, f_{milk} and f_{aq} are the feed data for milk products and aquatic products respectively, S is the set of all fodder products. D' is the fodder demand for livestock commodity c, C is the set of all livestock commodities. The global production requirement for fodder product k is then

$$R_k(n) = \sum_{a\in A} r_{k,a}(n) \tag{2.14}$$

In the same way as crop production for food, the fodder crop production demand is allocated based on historical production of the fodder products. The production allocation (q) for fodder product k for country a is

$$q_{k,a}(n) = \frac{M_{k,a}}{\sum_{a\in A} M_{k,a}} * R_k(n) \tag{2.15}$$

where M is the five year mean production mass for fodder product k and A is the set of all countries. In the case where the product has been considered as a food commodity and thus a yield and production allocation has already been calculated, the additional production allocation for fodder is simply added to the nations existing production quota of the commodity for food. In some cases, it is necessary to perform a yield projection in the same manner as described in section 3.3. Following this stage, each country has a production quota for each year for each commodity, used for food, animal feed, or both, along with a corresponding yield trajectory.

2.3.5 Land use

Crop land use

A simple division of yearly crop production allocations by national crop yield projections produces a yearly land demand trajectory for each crop within a given country. Since the model objective is to explore sensitivities rather than absolute land-use values, land-use is projected from the most recent value in the FAOSTAT data: a calibration factor is used to align the 2017 value of the projected values with the 2017 historical value, for each crop. In the case that total land demand for crops is less than the previous year, the land difference between the years is put into a ‘freed land’ class. In FALAFEL this land is then used for either afforestation or energy crops, while C-LLAMA does not currently process this further. In reality land use change is multidimensional; the abandonment of agricultural land varies greatly between areas and industrialisation levels, influenced by climate, land productivity, tradition and governance Lambin & Meyfroidt (2011); Lambin *et al.* (2003). C-LLAMA currently does not consider non-agricultural land use. Further development to include more complex handling of land-use is intended.

Livestock land use

As mentioned in section 3.4, the land requirements for livestock (in addition to fodder crop production) in C-LLAMA come entirely from their pasture area; the implication being that all fodder fed animals are under roof, while their foraging counterparts graze pasture. This is generally not the case for foraging pigs and chickens, so a pasture factor (ρ) of 0.1 is applied to reduce their land footprint from that of cows and sheep (Tufarelli *et al.*, 2018).

The land used for livestock pasture is calculated using an effective pasture yield. First, the historical energy obtained from pasture by livestock was estimated using a similar process to the method adopted in Haberl (2007); for each country, available feed is subtracted from a livestock feed demand, calculated using historical production energy and feed conversion ratios between 1961 and 2017. This leaves animal food acquired through forage. Dividing this quantity by land-area used for pasture in a given year results in the historical effective pasture yield – animal product energy produced per hectare of pasture. The land-area data used is taken from the FAOSTAT database (FAO, 2021a). The historical effective pasture yield (Y) for animal products in country a is

$$Y_a = \frac{1}{L_{\text{pasture}}, a} * \left(\sum_{j \in J} [M_{j,a} * \text{FE}_j * \rho_j] - \sum_{k \in K} f_{k,a} \right) \tag{2.16}$$

where L_{pasture} is the country's pasture land area, M is the production mass of an animal product j, FE_j is the feed conversion ratio for the animal product and J is the set of animal products. f is the quantity of available feed product k and K is the set of all feed products. The historical trajectory is linearly projected to 2050; the pasture yield and pasture production mass demand together give a projected pasture land requirement for each livestock commodity. Since there is no historical data to calibrate the yield value to, the yield value is scaled such that the projected 2017 pasture land-use matches the 2017 historical pasture land-use. The value is calibrated to the anchor scenario described in Section 5, rather than being scenario specific, to address counter-intuitive model behaviour, discussed in the Appendix (Figures A.4 and A.5). Because this can result is minor discontinuity when running non-anchor scenarios, the projected land-use is then calibrated to the historical land-use too. This method is coarse but offers a catch-all method of translating a production demand into land-area for every country in C-LLAMA.

2.4 MODEL OUTPUT

C-LLAMA produces a land-use trajectory from 2013 to 2050 for each food commodity and commodity group within a country, output as a comma separated variable file. Animal product land-use is aggregated as pasture, explained in section 3.4. All crops have individual land-use trajectories. An output with crops aggregated into either crops or specifically fodder crops is also produced. Data from intermediate stages of the model such as food supply, production, and crop yield projections is retained upon completion of the model run. However, given that calibration of the model occurs at the final stage rather than at every intermediate stage, these trajectories should be viewed with this in mind. Food supply and crop yield projections are both direct projections of historic data and so are exempt from this. For the sake of model run time, intermediate outputs are stored in a serialised format using the 'pickle' library, part of the Python standard library (Van Rossum & Drake Jr, 1995).

2.4.1 ANCHOR SCENARIO

C-LLAMA is based around an anchor scenario, in which all parameters take default values based on literature and projections from historical data are made to 2050. This scenario aims to be as close an approximation to the real world as possible in the framework of the model, with targets for efficiency and industrialisation being set at middle of road values. Table D1 in shows key parameters and their values in the anchor scenario. Regionally aggregated land-use types in the anchor scenario can be found in appendix E.

Figure 2.2 shows agricultural land-use at the continental level for historical FAOSTAT data and in the C-LLAMA anchor scenario. All continents aside from Oceania see an increase in land-use for both crop and animal production, with the rate of increase slightly decreasing toward 2050, particularly in Africa. The greatest rate of increase occurs in Asia and the least in Africa and Europe. In all cases, the rate of increase for pasture is greater than that of cropland, with cropland for fodder crops lying in between. The direction of the projected land-use aligns with that of the historical data in the Americas, Africa, Oceania, and Asia. However, in Europe a slight reversal of the direction of change occurs, a result of the significant historical production of beef and dairy production in Russia; Russia produced 4% of the World's bovine meat in 2013, hence is allocated a significant portion of beef production in the model processes and resultant pasture area increase.

Figure 2.3 shows the projection of mean diet at the continental level in the C-LLAMA anchor scenario. All continents undergo an increase in total calorific intake toward 2050. With the magnitude of change being similar at around 400 kcal for every continent with the exception of Europe, which sees a lesser increase of approximately 200 kcal by 2050. The proportional increase varies however, with the greatest proportional increase occurring in Africa. The consumption of non-egg and dairy animal products increases in across all continents, although only slightly in Africa. The consumption of cereals decreases slightly in Asia and Europe, but increases slightly elsewhere, with the strongest increase in Africa. The demand for oil crops sees similarly proportional increases in every continent, with Europe and Oceania consuming more.

COMPARISON WITH FALAFEL

The globally summed land-use output of the C-LLAMA anchor scenario can be compared with the land-use trajectory of an analogous business as usual scenario produced in FALAFEL. In the same way as C-LLAMA, the FALAFEL model allows prescribed increases in efficiency – for example a forced reduction in animal product consumption. To produce the business as usual scenario in FALAFEL, linear

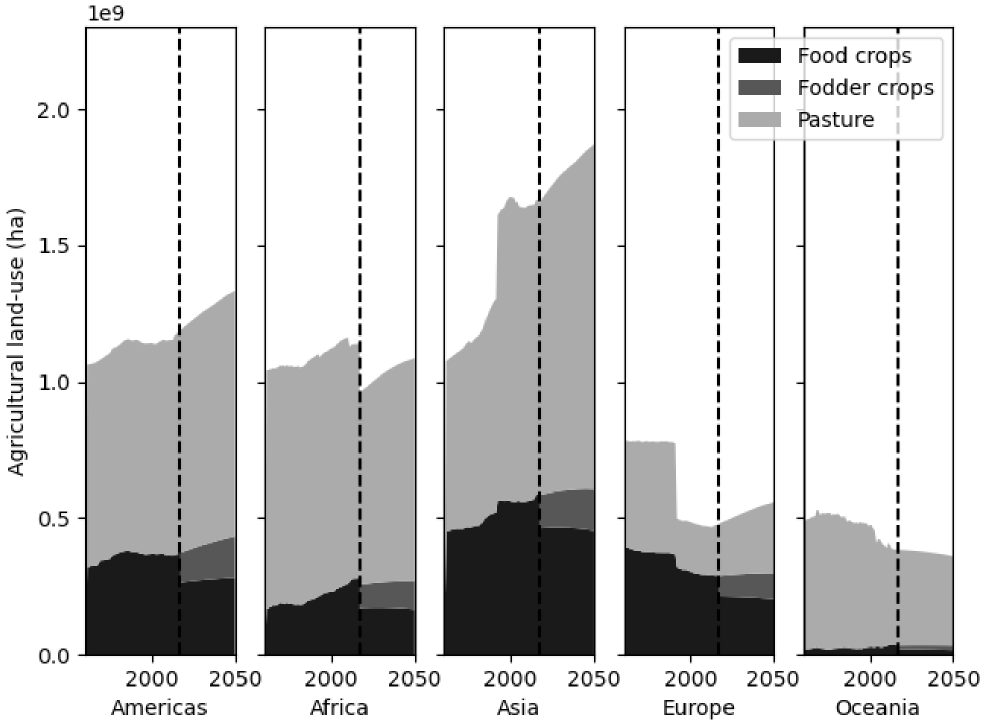

Figure 2.2: Agricultural land-use in FAOSTAT historical data and C-LLAMA anchor scenario projection for five continental regions. The transition from historical to modelled data is denoted by the dotted black line. Discontinuity at the dotted line is due to the countries not included in C-LLAMA for various reasons described in section 3. 99.7% of this discrepancy is the result of unavailable food balance data for Libya, Somalia, Sudan, the DRC, and Papua New Guinea. Also note the sudden increase of land-use in Asia and corresponding decrease in Europe in the early nineties, the result of the dissolution of the Soviet Union. As the FAOSTAT land-use does not contain disaggregated crop-data for fodder and food, food crops also include fodder crops in the historical data.

projections are made where they are available and all prescribed efficiency changes are turned off. For comparison, the land-use data from both models is grouped into pasture, food crops (for human consumption), and fodder crops. The resulting land-use for both modelled scenarios is shown in Figure 2.4. The trajectory of both the FALAFEL scenario and the C-LLAMA anchor scenario reach just over 5 Gha by around 2050, with C-LLAMA reaching approximately 5.2 Gha, an increase of approximately 450 Mha. The difference in starting food crop area is slightly higher in C-LLAMA, and a small amount of additional growth occurs by 2050 in C-LLAMA. C-LLAMA starts with a lesser area of fodder crops but sees less proportional growth by 2050 than in

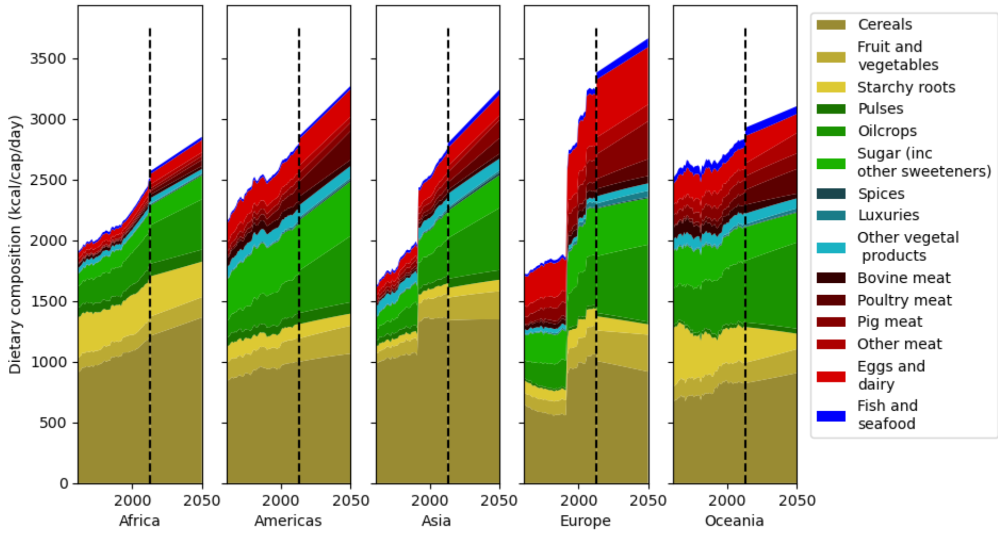

Figure 2.3: Calorific mean diet composition at the continent level in historical FAOSTAT data and the C-LLAMA anchor scenario. Some food commodities are grouped for clarity and the order of appearance from the origin for the groups aligns with the legend.

FALAFEL. Both models see an increase of approximately 90 Mha in total cropland by 2050. The largest difference lies in pasture, with C-LLAMA starting at just over 3 Gha and FALAFEL starting at around 2.6 Gha. Both models have a very similar pasture area in 2050 around 3.4 Gha. The method used to estimate pasture area in FALAFEL is completely different to that of C-LLAMA, using estimates of land-productivity and energy uptake by livestock, rather than calculating an empirical pasture-yield.

2.4.2 SENSITIVITY

Four key projections are made throughout the course of the model for each country. Diet and crop yields are projected directly from the historical data, whereas the food system efficiency parameter and effective pasture yield are internal values calculated from historical data, which are then projected. To explore the sensitivity of the final land-use output of C-LLAMA to these four projections, each was fixed at the mean value of their most recent five years and the land-use by 2050 compared with the anchor scenario. The results of this are shown in Figure 2.5.

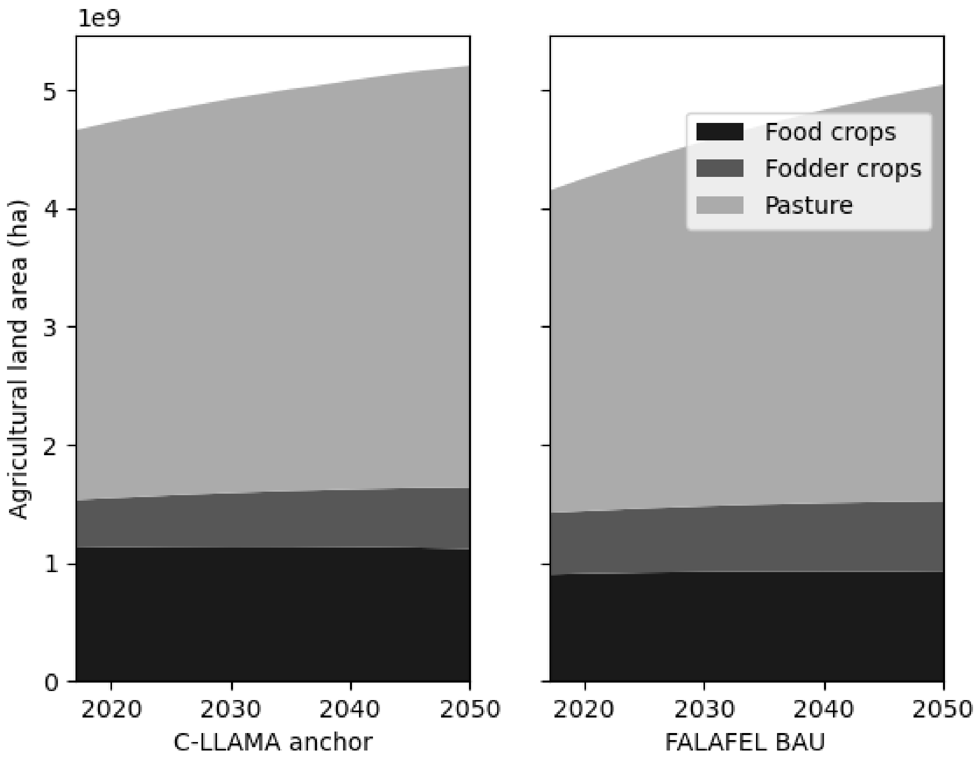

Figure 2.4: Aggregated global land-use for food production in the C-LLAMA anchor scenario and a 'business as usual' (BAU) FALAFEL scenario. FALAFEL accounts for the production of some non-food crops, however they are excluded for this comparative figure.

The impacts of each of these projections are within an order of magnitude of each other. Halting the projection of crop yields results in an increased agricultural land-use of approximately 300 Mha from the anchor scenario. This is consistent with the current trend of increasing crop yields in most areas of the world: a result of improving access to irrigation, agrochemicals and machinery (Ray *et al.*, 2012; Iizumi *et al.*, 2017). Suspending the projection of the food system efficiency parameter has the greatest impact on the total land-use with an increase of approximately 500 Mha. Suspending the food system efficiency parameter locks many countries in a state of lower efficiency, unable to meet the increasing food demand from the growing population. Halting changes in pasture yield leads to an increase in land-use of around 450 Mha. While the 'effective pasture yield' is not a real-world quantity, it aims to capture a wide range of factors that govern the output of grazed land. This quantity

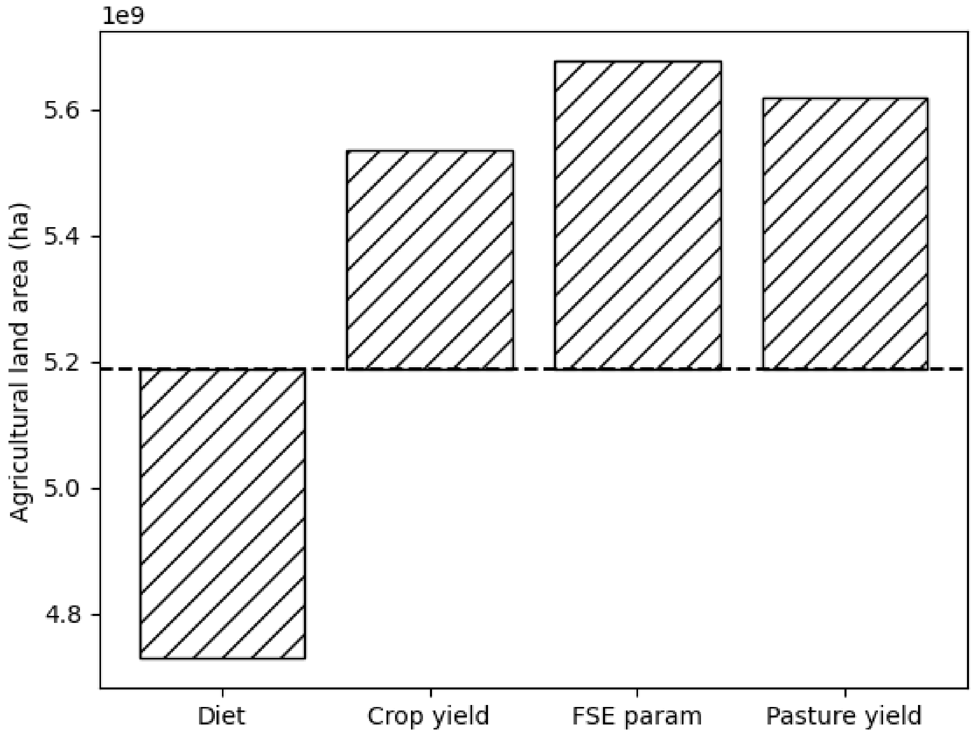

Figure 2.5: Difference in 2050 global agricultural land-use between the anchor scenario (dotted line) and when disallowing the progression of projections in the model by using the 5 year mean of historical values for each.

is increasing in the majority of countries, the result of livestock intensification by transfer to more intensive pasture or a covered system (Davis & D'Odorico, 2015; Thornton, 2010). Stopping the projection of dietary trends reduces the final land-use by approximately 450 Mha. Current global dietary trends are toward increased animal product consumption in developing countries and stagnation of animal product consumption in developed nations (Tilman & Clark, 2014; Van Zanten *et al.*, 2018). This combined with an increase in total calorie intake in the majority of countries explains the decrease in land-use when suspending the projection of diet.

Loss factors in C-LLAMA are dynamic, governed by the food system efficiency parameter. To explore the sensitivity of the model to loss factors every country was fixed at the lower and upper boundary values, equivalent to scoring every country at 0.0 or 1.0 respectively on the food system efficiency parameter. Figure 2.6 shows the

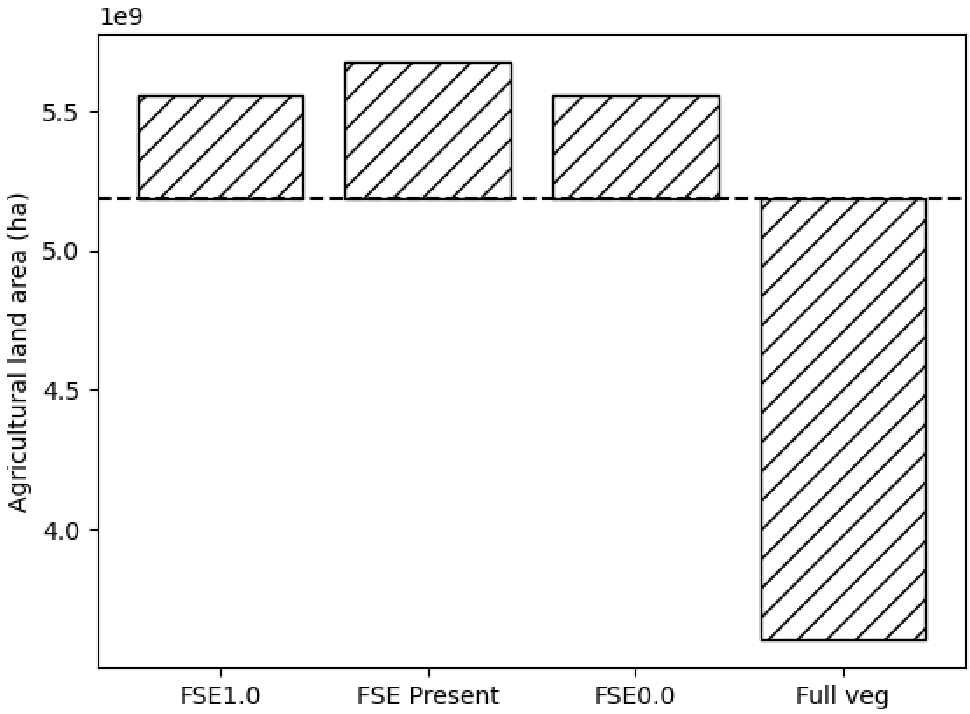

Figure 2.6: Change in 2050 agricultural land-use between the anchor scenario (dotted line), maximum, present, minimum efficiency, and full-vegetarian diet scenarios. Maximum and minimum efficiency scenarios are produced by setting the food system efficiency parameter to 1.0 and 0.0 respectively for all countries. The full-vegetarian diet scenario tends toward a 100% plant-based diet globally by the year 2050.

results of this analysis, along with a fully vegetarian (by 2050) diet scenario. Scores of 1.0 leads to a land-use increase of approximately 700 Mha by 2050, and a global score of 0.0 leads to an almost identical increase of just over 700 Mha by 2050. Scores of 1.0 and 0.0 both precipitate very high loss ratios from the start of the model of around 30% in post-production and production respectively. The present efficiency scenario is achieved by setting the food system efficiency parameter at its present values, identical to the 'FSE param' scenario in Figure 2.5. The fully vegetarian diet scenario sees a drastic land-use decrease of approximately 1.8 Gha by the year 2050, which is consistent with the previously discussed effective land-use inefficiency of animal products as food when compared to vegetal products.

2.5 DISCUSSION

Estimates of historical agricultural land cover, cropland harvests, and land-use change are plentiful (Erb *et al.*, 2017). There are a wide range of approaches from book-keeping to satellite imaging, the majority of which are available at high spatial resolutions (Fritz *et al.*, 2015; Winkler *et al.*, 2021; Hurtt *et al.*, 2011). These datasets are used as starting points for other modelling approaches such as IAMs or vegetation models but cannot be used to directly make projections of land-use. From these starting points, a great number of model and scenario drivers impact the land-use trajectories of IAMs, including economy, energy demand, commodity pricing and policy. IAMs are excellent tools for making holistic projections about a wide range of factors in given scenarios, but the land-use component is difficult to extract. The purpose of C-LLAMA is to explore the sensitivity of agricultural land-use to various drivers within the food system, not to make explicit predictions about land-use within specific countries.

The C-LLAMA anchor scenario projects cropland and pasture land-uses of approximately 1.64 Gha and 3.57 Gha respectively by 2050. The projected cropland value is within the range of projected values from IAM scenarios in the comparable SSP2 and broader AR5 databases, shown in Table 2, and well within estimates of cropland availability (Eitelberg *et al.*, 2015). However, the projected pasture value is slightly outside the range of other SSP2 scenarios, albeit only 70 Mha greater than the marker scenario. The majority of agricultural land expansion in SSP2 scenarios occurs in Africa and Latin America (Popp *et al.*, 2017). In C-LLAMA there are pasture expansions in these regions, along with expansion occurring in North America and Asia, due to the very limited trade mechanics of C-LLAMA. Note that the scenarios in these databases are based around key assumptions and pathways in the social and economic sectors, whereas the only prescribed trajectory within C-LLAMA is of population. As previously discussed, the intention of C-LLAMA is not to predict land-use futures, so this behaviour in these regions does not diminish the efficacy of the model as a means to explore sensitivities to drivers.

A fully vegetarian scenario in C-LLAMA sees a significant decrease in agricultural land-use of 1.8 Gha (a reduction of approximately 34%), in-line with the literature (Röös *et al.*, 2017; Swain *et al.*, 2018; Weindl *et al.*, 2017; Van Zanten *et al.*, 2018). The nutritional implications of such a diet were not considered in this scenario; which is likely to be a significant hurdle in the transition to sustainable diets (Duro *et al.*, 2020; Willett *et al.*, 2019). With the ability to prescribe trajectories for diet at a country level, C-LLAMA is well placed to explore such questions. Nutritional information could also be built into C-LLAMA for each commodity.

The strength of C-LLAMA lies in its simplicity: it can be easily modified, adapted, and improved. However, there are limitations to the approach and two key areas for improvement have been identified. One area with scope for improvement is in the allocation of crop and livestock production described in section 4.3. The current method uses a snapshot of current production to distribute the projected production of a crop; this approach works for earlier projected years since interannual changes to trade are relatively slow, being on similar timescales to changes in demand. However, long term changes to global trade are not captured, specifically those likely to arise from improved access to wealth and subsequent demand for luxury and animal products in developing countries. Improvements might include trade matrices for each food commodity, or a forward projection of the commodity production allocation, which would allow semi-dynamic trade representation without the need for any agent based or economically driven modelling. The other area with great potential for improvement is the representation of livestock and, more broadly, land-use within the model. The current method for estimating land-use for crops and livestock is effective for exploring questions surrounding global-scale changes and scenario options. However, a land class system with productivity, land-use transitions, and associated carbon exchange would facilitate a more nuanced exploration of the drivers of land-use and their consequences, particularly in the case of livestock, forests, and grasslands.

Including the DRC, Libya, Sudan, Somalia, and Papua New Guinea would be beneficial as together they account for a significant portion of the global land area (approximately 3%). Papua New Guinea and the DRC have humid, equatorial climates with highly productive land; excellent conditions for agricultural productivity (Kottek *et al.*, 2006). While not included in the food balance data, they are present in other FAO data, so it may be possible to construct an approximate food balance dataset from their available FAO data and regional averages. Another approach would be to construct food balances using other data sources, however this approach would contravene the internal consistency of C-LLAMA.

C-LLAMA takes a simple approach to modelling the drivers of land availability, offering transparency and adaptability where more complex modelling approaches do not. Of the many drivers of future land-availability, the simplicity and traceability of the model make it well placed to explore the impacts of broad scale drivers such as changes in livestock production systems, crop yields, dietary trends and food system efficiency on the future of land available for food agriculture, bioenergy and afforestation from a bottom-up perspective. For example, scenarios with prescribed increases to crop yields, consumption of specific commodities, calorie intake, or wasted food could be constructed. The structure of C-LLAMA also facilitates that these changes can be applied at regional or country levels. The model aims to be easily accessible to use and modify, using only open source data and software.

3

MODELLING THE IMPACTS OF DIET ON LAND AVAILABILITY

ABSTRACT

In this chapter the land-use implications of transitioning to both the EAT-Lancet planetary health diet and a fully plant-based diet are explored in C-LLAMA. Transitioning from business as usual diet projections to the EAT-Lancet planetary health diet leads to an increase in global agricultural land use of approximately 160 Mha by the year 2050, with land used to support animal production (pasture and fodder crops) decreasing by 670 Mha, and food crop area increasing by 830 Mha. The increased overall food supply in developing regions and transition to more nutritious vegetal products in the EAT-Lancet planetary health diet scenario offsets the land-use efficiency improvements made through reducing animal product consumption. When prescribing dietary changes regionally, regions with larger populations typically see greater agricultural land use sensitivity to diet. A fully

plant-based diet when prescribed globally leads to a complete reduction to 0 Mha of all fodder crop and pasture areas, and only a small increase in food crop area of approximately 100 Mha.

3.1 INTRODUCTION

The growth of populations, changes in total food supply, and dietary composition are the first in a series of driving forces behind the global food system and ultimately land-use for agriculture, outlined in Chapter 1 (Bahar *et al.*, 2020). The UN medium population scenario is constructed using the median trajectory of a set of several thousand projections for each country (KC & Lutz, 2017) and is used in the SSP2 and C-LLAMA anchor scenarios (Fricko *et al.* (2017), Chapter 2 Section 2.3), the total global population is projected to increase at a steady rate until 2050, at which point the rate of increase slows down, eventually stagnating around 2100 (see Figure 1.2). Increases in population mean there are more people to feed, inevitably leading to increases in food demand and hence land-use for agriculture. However, this relationship is not directly proportional, instead being heavily influenced by the quantity and composition of food consumed by the population. In the SSP2 marker scenario, overall calorie intake increases by 11% and 22% in the global North and South respectively, and animal product consumption increases by 20% globally (from 15% to 18% of all calories consumed) (Fricko *et al.*, 2017).

The trajectories of population growth around the world are fairly immutable in the context of climate change mitigation, so options for reducing the land required for food production are limited to changes in diet, food waste and losses, or productivity (crop and pasture yields). The focus of this chapter will be on diet, while later chapters will explore waste and productivity. There are two avenues through which diets can be changed to reduce land-use. The simplest is to reduce the quantity of food consumed; in many developed countries the average calorific intake is increasingly higher than necessary for a healthy diet (over-consumption), sometimes so high as to be detrimental to health (Cicatiello & Franco, 2018; Temme *et al.*, 2020; Bodirsky *et al.*, 2020). Indeed, over-consumption may be as significant a contributor to food-system inefficiency as post-production food waste (Alexander *et al.*, 2017). However, over-consumption is difficult to quantify as food supply estimates such as FAOSTAT food balances usually also include food that is wasted in the household (Schmidt & Matthies, 2018; FAO, 2021a). Additionally, under-nutrition and malnutrition remain prevalent in many regions of the world: over 2 billion people experienced food insecurity in 2019, which should be addressed as a priority in line with sustainable development goal 2 (end hunger, achieve food security and improved nutrition, and promote sustainable agriculture) (UN Department of Economic and Social Affairs, 2021). The second option to reduce the land-use impact through diets is to alter their composition.

With the goal of reducing the broader environmental impact of diets, the literature points overwhelmingly in the direction of reduced animal product consumption, in-part due to the considerable greenhouse gas emissions and water usage of livestock systems but also their high land footprints when compared with vegetal products (Swain *et al.*, 2018; Poore & Nemecek, 2018; Weindl *et al.*, 2017; Clark & Tilman, 2017). Ruminant meat (primarily bovine meat, and sheep and goats) is by far the greatest contributor to land-use for agriculture, with median land-use impacts an order of magnitude higher than that of pig meat and even more so than almost all vegetal products (Clark & Tilman, 2017; Poore & Nemecek, 2018). Eshel *et al.* (2016) assess the impact of replacing beef in the North American diet with entirely plant-based alternatives. Rather than modelling the land-use of the population this study assessed the land footprint 'per capita' of these diets, finding that in a suite of 1500 beef-replacement diets, on-average the replacement diet required only 10% the land of it's beef-consuming counterpart. There are also significant variations in the land-footprints of vegetal products, with cereals and starchy roots typically requiring less land to produce (per calorie) than pulses, vegetables, and fruits (Poore & Nemecek, 2018; Ramankutty *et al.*, 2018).

To remain consistent with the principles of the sustainable development goals, specifically sustainable development goal 2: which is to 'end hunger, achieve food security and improved nutrition and promote sustainable agriculture' (United Nations, 2019a), dietary targets should have both a sufficient calorie content and nutritional content as to be 'healthy'. Sustainable diets often have very limited animal product content, especially in the case of ruminant meat and dairy products (Hemler & Hu, 2019; Willett *et al.*, 2019; Steenson & Buttriss, 2020). Animal products contribute significant quantities of fats and protein to macro-nutrient intake in the diet, in addition to micro-nutrients such as iron, zinc, calcium, and iodine, so they must be replaced with vegetal products containing sufficient amounts of these nutrients (Steenson & Buttriss, 2020; Sha & Xiong, 2020). While most vegetal products contain a wide range of nutrients, legumes and vegetables are typically higher in nutrient content than cereals and starchy roots, which contain mostly carbohydrates (Liew, 2020). While it would certainly be possible to achieve an incredibly high land-use per calorie efficiency with diets comprised of only sugar products or cereals, such diets would not be suitable for sustained human consumption.

In this chapter, C-LLAMA is used to explore the land-use implications of prescribing a fully vegan diet globally, and the impacts of applying a diet, consistent with both planetary and human health goals, globally and at a regional level.

3.2 Method

3.2.1 The EAT-Lancet planetary health diet

The content of a healthy diet is subject to a number of factors individual to the consumer, including lifestyle and metabolism. For example, individuals who are more physically active will require a greater energy intake (Laquale, 2009). For a typical human, the same general guidelines for a healthy diet can be applied, although factors such as pregnancy or infancy may change these (World Health Organization, 2019). The EAT-Lancet commission present a 'planetary health diet' reference diet, the purpose of which is to operate within a safe space for both human health and planetary boundaries: it could theoretically be sustainable for every member of the population to consume this diet (Willett *et al.*, 2019). Table 3.1 shows the composition of the EAT-Lancet planetary health diet (EL diet). The presented diet is based on a total calorie intake of approximately 2500 kcal per day, however as the intake is adjusted to account for lifestyle and metabolism the energy contribution from each food should remain the same. This diet permits the continued consumption of animal products, albeit at a severely reduced rate for many regions of the world such as North and South America, Europe, Southern Africa, and Oceania. A reduction in animal product consumption is a significant social hurdle to overcome in the transition to sustainable food consumption (Culliford & Bradbury, 2020). This is especially true in middle-income countries such as India and China, where increasing wealth has increased demand for these products (He *et al.*, 2018): the global production of poultry and ruminant products has increased by factors of nearly 5 and 1.5 respectively since 1960 (Godfray *et al.*, 2018, 2010).

The EAT-Lancet planetary health diet is an excellent candidate for an idealised target diet to strive for: it is generally applicable since it allows for flexibility within constituent food groups (Willett *et al.*, 2019). To make the transition to the EL diet, the usual projection (see Section 2.4.1) is used until 2021, at which point a linear transition to the diet by 2050 occurs. The EL diet is expressed in terms of food groups rather than specific commodities, allowing for some variation in the makeup of each group. There are a number of steps needed to prescribe the EL diet in C-LLAMA. First, commodities as grouped in C-LLAMA are aggregated to align with the groups in the EAT-Lancet diet. For example, all cereals are aggregated (in addition to the 'other cereals' commodity) and grouped into 'whole grains'. A list of these aggregations can be found in Table 3.2. Secondly, the proportion of commodities within the aggregated

Food group	Constituent products	Macronutrient intake (g/day)	Calorie intake (kcal/day)
Whole grains	*Cereals*	232	811
Tubers and starchy roots	*Potatoes, cassava etc*	50	39
Vegetables	*Vegetables*	300	80
Fruits	*Fruits*	200	126
Dairy foods	*Milk and equivalents*	250	153
Protein sources	*Beef and lamb*	7	15
	Pork	7	15
	Poultry	29	62
	Eggs	13	19
	Fish	28	40
	Legumes	100	426
	Tree nuts	25	149
Added fats	*Oils and equivalents*	52	450
Added sugars	*Sugar and other sweeteners*	31	120

Table 3.1: The EAT-Lancet planetary health diet, based on a daily calorie intake of 2500 kcal, adapted from (Willett *et al.*, 2019). Presented macronutrient values are the modal of a range. Vegetable calories can vary dependant on the type of vegetables consumed. Pork and red (beef and lamb) meat calories are also interchangeable.

group are projected as normal (see Section 2.3.1): the makeup of the group is allowed to change over time. For example, if a country has an increasing contribution to diet from wheat more so than other cereals, the contribution from wheat to the whole-grains EAT-Lancet group will increase toward 2050.

There are some assumptions being made here; commodities in C-LLAMA also includes derivative products. For example, the wheat commodity includes raw wheat but also includes wheat flour and further derivatives such as breads. The included derivative products in these categories are adjusted to reflect the calorie contribution from the commodity (FAO, 2021a). Therefore, wheat as presented is actually an effective 'wheat-equivalent' value, so this should have no impact on the related agricultural land-use since it will propagate through the model as wheat (when relating to yield and production). This also presents a slight inaccuracy in the transition to the EAT-Lancet diet from the C-LLAMA projection, since cereals are commonly refined, altering their nutrient content (Bazzano *et al.*, 2005). Meaning

EAT-Lancet group	C-LLAMA commodities
Whole grains	wheat, rice, maize, other cereals
Tubers and starchy roots	potatoes, cassava, other starchy roots
Vegetables	vegetables
Fruits	fruit (excluding wine)
Dairy foods	dairy
Beef, lamb and pork	bovine meat, mutton and goat meat, pigmeat, other meat
Poultry	poultry meat
Eggs	eggs
Fish	fish, seafood
Legumes	pulses, soyabeans
Tree nuts	nuts, seeds
Added fats	palm oil, oilcrops, vegetable oils
Added sugars	sugar, other sweeteners

Table 3.2: C-LLAMA food commodities as they are grouped into the EAT-Lancet planetary health diet food groups. A detailed discussion of the C-LLAMA food groups and commodities can be ground in chapter 2. Beef, lamb and pork are all grouped together since their energy contributions to the EAT-Lancet diet are interchangeable.

that their nutrient content may not be the same as if the group was comprised entirely of true whole grains, although the calorie content will be the same.

The third step in implementing the EL diet into C-LLAMA is to consider post-production waste. The EAT-Lancet diet is not equivalent to food supply: the food supply projected as part of C-LLAMA also includes post-production waste; that is food wasted either in the household or by commerce and retail (see Section 2.3.1. To avoid inadvertently also prescribing a drastic reduction in post-production waste, the EAT-Lancet diet must be adjusted to account for this. This was done by estimating the portion of food wasted in this way in the country using the food-system efficiency metric, detailed in Section 2.3.2. This waste estimate is then used to scale the EL diet to include post-production waste. The relative proportion of each food group remains the same during this process. The post-production waste estimate is permitted to change with time (as it does in C-LLAMA), so if a country sees an increase in post-production waste by 2050 this will be reflected in the calories required to meet the dietary target.

The calories C in year n, between 2021 and 2050, contributed to the diet by EAT-

Lancet diet food group g, before post-production waste is accounted for, are

$$C_g(n) = C_g(2021) + \frac{n-2021}{2050-2021}(g_{\text{target}} - C_g(2021)), \quad (3.1)$$

where g_{target} are the calories contributed to the EAT-Lancet planetary health diet by group g. $C_g(2021)$ is the sum of calories contributed to group g by component food commodities i (detailed in Table 3.2) in 2021. $C_g(2021)$ is derived from FAOSTAT food supply data f as opposed to diet data; the food supply value is reduced using the estimated post-production waste μ_{post}, calculated using the food-system efficiency parameter, described in Section 2.3.2. $C_g(2021)$ is thus

$$C_g(2021) = (1 - \mu_{\text{post}}(2021)) \sum_{i \epsilon g} f_i(2021) \quad (3.2)$$

where f_i is the contribution to the total food supply from food commodity i and $\mu_{post}(2021)$ is the estimated post-production waste in 2021. The estimated post-production waste trajectory is then used again to translate the diet trajectory back into food supply trajectory:

$$F_g(n) = C_g(n) \frac{1}{\mu_{\text{post}}(n)} \quad (3.3)$$

where $F_g(n)$ is the supply (including post-production waste) of food group g in year n. The total food supply $F(n)$ is then the sum over all groups of $F_g(n)$.

REGIONAL TRAJECTORIES

The EL diet applied within C-LLAMA produces food supply trajectories for each country, aggregated into regional means (weighted by population) in Figures 3.1 to 3.4. Note that in these figures commodities have been grouped for visual clarity. Figure 3.1 shows the prescribed food supply trajectory for regions in the Americas. Northern America (the USA and Canada) see reductions in sugar products and animal

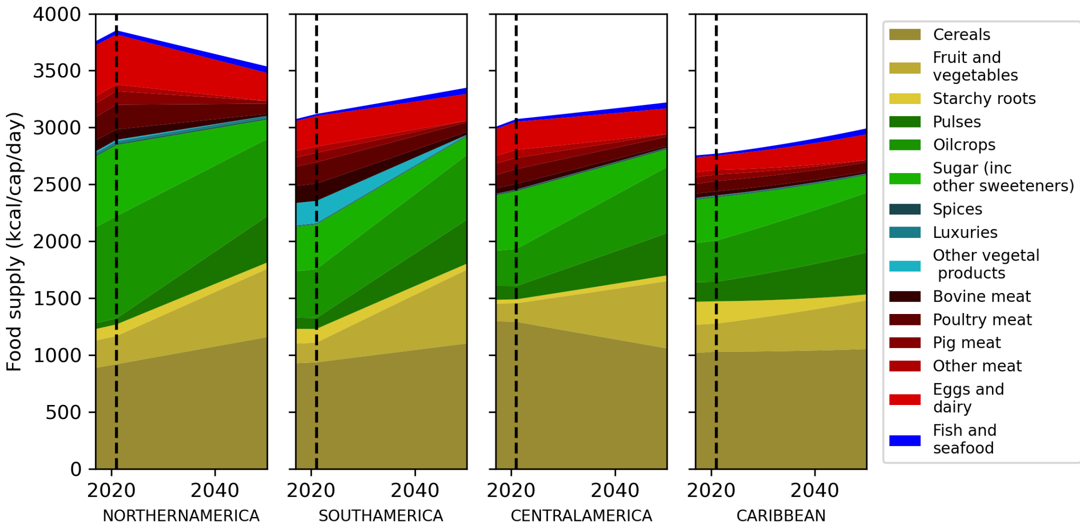

Figure 3.1: Prescribed food supply trajectories for regions in the Americas (weighted by population).

product consumption by approximately half, increases in cereals and fruit, and an increase by a factor of 4 in the consumption of pulses. The 2050 total food supply in this region is approximately 3500 kcal/capita/day in the EL diet scenario, a significant reduction from approximately 4200 kcal/capita/day in the C-LLAMA anchor scenario. Both these countries score 1.0 on the food-system efficiency metric scale, so the decrease in total food supply is indicative of initial over-consumption. Central and South America follow similar trends in composition to that of North America, but undergo an overall increase in total food supply. A handful of countries in these regions have less than 2500 kcal total food supply in 2017 (Haiti, Guatemala, Ecuador, Bolivia, Antigua, and Grenada, populations accounting for approximately 25%, 25%, and 6% of the Caribbean, and Central and South America respectively), contributing to the increasing regional food supply alongside post-production waste. Central America sees a decrease in cereal consumption and the Caribbean doesn't undergo much change in overall animal product consumption, contrary the other regions in the Americas.

All African regions see an increase in fruit, vegetables, and pulses consumption, shown in Figure 3.2. There are also dramatic reductions in the consumption of starchy

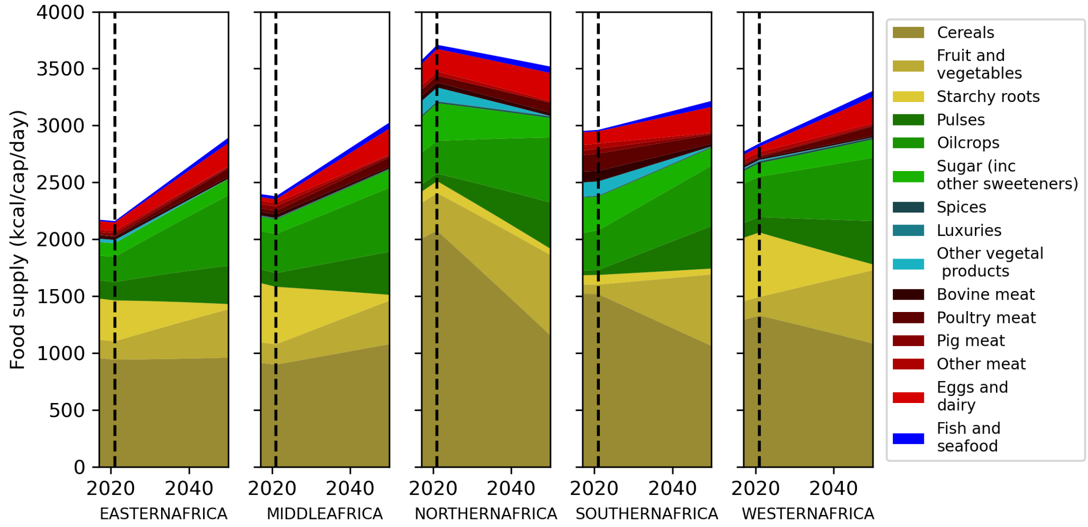

Figure 3.2: Prescribed food supply trajectories for regions in Africa (weighted by population).

roots and cereals in many of these regions. These groups are dominated by cassava, sorghum, and maize: staple crops in large areas of the continent (Belton & Taylor, 2004; Nweke *et al.*, 2002). All but Northern Africa undergo an increase in total supply; a combination of development, increases in post-production waste, and initial under-nutrition in some regions. Animal product consumption is initially low in all African regions and dominated by eggs and dairy when compared with other continents. All regions but Southern Africa see a small increase in total animal product consumption, with the majority of this increase coming from eggs and dairy products.

Similar to the trends in the Americas, all regions in Europe see increases in fruit, vegetables and pulses consumption, and a decrease in animal products and sugar consumption (Figure 3.3). Northern Europe undergoes a slight increase in total supply; Lithuania, Estonia, and Latvia score slightly less than 1.0 on the food-system efficiency metric at the start of the trajectory. Australia and New Zealand follow a very similar trajectory to regions in Europe and the Americas; reduced animal product consumption and increased fruit, vegetables, and pulses (Figure 3.4). Polynesia also follows a similar trend, but has a slight increase in total food supply whereas Australia and New Zealand do not.

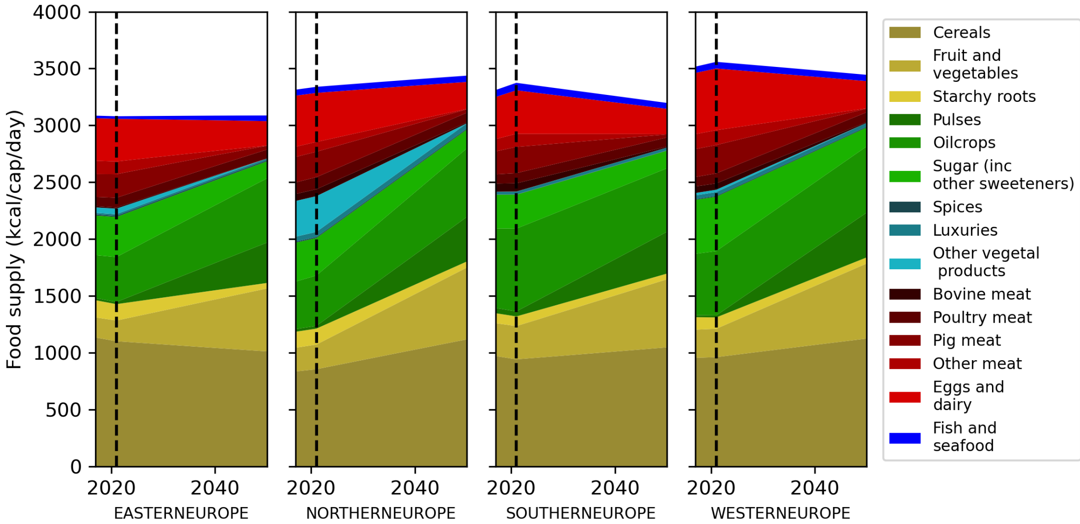

Figure 3.3: Prescribed food supply trajectories for regions in Europe (weighted by population).

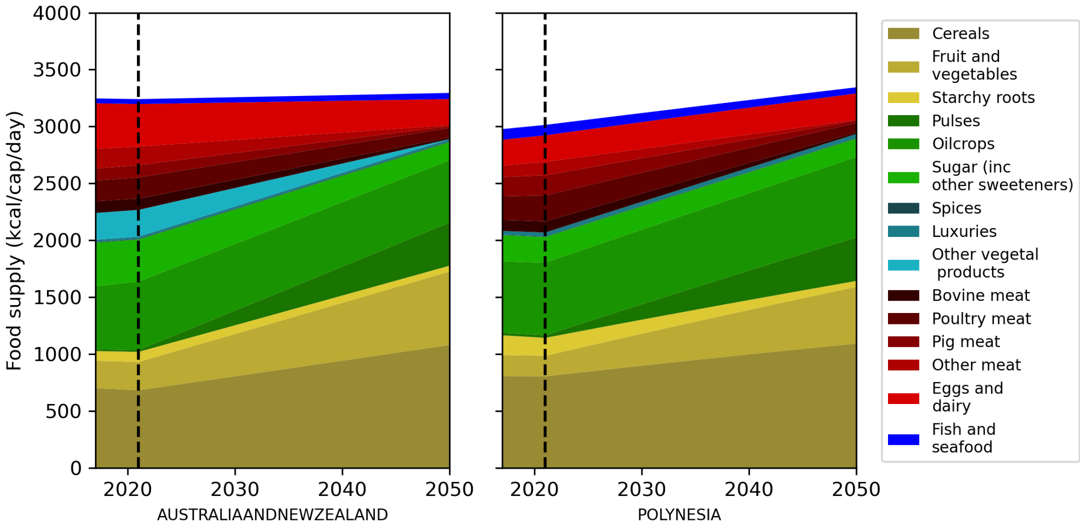

Figure 3.4: Prescribed food supply trajectories for regions in Oceania (weighted by population). Melanesia is excluded since none of it's constituent countries are present in C-LLAMA processes (the largest of which is Papua New Guinea, excluded for reasons detailed in chapter 2, accounting for more than half the population of the region at approximately 8 million people).

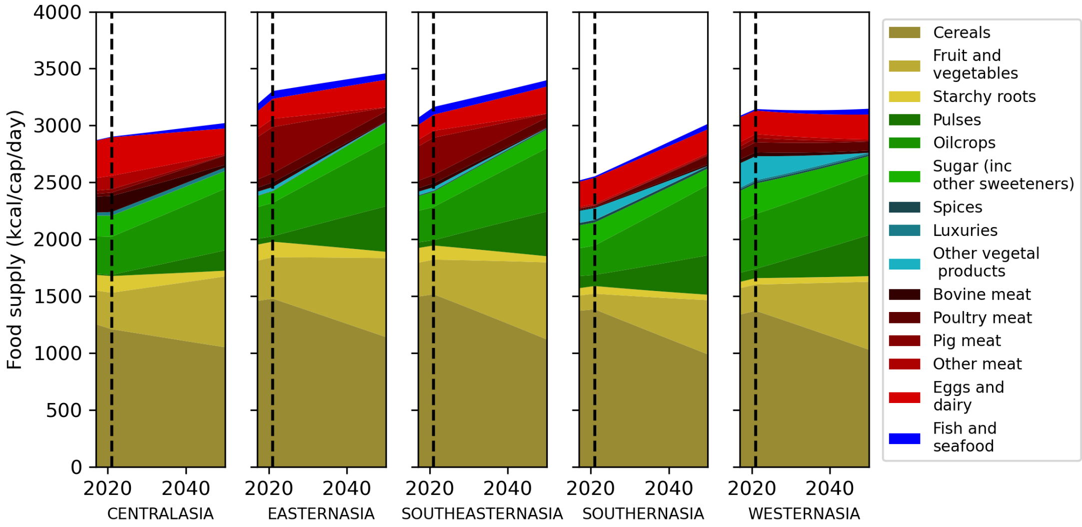

Figure 3.5: Prescribed food supply trajectories for regions in Asia (weighted by population).

The general trend in vegetal products is the same across the Asian continent (Figure 3.5), there is a consistent decrease in cereal consumption and an increase in fruit, vegetables, and pulses consumption. South-Eastern (including Brunei, Cambodia, Indonesia, Lao, Malasia, Myanmar, Phillipines, Sinapore, Thailand, Timor-leste, and Vietnam) and Eastern Asia (including China, North and South Korea, Mongolia, and Japan) both have relatively high initial levels of pigmeat consumption, reducing by more than half by 2050. Other regions in Asia begin with very little pork consumption and see almost no increase by 2050; pork consumption in these regions is historically very low due to the dominant religious demographics of Islam and Hinduism (Babji & Ghassem, 2010; Ro'I & Wainer, 2009). Animal product consumption in Central, Western, and Southern Asia is dominated by eggs and dairy. The most significant initial beef consumption and also reduction by 2050 occurs in Central Asia.

3.2.2 PLANT-BASED DIET

A scenario in which a fully plant-based diet is adopted globally by 2050 was produced in C-LLAMA. This scenario was constructed by replacing all animal product calories with vegetal product calories, starting in 2021 and finishing at 100% vegetal product calories in 2050. The ratio of food commodities within the vegetal product remit were projected using the same ratio projections as in the C-LLAMA anchor scenario, such that the total portion of vegetal products in the diet increased, but the contributions from each commodity are the same as the anchor scenario. This allows the makeup of the plant commodities to vary between countries based on their historical consumption. This scenario is not equivalent to the vegetarian scenario described in chapter 2, which permitted the consumption of non-meat animal products and fish. The nutritional value of the diet was not considered in the production of this scenario. Unlike in the EAT-Lancet planetary health diet, grains and starchy roots would remain a significant contributor to the calorie intake in many developing regions. Protein in particular would be drastically underrepresented when animal products are removed from diets of many developing regions that typically have high quantities of grains and roots in their diets (Sharma *et al.*, 2020).

3.3 RESULTS AND DISCUSSION

3.3.1 THE EAT-LANCET PLANETARY HEALTH DIET

The impact on global land use of the regional application of the El diet is shown in Figure 3.7. Figure 3.6 shows the proportional change from the C-LLAMA anchor scenario in *global* land use for each agricultural land use category when prescribing a trajectory toward the EL diet to each region in turn (21 scenarios). Figure 3.7 shows the global quantity of land used for each category for the same set of scenarios. The sensitivity of land-use to changes in diet will inevitably be skewed in favour of the most populous regions. This is evident in the dramatic changes seen when applying the diet to Southern Asia and Eastern Asia (the two most populous regions in the world, containing India and China respectively), and the almost undetectable changes when applying the diet to regions with small populations such as Polynesia.

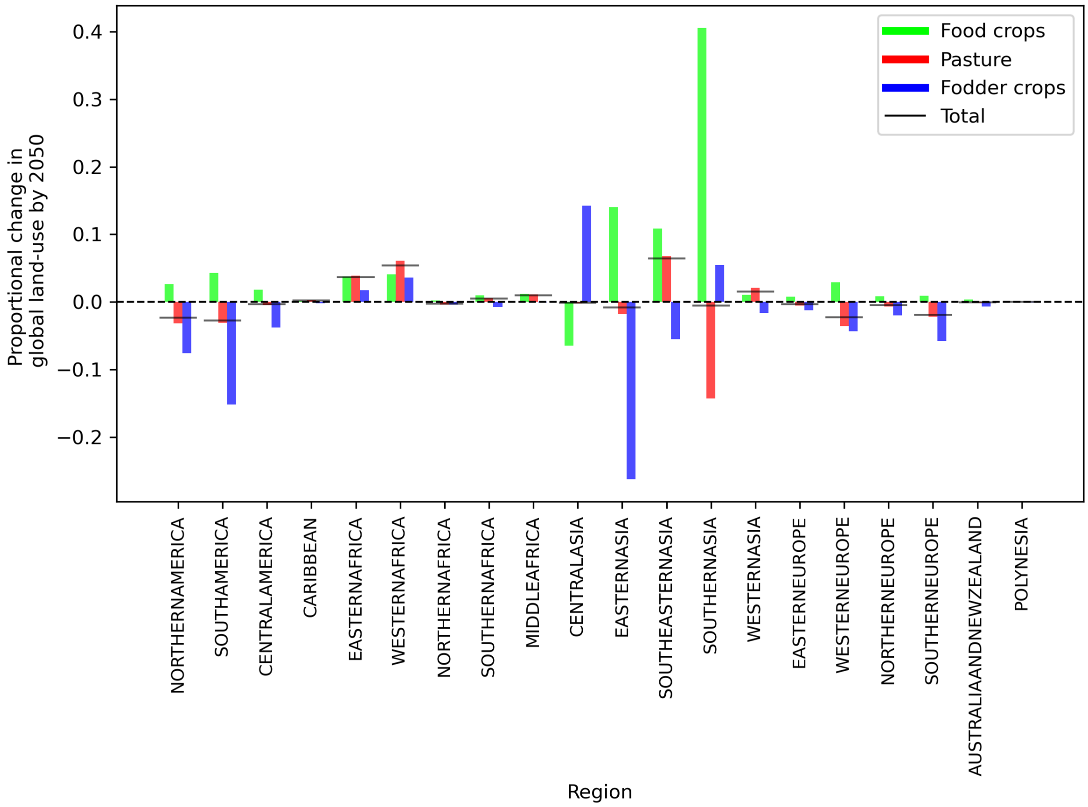

Figure 3.6: Proportional change from the C-LLAMA anchor scenario in global land-use in each category when prescribing a diet trajectory to the EAT-Lancet diet for the year 2050 to each of the 21 regions in C-LLAMA. Solid horizontal lines represent the change in total agricultural land use (the sum of the three categories.

There are 10%, 15% and 40% increases in global food crop area when applying the diet to South-East (including Brunei, Cambodia, Indonesia, Lao, Malasia, Myanmar, Phillipines, Sinapore, Thailand, Timor-leste, and Vietnam), East (including China, North and South Korea, Mongolia, and Japan), and Southern Asia (including Afghanistan, Bangladesh, Bhutan, India, Iran, Maldives, Nepal, Pakistan, and Sri Lanka) respectively. By far the most consumed vegetal product in each of these regions is rice, which is fairly high yielding when compared to fruits, vegetables, and pulses. The 2017 food supplies for Bangladesh, Sri Lanka, and India contained approximately 1700, 1000 and 800 kcal worth of rice respectively, almost 70% of the total food supply for Bangladesh. Pakistan (the second most populous country in Southern Asia) obtained approximately 40% of it’s food supply energy from wheat in the same year. China is the most populous nation in the world (in 2021) with

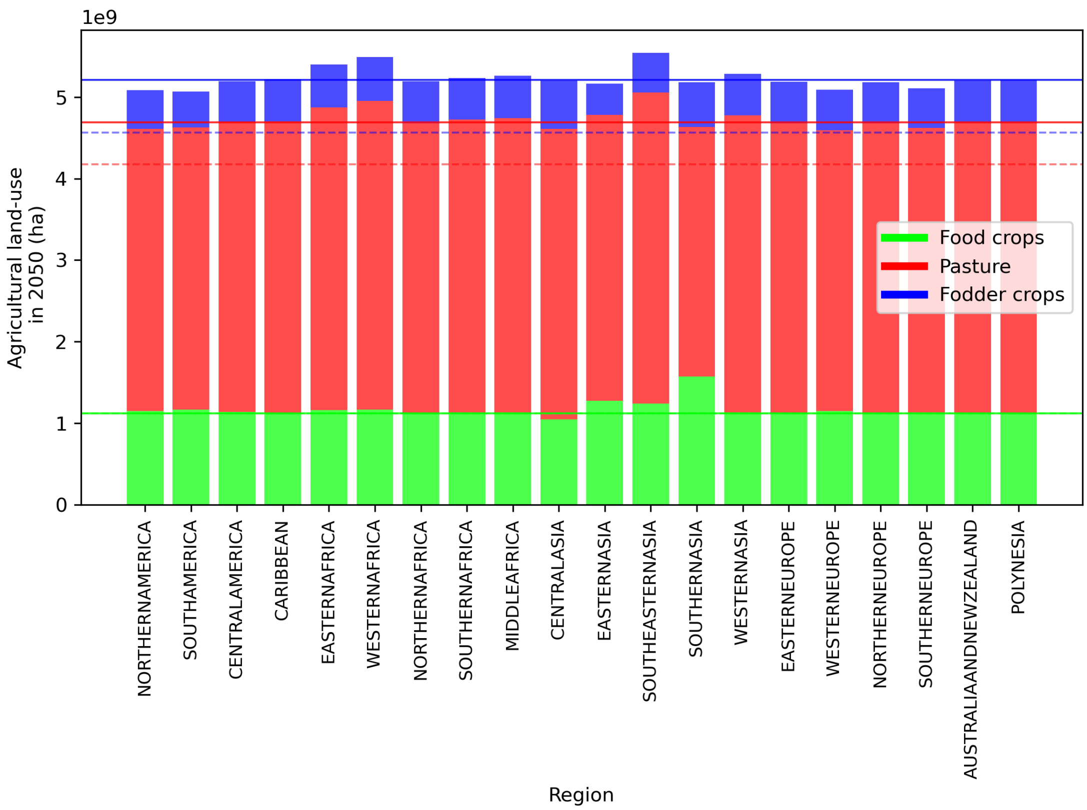

Figure 3.7: Global agricultural land used by each category in 2050 for the same 21 regional scenarios. The global land used by each category in 2050 and 2021 in the C-LLAMA anchor scenario are represented by solid lines and dashed lines respectively.

1.41 billion people, compared to India's 1.38 billion; it is surprising then that the impact of applying the EAT-Lancet diet to Eastern Asia (including China) is much less than in Southern Asia (including India), but less so when considering the projected growth in India's population, which (in the UN medium population scenario) is expected to overtake that of China around 2030 (KC & Lutz, 2017). China's food supply contained around 800 kcal of rice in 2017, a decline from the previous 20 years but comparable to that of India. However, the overall food supply in China has increased much more rapidly than in India in the past 60 years, overtaking India in the early 1980s (illustrated in Figure 3.8). For this reason China scores higher than India (with a greater rate of increase) on the food system efficiency parameter and hence undergoes less of an increase in food supply when the projected post-production food waste is applied to the projected food supply.

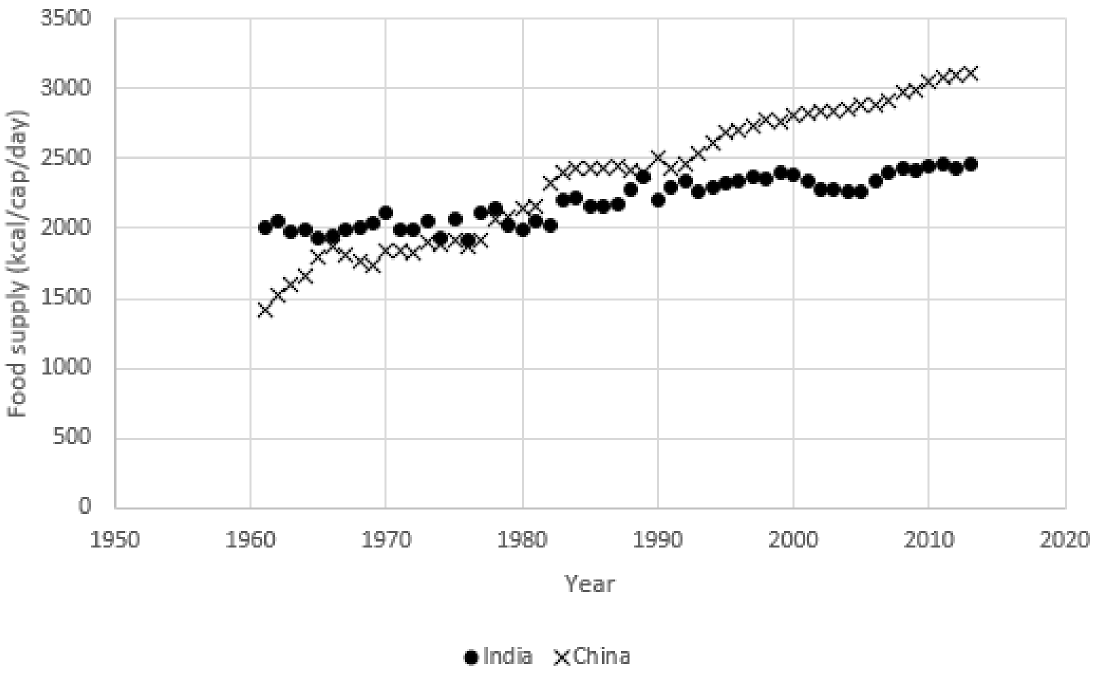

Figure 3.8: Historical total food supply in China and India for 1961 to 2013, produced using FAOSTAT food balance sheet data.

The change in vegetal products is a worthwhile one: rice and wheat (and other cereals) are low in nutrient content while being high in calorie content, unlike fruits and vegetables which typically have a high nutrient content. However, to provide these rapidly growing populations with a nutritionally sufficient diet will require a significant change in crop production in these regions away from rice and simple grains, and toward vegetables and legumes. This will almost certainly lead to an increase land use for food crops when compared with allowing current diet trends to continue, due to the lower yields of these non-starchy vegetal products (Sharma *et al.*, 2020).

The EAT-Lancet diet contains 30 kcal per day of beef, lamb, and pork. In this set of model runs, the diet was prescribed to all regions regardless of cultural backgrounds. Realistically however, such an increase in the consumption of these products is unlikely in Southern Asia without significant cultural change. Goats and poultry are important livestock in Southern Asia, especially in India; the reduction in pasture area and increase in fodder crops are likely due to a reduction in these products and a (potentially unlikely) increase in bovine and pig meat consumption in the EAT-Lancet diet. In this region, poultry rely heavily on feed. Additionally, cattle, oxen, and most importantly buffalo are commonly raised for dairy and labour rather than meat, being found in small herds in and around cities (Teufel *et al.*, 2010). Unlike Southern Asia, Eastern Asia and South-East Asia both have initially high levels of pork consumption and then a strong reduction by 2050. Pigs in these regions are typically raised in relatively intense conditions, and are given a high effective yield by the pasture land use calculation in C-LLAMA, leading to the large decreases in fodder crop land use (Liu *et al.*, 2021; Huynh *et al.*, 2007).

When prescribing the EAT-Lancet diet to Northern and Central America, food crop areas increased by less than 3% globally when compared to the anchor scenario in each case. When applying the diet to regions in Europe the increase in food crop area is similar, with Western Europe causing the greatest increase of approximately 3%. The opposite is true for pasture and fodder crop areas in these regions and in all cases the greatest proportional change is in fodder crop area. Note that in Figure 3.6 a 10% change in fodder crop area is not equivalent in land use change to a 10%. This is consistent with the initially high levels of animal product consumption and presence of over-consumption in these regions. The trends when prescribing the EAT-Lancet diet to South America are similar, but have a larger magnitude; since Southern America has a smaller population than both Europe and North America, the magnitude of the change is almost entirely due to the relatively greater reduction in bovine meat consumption, even as overall food supply is increasing. Applying the diet in Oceania has little impact on global land-use compared to the anchor, with only a very small decrease in fodder crop land area and imperceptible changes to other land-uses. Oceania is responsible for significant beef production at approximately 4% of the global total; it is also the second largest beef exporter, predominantly to Asia and Russia (Bell *et al.*, 2011; Kahn & Cottle, 2014).

A salient feature of Figure 3.6 is that the mean of the total proportional changes is greater than zero; implying that if the global population switched to this diet whilst simultaneously undergoing a net increase in post-production waste (as countries develop), the result would be a greater overall agricultural land-use in 2050 when compared with the anchor scenario. This is more clearly shown in Figure 3.9, which shows the mean proportional change compared to the anchor scenario when applying the diet to each region. There are significant deviations from the anchor scenario in food and fodder crop areas, and a smaller change in pasture area. However, this is not equivalent to applying the diet to every region at once, so to explore this result further an additional scenario was produced in which the EL diet was applied to all regions simultaneously. The globally aggregated results of this scenario are shown in Figure 3.10. In this scenario, the general trends implicated by the 21 individual regional scenarios still are present; food crop area in 2050 is greater than in the anchor scenario by approximately 830 Mha, fodder crop and pasture areas are less by approximately 270 and 400 Mha respectively. The total increase in agricultural land-use is approximately 160 Mha, about 3% more than in the anchor scenario.

In an EAT-Lancet planetary health diet scenario produced by the Lancet commission with no improvements to crop-yield or reductions in food waste and losses, transitioning to the EL diet lead to an approximately 60% increase in global crop-land area, which is comparable to the crop-land area change in the C-LLAMA EAT-Lancet scenario (The Eat-Lancet Commission, 2019). There is no reference to a pasture-area change in the EAT-Lancet scenario with which to compare the C-LLAMA pasture reduction. The C-LLAMA scenario also includes 'normal' projections of crop yield and food waste, leading to an overall food system efficiency increase.

The increased overall food supply in developing regions and transition to more nutritious vegetal products in the EL diet C-LLAMA scenario offsets the land-use efficiency improvements made through reducing animal product consumption. Africa undergoes the second greatest population growth but doesn't reach a per capita

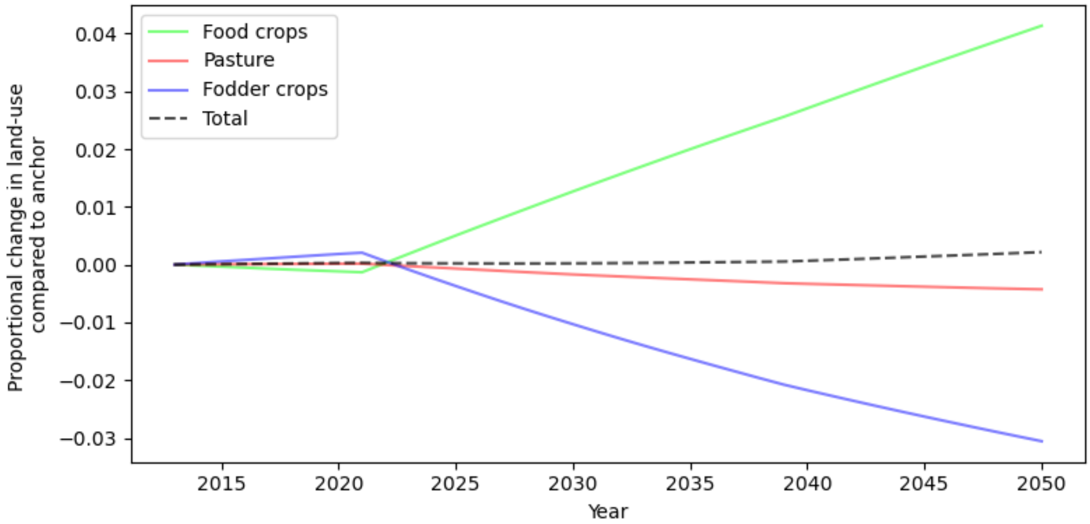

Figure 3.9: Mean of the proportional change when compared with the C-LLAMA anchor scenario in global land-use in each category when prescribing the EAT-Lancet diet regionally, from 2014 to 2050. This represents the mean of 21 model runs and is not equivalent to applying the diet to all regions at once.

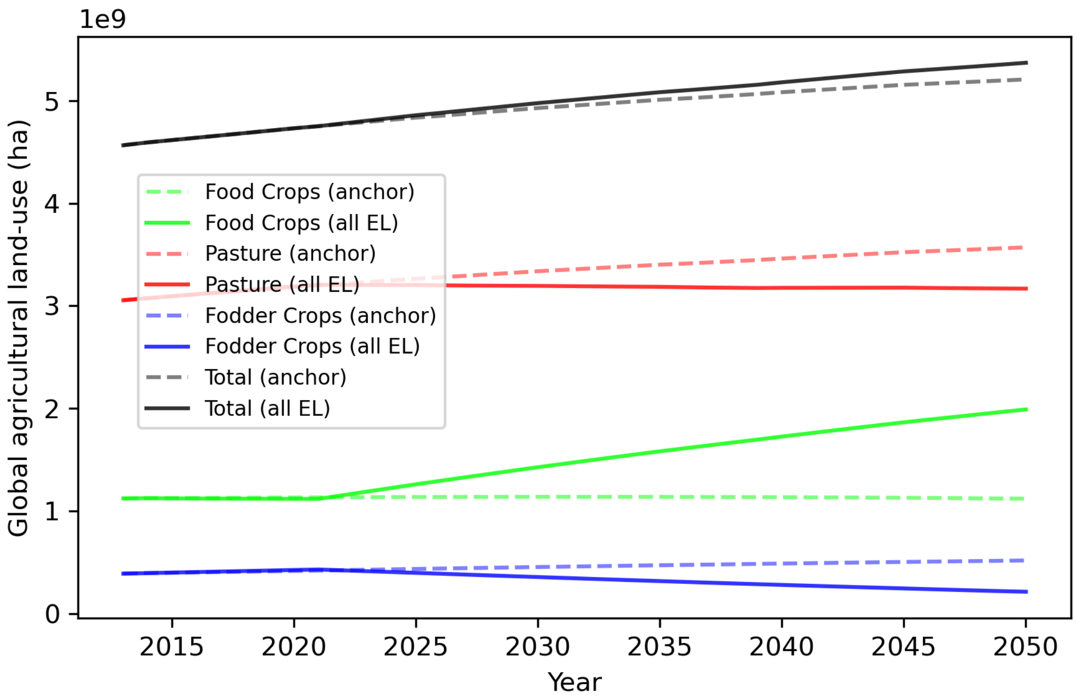

Figure 3.10: Global land-use in each category compared to the anchor scenario in a scenario in which the EAT-Lancet diet is applied to every region at once in C-LLAMA. The anchor scenario and EAT-Lancet diet scenario are represented by dashed and solid lines respectively.

food supply of 3000 kcal per day in the anchor scenario, whereas the EAT-Lancet diet combined with development (hence increased post-production waste) takes the continental average to just over 3100 kcal by 2050. The rapid population growth in Asia coupled with the discussed transition to less land-efficient but more nutritionally valuable vegetal products also contributes to the approximately 80% global increase in land-use for food crops when compared to the anchor scenario.

Pasture area remains surprisingly consistent overall despite the general trend toward a reduction in animal product consumption, undergoing a decrease of only 7% compared to the anchor scenario. The pasture changes shown in Figure 3.10 indicate that increases in pasture in Eastern and Western Africa, along with South-Eastern Asia are responsible for offsetting the decreases in South Asia, Europe, and America. Livestock systems are significantly more extensive in the former regions than the latter so this result is well-founded. It is important to note that the results presented in Figure 3.6 are relative to the anchor scenario; the total agricultural land area in both the anchor scenario and the EL diet C-LLAMA scenario increases by approximately 640 Mha from 2017 to 2050.

3.3.2 Plant-based diet

A diet with a (near) 100% reduction in animal product consumption by 2050 when prescribed globally in C-LLAMA leads to a decrease in total agricultural land-use of approximately 3.5 Gha from 2021, shown in Figure 3.11. Pasture and fodder crop areas disappear entirely by 2050 and only a very small increase in food crop area occurs. This is not surprising since C-LLAMA is highly idealised; a complete lack of demand for animal products precipitates zero production. This result is within the boundaries of the literature, which suggest that a fully vegan diet applied globally could theoretically lead to agricultural land-use decreases of upward of 70% (Aleksandrowicz *et al.*, 2016; Poore & Nemecek, 2018). This is an extreme scenario and realistically unlikely to be achievable by the year 2050. This scenario also does not

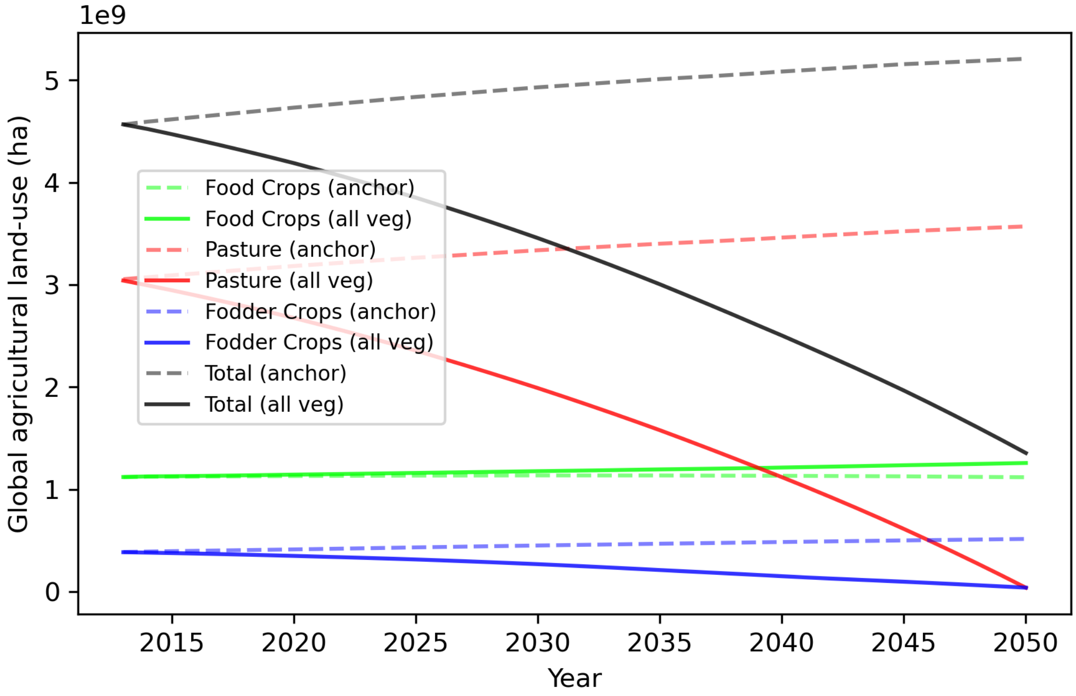

Figure 3.11: Global agricultural land-use in the C-LLAMA anchor scenario and a scenario with a 100% reduction in animal product consumption by 2050. Note that the actual reduction in animal product consumption is 99.99% to avoid errors during model runtime.

take into account nutrition as discussed in Section 3.1: animal calories are replaced by vegetal products using the ratios projected from the country's historical food supply. In practice this means that for most regions of the world, the diet in this scenario tends toward the consumption of grains, primarily wheat and rice.

3.4 CONCLUSION

In this chapter, the sensitivity of agricultural land-use to changes in diet was explored using C-LLAMA at a regional level. There is evidently the potential for significant land-use efficiency improves attainable through diet, it is also clear that the impact of switching to a sustainable diet is greater in regions with large populations - an expected result. However, as illustrated by the regional analysis in C-LLAMA, these impacts may not always lead to a reduction in overall land agricultural land-use.

Moreover, the EAT-Lancet diet comes at a cost; Hirvonen *et al.* (2020) found that the average cost of the diet is greater than the household income (per capita) for over 1.58 billion people.

The change in total agricultural land use area in the scenario where the EAT-Lancet diet is adopted rapidly across all regions is very similar to that of the C-LLAMA anchor scenario. However, the make-up of 2050 agricultural land in the two cases is different. Pasture area increases only a small amount and fodder crop area decreases in the EAT-Lancet scenario, while food crops increase significantly, whereas in the anchor scenario it is pasture that increases. These results are consistent with the findings of the EAT-Lancet planetary health report, which highlights the fact that no single intervention strategy is sufficient to remain within all planetary boundaries at once; yield gaps (as described in Section 5.1.1) are closed to 75%, and food waste and losses (see Section 4.1) are halved to facilitate the global adoption of the planetary health diet (The Eat-Lancet Commission, 2019).

The transition to food crops from pasture presents additional options for reducing the land footprint of the food-system. In many parts of the world, especially less developed regions, current crop yields are lower than their attainable maximums (Mueller *et al.*, 2012). The difference between attainable and actual yields are often referred to as ‘yield-gaps’, which will be explored in Chapter 5. Additionally, emerging technologies such as vertical farming have the potential to drastically increase crop yields, albeit it a high cost compared to traditional farming (Benke & Tomkins, 2017; Specht *et al.*, 2019). Moreover, crop production is far less constrained by the potential ethical concerns surrounding the intensification of livestock production (Pietrosemoli & Tang, 2020).

These results illustrate the potentially important role that diet could play amongst a suite of strategies for reducing the land footprint and improving the sustainability of the food system as a whole, especially in the context of land available for bioenergy and afforestation.

4

Modelling the impacts of food waste and losses on land availability

Abstract

The global food system is inefficient, but not inherently so. Between one third and one half of the total food produced in a given year (by mass) is wasted or lost through avoidable channels. The necessity for increasing food production to meet the requirements of growing populations is being artificially 'inflated' by the food that never makes it to the consumer, in-turn increasing the land footprint of the agricultural system. In this chapter we use the simplistic representation of food system efficiency in C-LLAMA to explore the potential for reductions in food waste (consumer, retail, and commercial waste) and losses (production, processing, and distribution) to reduce the land used directly and indirectly to produce food,

and therefore increase land availability for land-intensive climate change mitigation strategies (bioenergy, afforestation, and BECCS). Reducing post-production waste by half by 2030, in accordance with sustainable development goal 12.3, reduces the land requirement compared with the C-LLAMA anchor scenario in 2050 by approximately 700 Mha. Reducing processing and distribution losses by half in the same time frame leads to a smaller reduction in global land-use of 430 Mha by 2050. Applying a trajectory toward a 'best-case' scenario based on real-world waste values leads to a global reduction in agricultural land-use of 1000 Mha. Reducing waste at a regional level is most impactful in Southern Asia (containing India), and it is shown in general that reducing waste and losses in regions with larger populations has a greater impact on agricultural land-use.

4.1 Introduction

The United Nations Environment Programme (UNEP) defines food loss in their 2021 Food Waste Index report as any human edible animal or plant food commodity that completely exits the food supply chain without re-utilisation in some other form (e.g. animal feed) (United Nations, 2021a). Similar to food loss but slightly distinct is food waste; defined in the same way as food loss but with the caveat that it was deliberately discarded, either due to quality control standards or poor management (in the home or in the supply chain). For the purpose of this chapter losses and wastes are treated in kind: they both contribute to food production demand inflation and hence the inflation of agricultural land-use in turn. It is estimated that one third of all produced food is wasted yearly (Katt & Meixner, 2020).

Figure 4.1 represents general inefficiencies and stages of loss in the food system. In this chapter the central three loss stages will be considered: storage and transport (distribution), processing losses, and food waste by consumers (referred to as post-production waste throughout this thesis), all of which occur before 'harvested crops'.

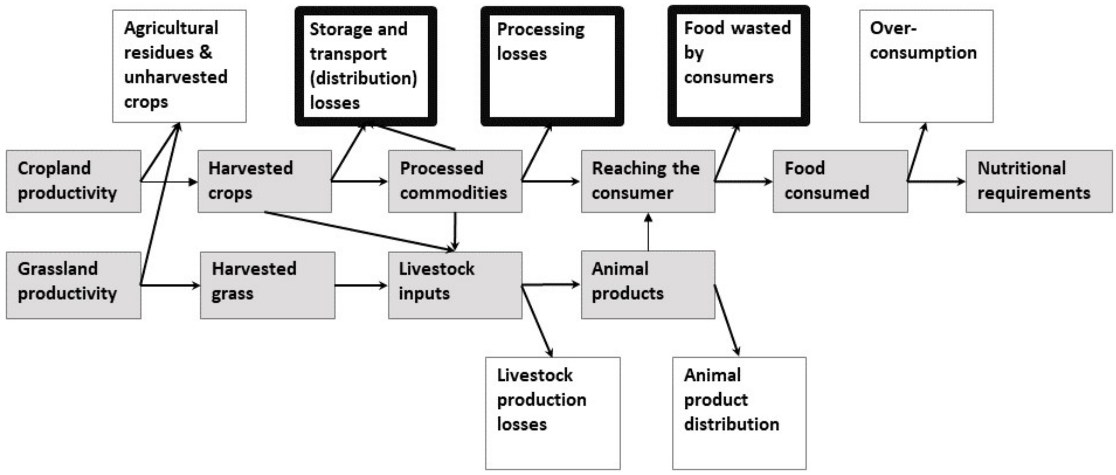

Figure 4.1: Stages of the food-system and associated losses. The top-central boxes are the focus of this chapter, outlined in bold. Food-system stages are shaded in light-grey. This figure is adapted from Alexander *et al.* (2017) (Figure 1).

The final stages (nutritional requirements and over-consumption) fall under the remit of diet and are discussed in Chapter 3.

The first avenue for food loss is during production, most commonly due to poor crop management, disease, weeds, and pests. This loss factor is usually greater in developing regions with limited access to pesticides, fungicides, machinery, and other management practices (Savary *et al.*, 2019; Oerke & Dehne, 2004; Alexander *et al.*, 2017). Losses due to climate and ecological factors can also occur, which may become more prevalent with the ubiquitous impacts of anthropogenic climate change (Ray *et al.*, 2019; Kukal & Irmak, 2018). Losses due to climate and ecological factors will not be considered in this chapter, since they are captured in yield data in the FAOSTAT database which are derived from production quantity and harvest area (rather than being measured empirically) (FAO, 2021a). Harvest residues also occur at the production stage but are not losses of food in the conventional sense as they are not suitable for human consumption; C-LLAMA has the capacity to divert these losses to animal feed as discussed in Chapter 2, and in the real world they may also be used as biomass for energy generation (Kalt *et al.*, 2020).

Storage and transport losses, together referred to as distribution losses, are distinct types of loss but often occur in conjunction. Storage losses are the result of poor storage conditions during intermediate stages of the food system, usually a lack of suitable refrigeration, excess humidity, or the presence of rodents, fungus, or parasites (Gustavsson *et al.*, 2011; Bradford *et al.*, 2018). Not only are poor storage conditions a cause of inefficiency in the food-system, they can also be harmful to human health if foods contaminated with fungal or insect infestation are ingested, either due to necessity or lack of awareness (Bradford *et al.*, 2018). Storage losses are greater in regions of lower development (an estimated 22% in developing countries versus 9% in developed countries), where access to refrigeration or suitably dry conditions are limited, or in the case that refrigeration is available, it may not be persistent due to inconsistent power supply (Kitinoja, 2013).

Food can be lost during transportation in two ways: the first is that food can become damaged due to poor road surfaces. The second is that the time taken is too great for the conditions of transit; food spoils before it reaches its destination (often due to a lack of refrigeration) (Lipinski *et al.*, 2013). Insufficient packaging can also contribute to both storage and transportation losses. Fruits and vegetables are particularly susceptible to losses at this stage: they are more fragile than grains and starchy roots and more prone to spoilage (Kitinoja, 2013; Gustavsson *et al.*, 2011). As Figure 4.2 shows, fruits, vegetables, grains, and seafood account for the bulk of food wasted globally in terms of both mass and energy. Losses in the remaining categories (roots, oil crops, pulses, dairy, and meat) account for approximately 20% in both cases. Energy losses are skewed toward grains due to their higher energy content (and visa versa with mass losses for fruits and vegetables).

It is estimated that around one third of all produced food (by mass) is wasted at this stage (Kumar & Kalita, 2017). As described in Section 2.3.2, distribution losses are much higher in the developing world than the developed world. Estimated losses at this stage are as high as 40% in Sub-Saharan Africa and up to 80% in severe cases (Kumar & Kalita, 2017), whereas in highly industrialised countries such as the

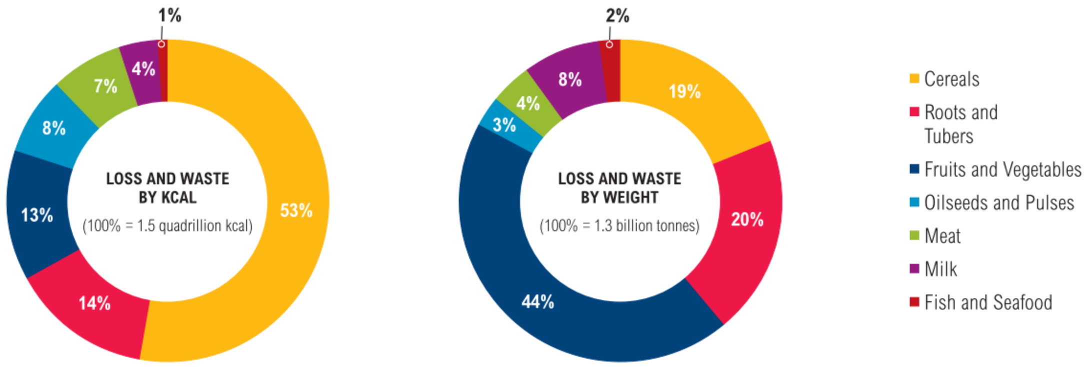

Figure 4.2: Estimated food wastage globally by production energy and production mass for the year 2011, from Lipinski *et al.* (2013), based on 2011 FAOSTAT data.

USA or the UK distribution losses range from 2% to 20% (for grains and fruits / vegetables respectively) (Parfitt *et al.*, 2010). Estimates for distribution losses can be made using export, food supply, and processing data: food produced but not reaching the consumer, processed, or exported within a country must have been lost to distribution (FAO, 2021a; Alexander *et al.*, 2017).

Processing losses are the smallest contributor to overall food waste, as well as being the least avoidable. Food processing is divided into three categories. Primary food processing occurs immediately post-harvest and includes drying, threshing, shelling, or similar of cereal crops and pulses; reducing weight, removing inedible product, and extending the lifetime of these products (Grumezescu & Holban, 2018). The waste product produced at this stage are referred to as harvest residues (distinct from field residues, which is biomass left on-site at harvest), and are not considered to be a true 'loss', since they are not suitable for human consumption. Additionally, primary processing losses are captured as part of yield data: production and yield data are usually expressed in terms of the dry mass of product *post*-primary processing, for example in the case of cereals, data represents the mass of dry grain only (FAO, 2021b). Processing losses in this chapter will be limited to secondary and tertiary; since primary losses are usually captured in yield data they will be discussed in Chapter 5. Secondary and tertiary processing losses occur post-harvest, usually off-site. Secondary processing includes procedures that alter the state of the raw product, such as cleaning, milling, or splitting (in the case of legumes and grains). Tertiary processing is the production of a 'final product' from secondarily processed commodities, usually on large scales for commercial outlets such as supermarkets (an example of this might be packaged ready meals) (Grumezescu & Holban, 2018; Hitzmann & Ahmad, 2017).

Losses at the secondary and tertiary processing stages occur due to mishandling or intrinsic tolerances in the processes - spillages, sorting errors, and spoilage due to mismanagement are all examples of losses at this stage (Jeswani *et al.*, 2021). Processing losses are less dependant on development level since processing is generally carried out on commercial scales and are more specific to the process and food commodity, so estimates for losses at this stage vary dramatically even within development levels; 13% to 20% in Egypt (Ali *et al.*, 2021), 5% to 18% globally (Gustavsson *et al.*, 2011), 19% in Switzerland (Dora *et al.*, 2020), 21% for the milling of rice in South-Eastern and East Asia (Kumar & Kalita, 2017), and as low as 1% for Australia, New Zealand, and North America (Porat *et al.*, 2018). Additionally, the boundary between tertiary processing losses and post-production food waste can be somewhat blurred: preparation of food for mass food-service (for example, fast food restaurants) takes place in large scale processing plants before distribution to restaurants, so can potentially be included with 'food-service' waste, which will be discussed in the next paragraph.

The post-production stage is the final avenue for food losses, almost all of which can be categorised as waste. Post-production waste can be split grouped into three categories: 'food-service', retail, and household wastes. Food-services are food outlets - distributors of prepared food products, for example restaurants, hotels, educational institutions, and prisons (Dhir *et al.*, 2020; United Nations, 2021a). Food-service is sometimes referred to as hospitality however that fails to capture prisons and potentially education. Retail is the sale of food products to the general public, for example at markets or supermarkets, and household waste is food discarded by consumers in homes (United Nations, 2021a). All three of these waste streams are linked heavily to consumer behaviour, wastage here is much higher in developed countries (Stancu *et al.*, 2016), although it is prevalent across all seven continents (United Nations, 2021a).

Estimates for post-production waste include 22% in the household in the UK (Stancu *et al.*, 2016), 7% to 24% at the consumer stage in the EU (Roodhuyzen *et al.*, 2017), and 40% during post-production in North America, Australia, and New Zealand combined (Porat *et al.*, 2018). There is a significant lack of data availability for post-production food waste outside developed countries; with 77% of studies in the 2021 Food Waste Index Report coming from upper-middle and high income countries (United Nations, 2021a). Additionally, only two low-middle income country studies provide an estimate for household waste in the 2021 Food Sustainability Index (94 and 121 kg/person/year in India and Indonesia respectively) (The Economist Intelligence Unit, 2021). Examples of waste in food-service are trimming scraps (up to 12% in the case of potato fries in fast food outlets (Gustavsson *et al.*, 2011)), quality control, and industry standards or company policies. Retail food losses are linked to quality control, poor communication between stages (leading to over-purchasing or insufficient storage) in the (retail) supply chain, and high consumer standards for appearance (eg. 'ugly vegetables' that are perfectly edible) (de Moraes *et al.*, 2020; Porter *et al.*, 2018).

Household waste is the greatest contributor to food waste in the post-production stage in high-income countries (Roodhuyzen *et al.*, 2017). Food is wasted in the household due to poor purchase planning, scraps produced during food preparation (eg - vegetable peels), poor 'leftover management', and general misinformation regarding food safety (Schanes *et al.*, 2018; Porter *et al.*, 2018; Kavanaugh & Quinlan, 2020; Toma *et al.*, 2020). Misunderstanding by consumers of labels applied to food in retail contribute significantly to household food waste (Toma *et al.*, 2020; Kavanaugh & Quinlan, 2020). For example, 'best-before' and 'sell-by' date indications have no bearing on food safety, but are commonly interpreted to mean as such by consumers, leading them to discard perfectly edible food (Porter *et al.*, 2018; Kavanaugh & Quinlan, 2020). Flexible 'best-before' dates have already been shown to reduce food losses in the distribution and processing stages, however these labels are commonly misinterpreted by consumers at the retail stage (Dobon *et al.*, 2011).

Food losses and waste have a direct impact on food demand: the elimination of a source of loss or pressure would take pressure away from the food system to deliver that food to consumers. Nearly one third of all food produced is wasted globally, while some food waste and loss is inevitable and this does include some unavoidable losses (for example eggshells, coffee grounds), there is the potential for a third reduction in food demand (Katt & Meixner, 2020). While this wouldn't necessarily reduce land-use by agriculture by one-third, land-use is almost directly proportional to demand, so the potential for increasing land availability is large (Cattaneo *et al.*, 2021).

4.1.1 FOOD WASTE AND LOSS IN C-LLAMA

Food losses and waste are represented simplistically in C-LLAMA, with each country being assigned a value for each of the three stages of loss and waste: distribution, processing, and post-production. In reality there are multiple sub-stages of loss and waste within each of these that vary based on the commodity in question (Koester & Galaktionova, 2021). A case-by-case approach for each country was not feasible given the number of countries in C-LLAMA, in addition to the lack of a coherent global dataset for food losses and waste. The Sustainable Development Goal indicators, the Food Waste Index (FWI) and Food Loss Index (FLI) were initially classified as tier three indicators in 2018, although have since been updated to tier two indicators (there are no longer any tier three indicators), meaning that while 'the indicator is conceptually clear, has an internationally established methodology and standards are available', 'data are not regularly produced by countries' (United Nations, 2021c). It was this lack of data availability and consistency that excluded the possibility of an empirical waste and loss system in C-LLAMA, instead using the food-system efficiency parameter to assign approximate values for each country.

Figures 4.3 and 4.4 show the availability of food loss data for two middle-high income countries, the USA and Italy respectively between the years 1981 and 2021, in the Food Loss Index (Koester & Galaktionova, 2021). While it would have been possible to achieve high levels of real-world accuracy in countries with high data-availability such as the USA, the large number of countries with scattered data availability precluded the possibility. Additionally, there are a vast number of commodities listed in this index; the data points for Italy are (exhaustively) for tomatoes, eggs, wine, fruits, legumes, and 'other vegetables', while the USA data includes commodities such as 'grapefruit juice' and 'carrots and turnips'. Unfortunately, homogenising this data (for example the conversion of grapefruit juice to grapefruits as part of the food supply) was well outside the scope of development for C-LLAMA.

To explore the impact of food waste and loss on agricultural land-use using C-LLAMA, subcategories of waste such as household and retail waste must be aggregated into one of the three types of waste in the model. Since food losses are so dependant on income level and development, the country-level structure of C-LLAMA place it in a good position to explore the impacts of food losses on land-use. In this chapter the effect of reducing food waste at different stages of the food system on agricultural land globally will be explored.

4.2 METHODS

4.2.1 REDUCING POST-PRODUCTION WASTE

To explore the impact of reductions in food waste, three different sets of model runs were conducted in C-LLAMA. The first is an exploration of sustainable development goal (SDG) 12.3: 'by 2030, halve per capita global food waste at the retail and

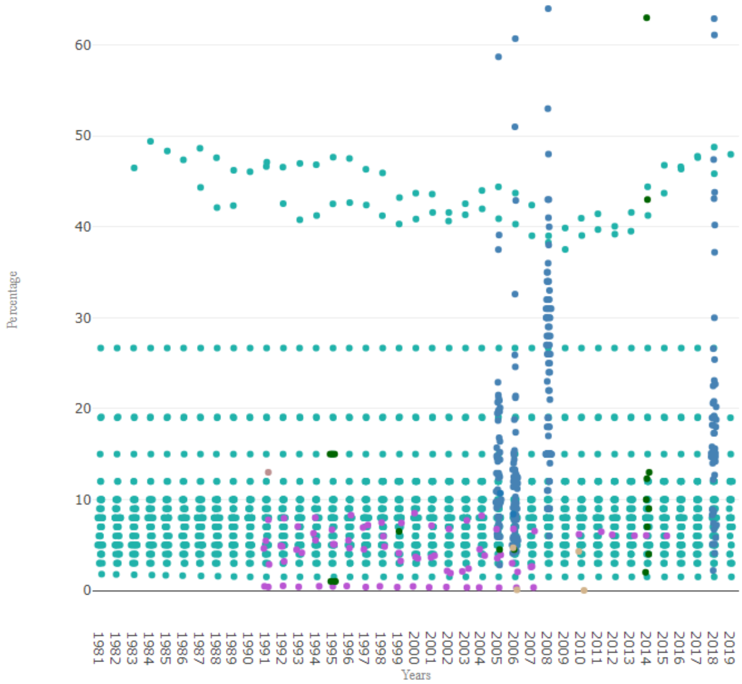

Figure 4.3: Data points in the Food Loss Index for the USA for the years 1981 to 2021 (Koester & Galaktionova, 2021). Each point represents a quantifying study of the wastage or loss of a particular commodity or group of commodities in a given year within a country. Colours indicate the method of data collection used in the study, they include case-studies census, controlled experiments, expert opinion, literature reviews, national accounting, modelling, and FAO annual surveys. For the illustrative purpose of this plot, the legend has been omitted.

consumer levels and reduce food losses along production and supply chains, including post-harvest losses' (United Nations, 2021b). The includes inedible food-waste in the household, for example eggshells or bones (United Nations, 2021a); since these are included in food-supply data used by C-LLAMA the definition of edible vs inedible food waste should have no bearing on the outcome. The focus of this scenario is on the first half of SDG 12.3: reducing retail and consumer waste (post-production waste) by half by 2030. This is a very achievable goal from a technical perspective: all waste generated here is due to consumer behaviour, which in theory could change overnight. In reality motivating such large changes will almost certainly require significant policy intervention (FAO, 2011).

A trajectory for 'post-production waste' was prescribed to each country from 2021 to 2030, such that the 2030 value is half that of the 2021 value; the trajectory then

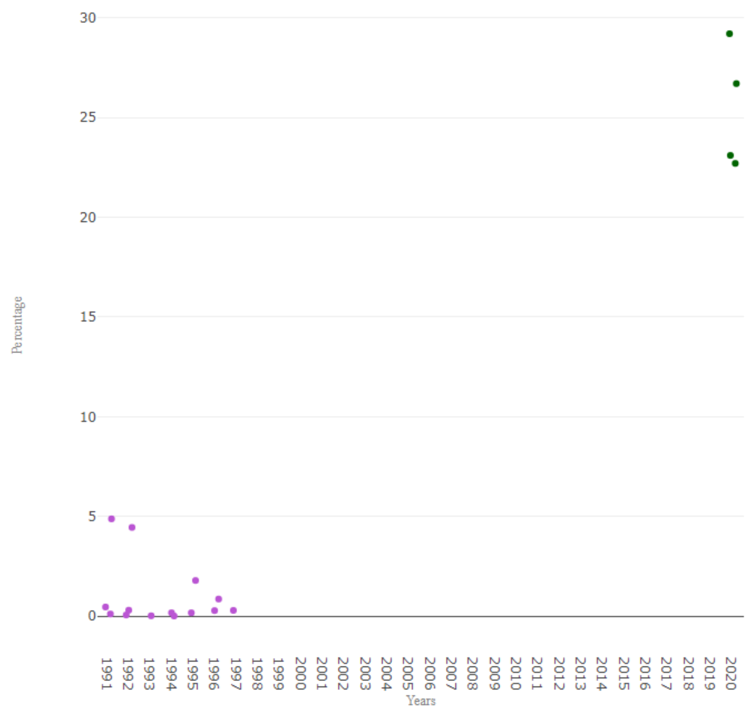

Figure 4.4: Data points in the Food Loss Index for Italy for the years 1981 to 2021 (there are no data points prior to 1991) (Koester & Galaktionova, 2021). Each point represents a quantified study of the wastage or loss of a particular commodity or group of commodities in a given year.

remains constant from 2030 to 2050. Assuming SDG 12.3 is achieved, this is the most conservative possible outcome for the scenario: the development goal was met and then no further action taken. A linear decay was used for the trajectory (such that the 2030 value is half that of the 2021 value), so that the new post-production waste ratio for a given country is:

$$M_{\text{post}}(n) = \begin{cases} \mu_{\text{post}}(n), & \text{for } n < 2022 \\ \mu_{\text{post}}(2021) * \left(1 - \frac{n-2021}{2*(2030-2021)}\right), & \text{for } 2022 < n <= 2030 \\ \mu_{\text{post}}(2021) * \frac{1}{2}, & \text{for } 2030 < n <= 2050 \end{cases} \tag{4.1}$$

where $M_{\text{post}}(n)$ is the new fraction of food wasted during post-production in year n and $\mu_{\text{post}}(2021)$ is the previously calculated post-production food waste fraction in 2021, calculated using the food system efficiency parameter described in Section 2.3.2. Figure 4.5 gives examples of the post-production waste trajectory for six

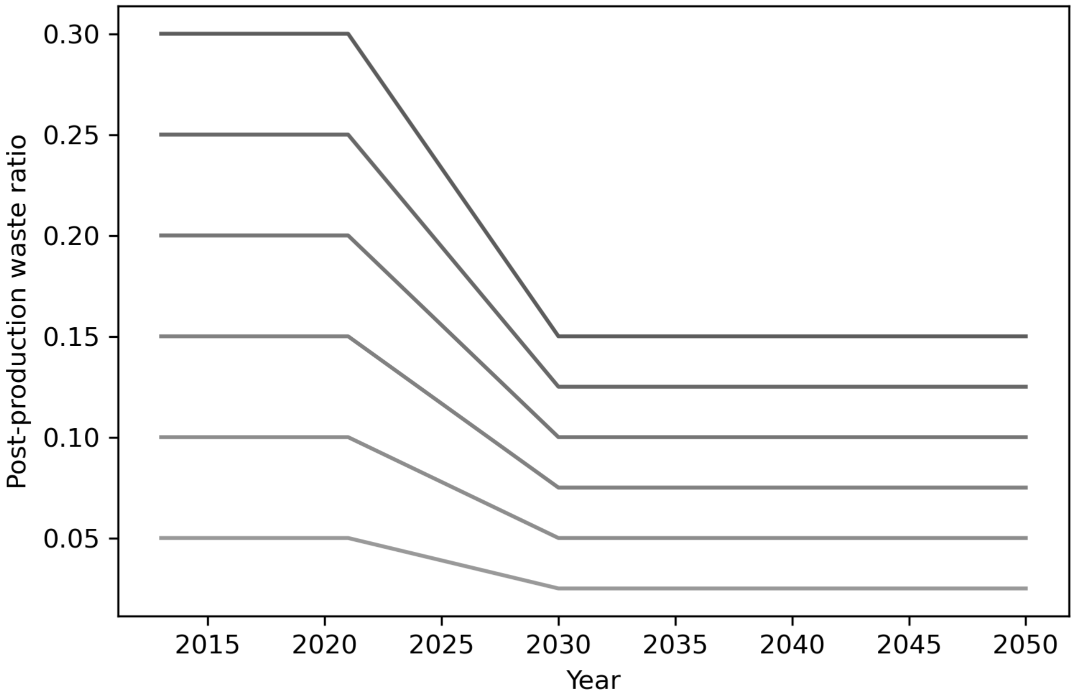

Figure 4.5: Post-production waste trajectory for countries with initial (2021) post-production waste values from 0.05 (score of 0.0 on the food-system efficiency parameter) to 0.3 (score of 1.0 on the food-system efficiency parameter).

different values of $\mu_{\text{post}}(2021)$ from 0.05 to 0.3, corresponding to scores of 0.0 and 1.0 on the food-system efficiency parameter respectively.

Since food supply data inherently includes post-production waste, to implement the new trajectories into C-LLAMA, the projected food supply for the chosen country was first scaled down by the projected post-production $\mu_{\text{post}}(n)$ (leaving a hypothetical 'food-consumed' trajectory) then re-scaled upward using the new post-production waste trajectory $M_{\text{post}}(n)$. Evidently achieving this goal will require more drastic change and have a greater impact in high-income regions that have initially high post-production waste compared with low-middle income regions; while the proportional change is the same regardless of initial post-production waste, the magnitude of change is much greater given a higher starting value.

4.2.2 REDUCING PROCESSING AND DISTRIBUTION WASTE

Sustainable Development Goal 12.3 is more ambiguous regarding production, processing, and distribution losses (post-harvest): only aiming to 'reduce' losses at these stages without specifying a quantity (Koester & Galaktionova, 2021). In the absence of an analogous target, the trajectory used in Section 4.2.1 was applied to both processing and distribution wastes: both undergo a reduction of half between the years 2021 and 2030. Production waste was excluded, since it is usually included in yield calculations. As such, Equation 4.1 governs the trajectory for each waste stream, with μ_{proc} and μ_{dist} replacing μ_{post} in each case. These waste trajectories were applied to every country at once to produce a single scenario.

4.2.3 'BEST-CASE WASTE'

A final set of C-LLAMA model runs was conducted for this chapter, in which each region tends toward a 'best-case' value for each of the avenues for food loss and waste. As previously discussed, C-LLAMA does not differentiate between different types of post-production waste. To obtain a best-case value for post-production waste, the least wasteful example for each of household, retail, and food-service was taken from the Food Sustainability Index (FSI) (The Economist Intelligence Unit, 2021; United Nations, 2021a). The FSI ranks the G20 countries by metrics surrounding food loss, waste, policy, diet, and sustainable agriculture to produce an overall food sustainability index, in which Canada ranks first. Since a large portion of Canada's high score is due to policy and diet, rather than it having low food waste and loss values, the metric scores for waste at each stage were used instead. Russia produced the lowest household waste per capita at 33 kg/capita/year, followed by South Africa and India at 40 and 50 kg/capita/year respectively. Italy and the UK produced the lowest retail waste at 4 kg/capita/year each (followed by Germany at 6 kg/capita/year). Japan produced the least food-service waste at 15 kg/capita/year

Waste stage	Country	Food waste (kg/capita/year)	Food supply (kg/capita/year)	Waste fraction
Household	Russia	33	888	0.016
Retail	Italy / UK	4	993 / 970 (980)	0.004
Food-service	Japan	15	603	0.025

Table 4.1: Best-case food waste values for each of the three 'end-user' waste categories in the Food Sustainability Index The Economist Intelligence Unit (2021). The retail waste fraction was calculated by weighting the total food supply quantities of Italy and the UK by their 2021 populations (The World Bank, 2021). The parenthesised 980 kg/capita/day represents the weighted (by population) mean of the Italian and UK food supplies.

(followed by the UK at 17 kg/capita/year).

To convert these waste values into a fraction for use in C-LLAMA, the score for each country was divided by the total food supply quantity (mass) in that country for 2021, producing best-case waste fractions of 0.4%, 1.6%, and 2.5% for retail, household, and food-service respectively. Summing these gives a total post-production waste fraction of 4.5%, which is almost an order of magnitude lower than most literature estimates of post-production waste in middle-high income countries, and the upper boundary of 30% used in C-LLAMA (see Section 4.1). However, it worth noting that the top scoring countries in each of these aspects do not score so well in other aspects, for example the UK produces 77 kg/capita/year in household waste, more than double that of Russia, which would give it an overall waste fraction of approximately 10%. The best-case scenario should therefore be considered highly optimistic, since no single country achieves comparably low wastage and losses across all aspects.

Processing and distribution losses are aggregated in the Food Sustainability Index as 'food loss', defined as food lost been the point at which production is measured (excluding losses before and during harvest) and before the consumer stage (excluding household, retail, and food-service) (The Economist Intelligence Unit, 2021). Once again Russia has the lowest losses in this regard, with a food loss estimate of 1.56% of it's total production. Because processing and distribution losses are summed in the FSI, they must be separated for implementation into C-LLAMA; the total 'food loss' was split according to the relative projected processing and distribution losses in the C-LLAMA anchor scenario for each country.

Once again a linear trajectory was prescribed from 2021 to 2050, this time to the idealised values for processing, distribution, and post-production waste fractions, to each region in turn in C-LLAMA, for a total of 21 model runs. As in Section 4.2.1, the food-supply projection for each country was scaled down by the projected post-production loss value, then re-scaled up using the new post-production trajectory.

4.3 RESULTS AND DISCUSSION

4.3.1 REDUCING POST-PRODUCTION WASTE

The global results of applying a 50% reduction in post-production waste by 2030, in line with the first target of sustainable development goal 12.3, are shown in Figure 4.6. The greatest decrease in land-use is with pasture area, with the 2050 area being approximately 500 Mha less than in the C-LLAMA anchor scenario (section 2.4.1). As described in Sections 4.1 and 3.2.1, developed regions typically have higher animal product consumption and post-production waste, so it is not surprising the greatest reduction in land-use occurs in pasture. Food and fodder crop areas decrease by approximately 150 and 50 Mha respectively. Given the structure of C-LLAMA it is expected that the trajectories for pasture, fodder, and food crops are approximately proportional to their anchor scenario counterparts. The change in fodder crop area is small compared to pasture and food crops; fodder crop and pasture areas are both dependant on the make-up of the animal products being consumed due to the ratios for forage and fodder feed discussed in Section 2.3.4. The total land use saving made by 2050 is 700 Mha.

While the gains made in land availability by 2050 through reducing post-production waste are significant when compared to the anchor scenario, the overall change in land use from 2021 is fairly small. Pasture and food crops undergo reductions

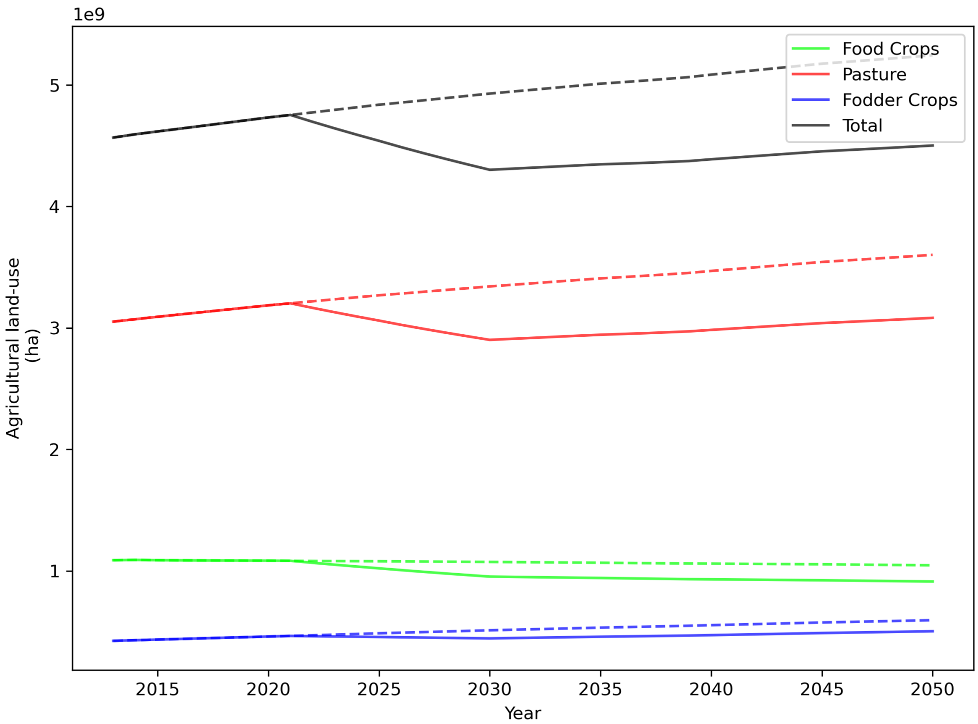

Figure 4.6: Global agricultural land-use when meeting the SDG 12.3 target of a 50% reduction in post-production waste by 2030 in C-LLAMA (solid line), compared with the anchor scenario (dashed line).

of 170 Mha and 120 Mha respectively between 2021 and 2050, while fodder crop area increases by 40 Mha. The continuing increase in food demand in the majority of regions is only marginally offset by the reduction in post-production waste, especially in the case of animal products. This suggests that while SDG 12.3 is a commendable initial target for improving efficiency within the food-system, alone it will not sufficiently increase land-availability for climate change mitigation strategies without further action beyond 2030. This result is also consistent with the findings of Chapter 3 and the EAT-Lancet planetary health diets report, in that 'no single intervention is enough to stay below all boundaries simultaneously' (The Eat-Lancet Commission, 2019).

4.3.2 REDUCING PROCESSING AND DISTRIBUTION WASTE

Reducing processing and distribution losses in C-LLAMA by the year 2030 (Figure 4.7) leads to a similar pattern in land use as when reducing post-production waste over the same period. Pasture area reduces by 310 Mha compared to the anchor scenario, significantly less than the 500 Mha reduction when reducing post-production waste. Animal products and especially ruminant meat and dairy are presently consumed more readily in developed regions where processing and distribution wastes are lower (Milford *et al.*, 2019). Food crops and fodder crops reduce by 110 Mha and 10 Mha respectively. Overall, 430 Mha of land is freed from agriculture by the year 2050 when halving processing and distribution losses by 2030 compared to the anchor scenario in C-LLAMA. Both the processing and distribution, and the post-production waste scenarios undergo rapid land-use reductions in the 2021 to 2030 period, then continue to climb again until 2050. This behaviour pattern is expected given the deterministic and simplistic structure of the model; there are no hysteresis behaviours in C-LLAMA.

4.3.3 'BEST-CASE WASTE'

Reducing global waste to the 'best-case' values described in Section 4.2.3 in every region simultaneously in C-LLAMA results in a total global agricultural land-use of approximately 4200 Mha in 2050, almost exactly 1000 Mha less than the C-LLAMA anchor scenario in 2050 (a reduction of 19%). This is also 510 Mha less than the 2021 land-use value (an 11% reduction from the present day). The land-use by different agricultural categories in this scenario are shown in Figure 4.8. Pasture land-use decreases by around 600 Mha, food-crops by approximately 300 Mha, and fodder-crops by just under 100 Mha.

It is estimated that approximately one third of all food produced is either lost or not consumed (Porat *et al.*, 2018). It is therefore tempting to set the theoretical maximum

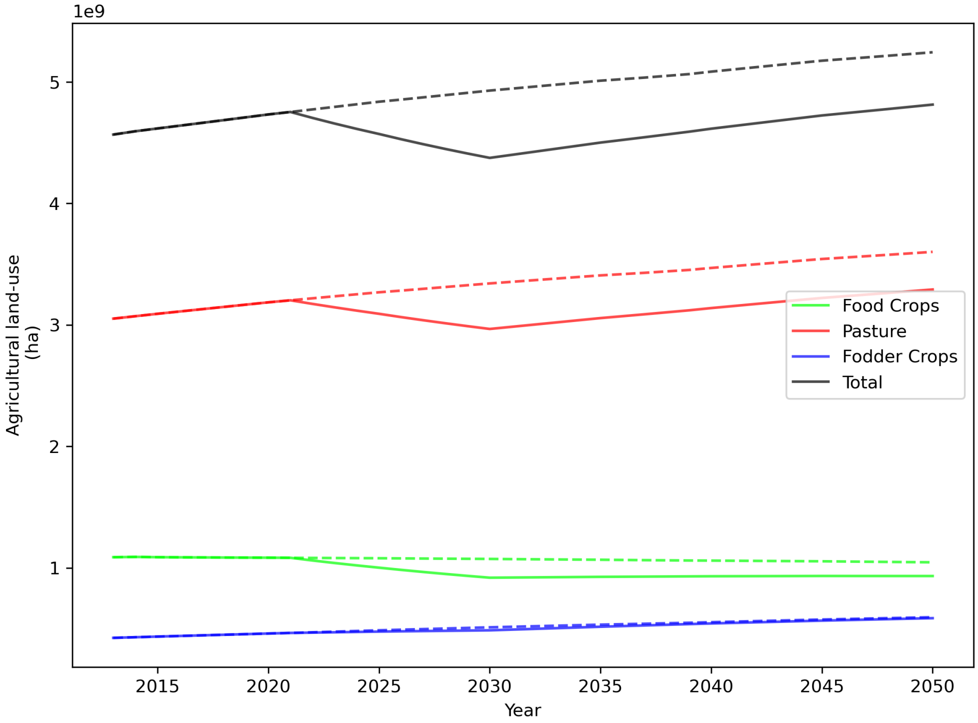

Figure 4.7: Global agricultural land-use when reducing processing and distribution wastes by half between the years 2021 and 2030 in C-LLAMA (dashed lines). The solid lines represent the C-LLAMA anchor scenario.

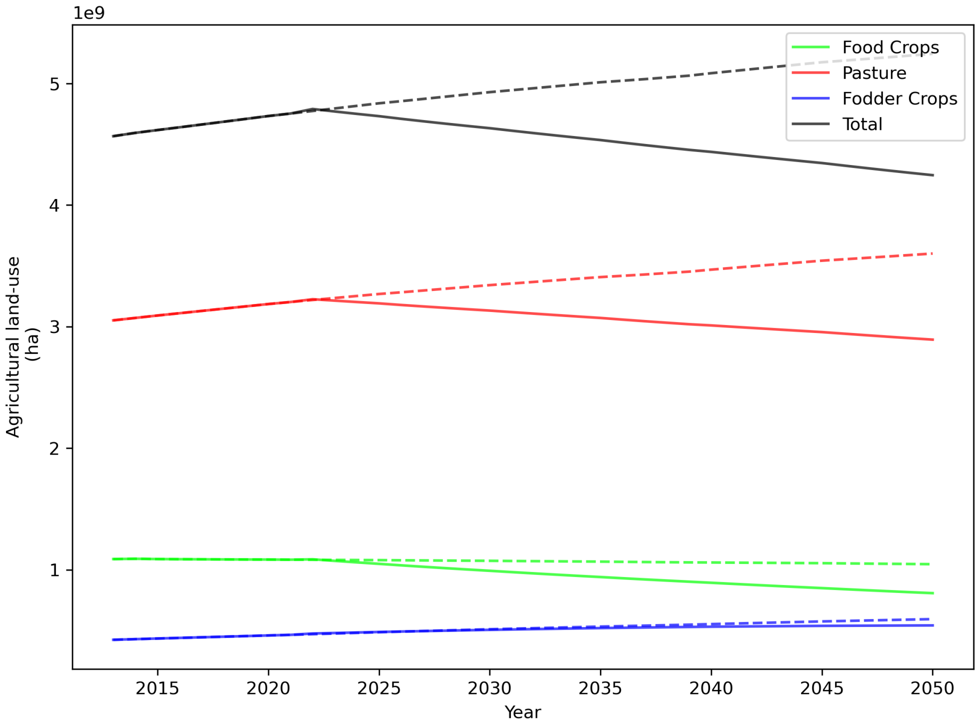

Figure 4.8: Global land-use for agriculture for a scenario in which a trajectory toward 'best-case' waste values in 2050 was prescribed to all regions at once in C-LLAMA.

land-use reduction also at third the present value (in the case in which all post-harvest food waste and losses are eliminated). However, different food products are wasted and lost in differing amounts: vegetal products are typically subject to greater waste and losses than animal products (likely due to the higher value of animal products) (Alexander *et al.*, 2017). Reducing the wastage of animal products leads to greater reductions in agricultural land-use, a result of the on-average higher land-footprint of animal products. This is reflected in these scenario results: by far the greatest reduction in land-use occurs in pasture. Kummu *et al.* (2012) estimates that food waste and losses are responsible for 25% of land use for crop production (in addition to the same proportion of extraneous water and fertiliser use).

While there are savings land-use to be made by reducing food wastage and losses, growing populations and demand for food products will continue to drive an increasing demand for agricultural land. With this in mind, an almost 20% reduction (compared to the 'business-as-usual' anchor scenario in 2050) in total agricultural land-use when prescribing a trajectory toward 'best-case' waste values is encouraging. The values chosen are observed values, so certainly attainable. However, they are from relatively developed countries (Table 4.1). While developing countries typically have very low rates of post-production food waste to begin with, empirically post-production food waste increases as development occurs and access to food and wealth are improved. To avoid 'repeating history' in countries that are developing, this increase in post-production waste must be minimised at the same time as allowing development (a strategy in-keeping with the sustainable development goals). As discussed in Section 2.3.2, losses in developing countries are much higher earlier in the food supply chain, and reductions to which are concurrent with the general development of the country (improved infrastructure, power grid reliability, etc).

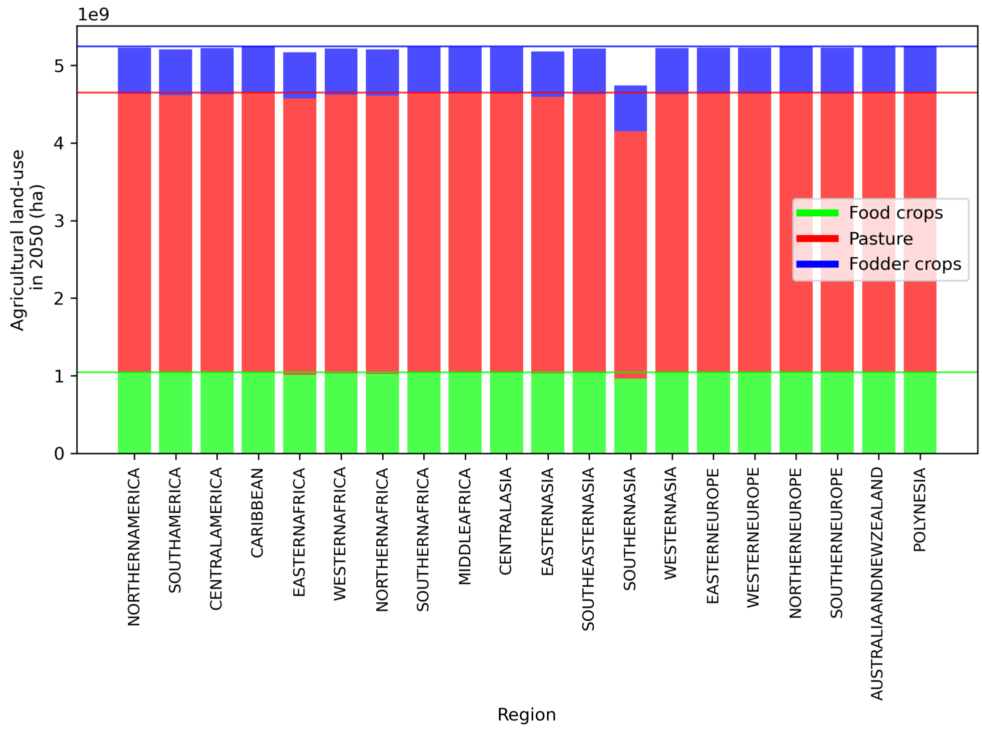

Figure 4.9: Global land-use for agriculture for twenty-one scenarios in which a trajectory toward minimal waste values was prescribed to each region in turn. Narrow horizontal lines represent the 2050 position of each of pasture, and food and fodder crops.

REGIONAL WASTE REDUCTION

The 2050 land-usage for each scenario in which trajectories toward the best-case waste and loss values are prescribed in each region, described in Section 4.2.3, are shown in Figure 4.9. By far the most significant change in global land-use occurs when reducing waste and losses in Southern Asia (the most populous country in which is India) with a reduction in land-use of approximately 400 Mha, the majority of which comes from pasture (just over 300 Mha). Food and fodder crops are both around 50 Mha less than in the anchor scenario. Prescribing the waste and loss reduction to Eastern Asia and Eastern Africa (the most populous countries in these respective regions being China and Ethopia) both lead to a reduction in land-use of around 100 Mha. In all scenarios there is at least some reduction in agricultural land-use, although for some regions this is imperceptible in Figure 4.9.

To emphasise the small changes when reducing waste in the majority of regions,

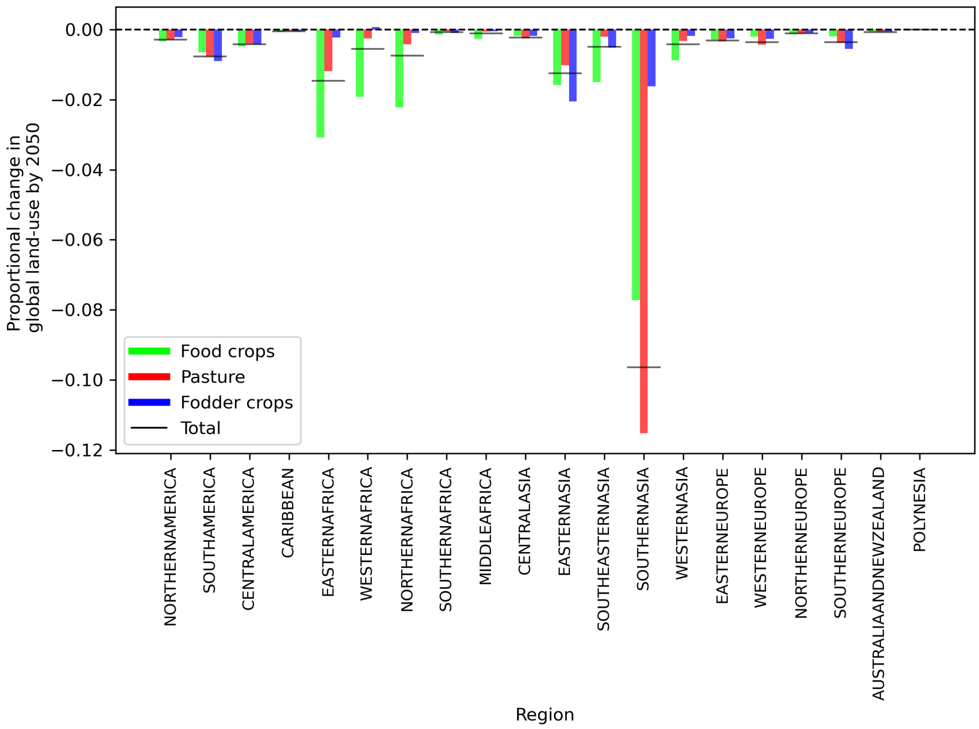

Figure 4.10: Proportional projected land-use change in 2050 relative to the anchor scenario, for the twenty-one scenarios in which a trajectory toward minimal waste values was prescribed to each region in turn.

Figure 4.10 shows the proportional land-use in 2050 relative to the C-LLAMA anchor scenario. All types of waste in C-LLAMA inflate food production demand, so it is no surprise that reducing waste leads to a reduction in production demand and hence agricultural land use in all cases. Reducing waste in Eastern, Western, and Northern Africa lead to global land-use reductions of between 1% and 2%, second only to Southern and Eastern Asia (approximately 10% and 1%). In SSP2, Africa undergoes a near doubling of population size from approximately 1 billion (2010) to 2 billion by 2050; the population in Asia also grows by approximately 1 billion in the same time period, but this is a much smaller proportional increase since the Asian population was 4 billion in 2010 (KC & Lutz, 2017).

Figure 4.11 shows the relationship between regional population in 2050 and the global land-use impact of reducing waste in that region. For each land-use category there are strong correlations between population size in 2050 and land use impact of reducing

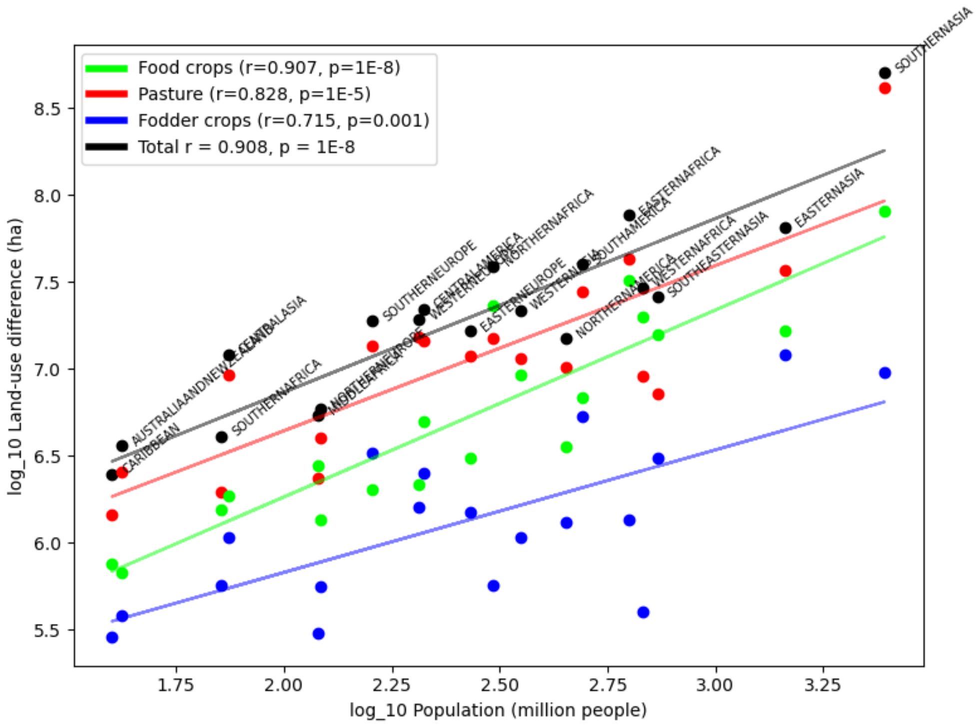

Figure 4.11: Log_{10} regional projected (UN medium population, 2050) population versus the difference in global land use from the anchor scenario in 2050 when applying a trajectory toward a 'best-case' waste scenario in that region. Positive values indicate a reduction in land use when compared with the anchor scenario (note all values are positive). Since it lies very far to the left with a projected 2050 population of less than one million, Polynesia is excluded from this plot for visual clarity (r values for all lines are greater when Polynesia is included).

food waste and loss, with fodder crops being the least correlated. Australia and New Zealand, Southern Asia, Central Asia, Southern Europe, Western Europe, Central America, South America, Northern Africa, and Eastern Africa all lie above the fitted line for total land use difference by 2050. This implies that reducing waste and losses in those regions has a greater impact *per capita* than in the regions below the fit line.

Figure 4.12 shows the land use difference when reducing waste in a given region compared with the anchor scenario, adjusted by the projected 2050 population for that region (from the UN medium population scenario). This is not a true per capita sensitivity since populations change over the 2021 to 2050 time period, however it gives a general sense of the individual impact of reducing waste and losses. Since both distribution and processing, and post-production losses are reduced in these scenarios, changes to land use are tied to both the population and diet of a region (demand), and the production of the region (supply).

Pasture area is more sensitive than cropland to waste and loss reductions in the majority of regions, with the exception of Northern, Western, and Middle Africa, and South-Eastern Asia. The per capita consumption of cereals and fruits and vegetables in these regions (as a portion of diet) are some of the highest in the World (see Section 3.2.1). Southern Asia remains the region with the greatest impact on land use when reducing processing, distribution, and post-production waste, with a change in land availability of approximately 0.20 ha/capita across pasture and cropland. Central Asia (which includes Kazakhstan, Kyrgyzstan, Tajikistan, Turkmenistan, and Uzbekistan) is inflated dramatically from it's pre-adjustment land use impacts at 0.16 ha/capita, where before reducing waste in this region lead to a global land use reduction of less than 1%. Adjusting for population swaps South America and Central America as the regions with the first and second greatest land use sensitivity to waste and losses in the Americas, with the continental range being 0.04 to 0.12 ha/capita. European regions have similar sensitivities of between 0.05 and 0.09 ha/capita, with Western Europe having the greatest land use impact.

4.4 CONCLUSION

This chapter has explored the agricultural land use implications of reducing waste and losses in the food system both during production and in post-production, along with regional trajectories toward best-case waste values. The waste and losses system in C-LLAMA is dramatically simplified due to the lack of a coherent data set of waste and losses for all countries, but has served as a tool for an exploratory set of analyses into the impacts of reducing waste on agricultural land-use. In all cases, reductions in waste and losses lead to significant reductions in agricultural land use when applied globally. However, the regional application of these reductions has much greater impacts in regions with high populations. Adjusting for population reveals that

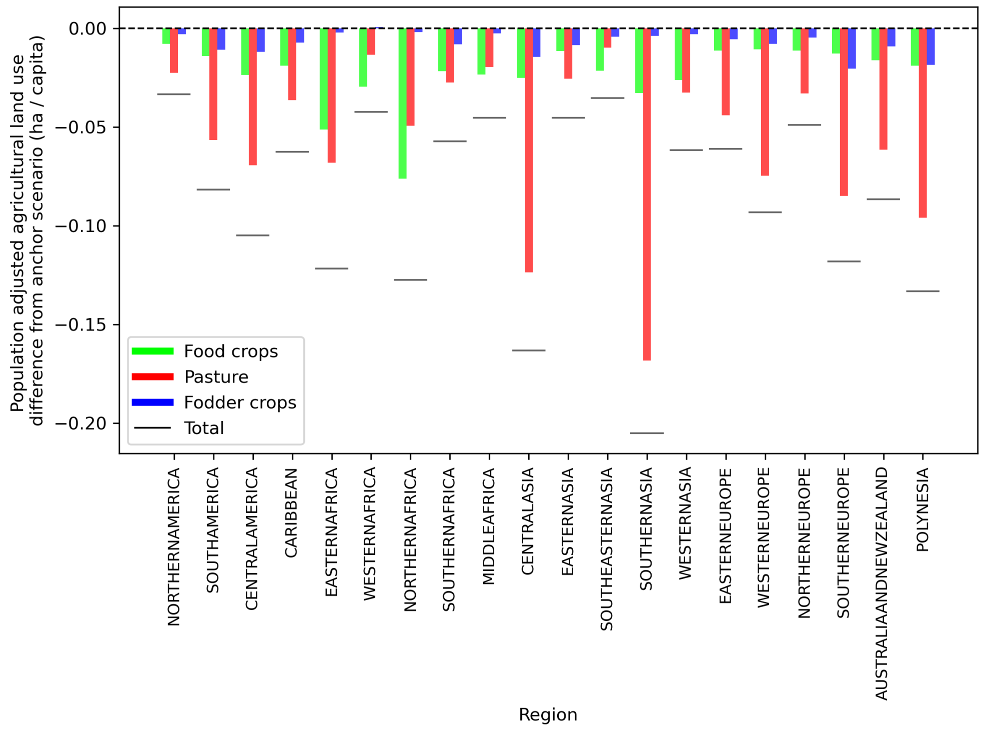

Figure 4.12: Population (UN medium population, 2050) adjusted land use impact of reducing waste and losses in a given region when compared to the C-LLAMA anchor scenario. All values are negative; lower values indicate a stronger land-use impact when reducing waste in that region. Black lines represent the aggregated land use impact for that region.

the per capita impacts of reducing waste in any region are between 0.04 and 0.20 ha/capita.

When applied globally, reductions in post-production and pre-consumer (processing and distribution) wastes lead to total land use reductions of 700 and 430 Mha respectively when compared with the C-LLAMA anchor scenario. As with all C-LLAMA scenarios, it is likely that the actual land use saving would be less; since agricultural land use change is a process rather than instantaneous as in the model. However, these are still significant land use efficiency improvements that together could contribute a significant portion of land toward land-intensive mitigation practices such as BECCS and afforestation.

Tending towards best-case waste and loss values for both pre-consumer (processing and distribution) and post-production waste and losses simultaneously ties the ultimate land footprint of a region to both its food demand and food production. To target waste and loss reductions at specific regions, a further exploration of the space using C-LLAMA could be informative, for example prescribing separate trajectories (such as the global scenarios in Sections 4.2.1 and 4.2.2) to each region in turn.

5

MODELLING THE IMPACTS OF YIELD ON LAND AVAILABILITY AND REGIONAL OPTIONS FOR IMPROVING LAND AVAILABILITY

ABSTRACT

In this chapter, the land use impacts of closing yield gaps (to maximum attainable yields) at a global and regional level were explored using C-LLAMA. Prescribing a trajectory toward maximum attainable yield for several major crops in every world region simultaneously resulted in a 200 Mha decrease in global crop land compared with the C-LLAMA anchor scenario. In the regional analysis, the general result is that closing yield gaps is much less effective in high and upper-middle income regions, while doing so in low and lower-middle income regions has a stronger effect,

between 2-3% change in global crop area. The regional yield gap closure was then compared with regionally prescribed EAT-Lancet diet, or 'best case' waste reduction scenarios. Applying the diet in some regions (especially those with low and lower-middle income) lead to increases in global land use of up to 4%, but was effective at reducing land use in upper-middle or high income regions (with land use decreases of up to 2%). Closing yield gaps was generally ineffective compared to waste and diet on the global scale, but decreased land use in the targeted regions more significantly. Reducing waste in Southern Asia lead to a dramatic land use decrease of 10% (530 Mha) when compared with the C-LLAMA anchor scenario.

5.1 INTRODUCTION

5.1.1 YIELDS

CROP YIELDS

Crop yields are a direct driver of agricultural land-use; the land area required to produce a given quantity of a crop is directly inversely proportional to the yield of that crop. Moreover, yields are defined empirically as the mass of product harvested per unit area (importantly, they are defined this way in FAOSTAT data (FAO, 2021b)). Mitigation scenarios consistent with 1.5°C warming generally assume significant improvement in yields whilst avoiding extraneous land-use change to facilitate the deployment of land-intensive climate change mitigation strategies (Daioglou *et al.*, 2019). Despite this assumption however, in recent years yield growth in major crops has been stagnating or halting completely in many regions, especially in the developed world. Between 1961 and 2008, in 24-39% of areas growing wheat, maize, rice, and soybean, yield growth didn't occur, stagnated, or collapsed, and nearly 50% of both rice and wheat sources are not currently seeing any increases in yield (Ray *et al.*, 2012). On the other hand, yields in a number of regions are lower than their potential physiological maximums, the difference between which is described as a 'yield-gap' (Mueller *et al.*, 2012; Tian & Yu, 2019; Battisti *et al.*, 2018).

There a wide range of factors that can influence the yield of a crop in a given region, with varying degrees of tractability. As with all organisms, plants favor certain conditions for growth. These include of temperature, nutrient access, light intensity, humidity, and water availability. With all of of these factors, each plant will have a minimum, maximum, and optimal value for growth, although some plants are more particular than others; the range for a suitable condition might be very narrow for some species (Schlenker *et al.*, 2006; Chapin *et al.*, 1987; Hatfield & Prueger, 2015). All of these conditions can be controlled precisely when growing crops in artificial conditions (such as in glass-houses). Outside the use of artificial environments, water and nutrient availability can be controlled through the use of irrigation and fertilisation. Temperature, light intensity, and humidity however, are entirely determined by the climate of a region (Iizumi *et al.*, 2017; Kukal & Irmak, 2018). Lobell & Field (2007) found that climate variables explained approximately 30% of the variation in annual crop yields for six major crop types.

YIELD GAPS

Potential yield (as defined by van Zeist *et al.* (2020) is the physiological maximum yield for a given crop, assuming perfect conditions and most productive strain. Attainable yields on the other hand, are the yields obtained by farmers under *economically* optimised conditions and (fertiliser and irrigation) inputs - i.e., maximum output is achieved with minimum input. In the real world, attainable yields are realistically maximum yields: unless crop production undergoes nationalisation the world over, farms will continue to effectively operate as businesses (van Zeist *et al.*, 2020).

Yield-gaps are the discrepancy between observed, actual crop yield and the attainable yield for a given crop, based on the climatic conditions of a region. Attainable yields are produced using modelling approaches or empirical studies (Grassini *et al.*, 2015).

As discussed previously, nutrient and water availability have significant impacts on crop productivity, so access to irrigation and nutrients are key determinants of yield gaps (Mueller *et al.*, 2012). In addition to irrigation and fertilisation, mechanisation is another land management practice that may serve to close yield gaps (Licker *et al.*, 2010). It is unsurprising then, that yield gaps are typically larger in lower income regions, since each of irrigation, fertilisation, and agricultural machinery require initial or continued financial investment.

By closing yield gaps, Mueller *et al.* (2012) identifies potential yield increases of 45 to 70% for major crop types, accounting for 76% of the agricultural land surface. Return on investment is high, especially developing regions: maize, wheat and rice, responsible for 57% of the world's food energy (Tilman *et al.*, 2011), could all be brought to 75% of their potential maximum output with relatively small changes to nutrient application and irrigation regimes.

In this chapter, the global land-use implications of 'closing' yield gaps at a regional level will be explored. In the real world, changes to yield might drive the economic value of food commodities up and down, which may affect the distribution of their production. However, since yield is a direct driver of agricultural land-use and economics are not considered in C-LLAMA, changes to yield will only affect land-use in the region in which they are applied.

CROP YIELD FRONTIERS

In addition to glasshouses as a controllable environment in which to produce vegetal products, aeroponics, hydroponics, and vertical farming have all seen increased interest in recent years (Garg, 2014). In aeroponics, the plant is suspended by an artificial support, allowing the roots to hang freely in air, with water and nutrients being delivered at regular intervals (usually as a mist). This allows precise amounts of water and nutrients to be administered to the plant (in addition to light and temperature under artificial conditions), improving water and nutrient efficiency by up to 99% and 50% respectively when compared to substrate-based farming (Lakhiar *et al.*, 2018). With similar benefits, in a hydroponic system oxygenated water (along with nutrients) is delivered to plant roots, either through submersion, intermittent flow, or constant flow (Sharma *et al.*, 2018). Water consumption is slightly higher in hydroponic systems but still between 70% and 90% less than traditional methods (Khobragade *et al.*, 2021).

A third method of cultivation - aquaponics, operates in the same manner as hydroponics, but with the addition of aquatic livestock. Waste produced by the aquatic livestock (crustaceans or fish) enters the water column and breaks down into nutrients that can be taken up by plant roots, acting as a fertiliser. This has the added benefit of removing the toxic waste products from the environment of the aquatic livestock, and while not as resource efficient as aero or hydroponics, it produces both vegetal and aquatic products (Palm *et al.*, 2018).

Vertical farming is the high-rise scaling of plant cultivation under climate-controlled conditions. Any one of aero, aqua, or hydroponics are used as the delivery system for water and nutrients, foregoing the need for growth substrate and facilitating the vertical engineering of the setup. This method lifts the yield constraints of traditional farming from crop production by allowing yields to scale upward, essentially infinitely (within the limits of water and energy usage) (Benke & Tomkins, 2017). Asseng *et al.* (2020) compared modelled wheat growth with experimental yields in controlled conditions on a vertical farm setup with 10 layers. They observed yields of 700 tonnes/ha, and modelled yields of up to 1900 tonnes/ha, 220 and 600 times greater than the average global wheat yield in 2020 (3 tonnes/ha).

In addition to relatively high setup costs, considerable means and energy inputs are required to maintain crop production in artificial conditions and as such, at present they are largely the domain of the developed world (Benke & Tomkins, 2017). Instead of looking for solutions within planetary boundaries, these technologies look to escape the constraints of traditional farming, and thus in the face of ever increasing food production demand, could play a key role in future food production, especially in urban environments (Benke & Tomkins, 2017).

LIVESTOCK

Quantification of yield is not limited to vegetal products; an empirical yield can also be defined for livestock. As with crops, this is simply the mass of livestock product generated per area in a given time-frame. Defining livestock yield in this way, maximum potential yields can be achieved when livestock are severely confined and fed entirely on dedicated feed (rather than grazing), thus their only land footprint is that of the fodder crops required to raise them. Such systems are not uncommon, for chickens and pigs in particular. In addition to high land-use efficiency, there are other environmental benefits to these extremely intense livestock systems since they facilitate the management of waste products such as manure, preventing issues such as water contamination and eutrophication (Pexas *et al.*, 2020). However, there exists a trade off between the environmental and land-use benefits, and the ethical considerations of such systems (Boogaard *et al.*, 2011).

At the other end of the spectrum, there are extensive pasture grazing systems, where a high portion of (or all) livestock feed is grazing or foraged. These systems are more commonly used to rear ruminant livestock, and are typically associated with better levels of animal welfare (Spigarelli *et al.*, 2020). They are also perhaps the least land-efficient food production system, in addition to producing detrimental environmental effects, including widespread soil degradation, biodiversity loss, and the motivation for deforestation (Poore & Nemecek, 2018; Kreidenweis *et al.*, 2018; De Oliveira Silva *et al.*, 2021).

The most obvious solution to the problem of animal product land-inefficiency is to simply forego the consumption of animal products (see Chapter 3). However in the absence of this possibility, livestock production systems can be intensified. In C-LLAMA, livestock production is essentially separated into either completely extensive or completely intensive, based on estimates of the portion of livestock fed through fodder and forage. Then a theoretical 'pasture-yield' is used to estimate the land requirement for animal products produced in the foraging systems, while the land footprint of fodder fed livestock is assumed to be entirely based on the fodder crop requirement (see Section 2.3.4 for details). As discussed in Chapter 3, due to the 'feed conversion' stage of livestock production, animal products (especially beef) are inherently less land-efficient than vegetal products, even in the most efficient possible production systems (Byerly, 1967).

Grazing animal land usage is calculated at the very end of the C-LLAMA model process and does not influence any other aspects of the model. Therefore applying an arbitrary pasture intensification trajectory in C-LLAMA would not be informative; an intensification of 15% in a region would lead to a 15% reduction in land use for pasture. The intensification of pasture will not be explored in this chapter, but is an inviting avenue for further development of C-LLAMA to include a head-count based livestock and land use model, with different grazing systems (as opposed to an empirically defined pasture yield).

5.1.2 FOOD SYSTEM OPTIMISATION

In order to meet the climate target of a maximum net global warming of 1.5 °C by 2100, it is likely that a significant quantity of land will be required to facilitate deployment of land-intensive mitigation strategies such as BECCS and afforestation (Gough *et al.*, 2018; Burns & Nicholson, 2017; Arneth *et al.*, 2019). This land requirement can be as great as 58 Mha per $GtCO_2e$ removed for BECCS, and potentially even higher for afforestation (Roe *et al.*, 2019). As discussed in detail in Chapter 1, the amount of suitable land currently available is not like to be sufficient to meet these climate targets. Suitable land could be recovered either from forests or from the agricultural system, however for BECCS and afforestation to be worthwhile as carbon dioxide removal methods, removing forests to procure the land is not a viable option (Harper *et al.*, 2018). The land must therefore be obtained by reducing the land used by the global food system.

Cultural differences, wealth and resource inequality, and trade amongst other things, give rise to an incredibly complex and interlinked global food system. The environmental impacts (especially land-use) of producing a single food commodity can vary drastically, sometimes even within the same administrative or climatic region (Poore & Nemecek, 2018). For example, in addition to it's extremely high land-use compared to other food products, beef production is one of the biggest emitters of greenhouse gases within the food system, and yet in some situations it can actually act as a greenhouse gas sink (Poore & Nemecek, 2018). The task of reducing the land-use required to feed the global population is complex, but there are a range of potential options available. These options can be made in three broad areas: food demand, food waste or losses, and food production. Undoubtedly, the implementation of improvements to all three of these broad aspects would lead to the greatest reductions in land-use, and sustainable food provision whilst meeting climate targets is certain to require some combination of the three (The Eat-Lancet Commission, 2019). The impacts of food demand (diet and population), and food waste or losses on land availability were explored using C-LLAMA in Chapters 3 and 4. In the first part of this chapter, the impacts of closing yield gaps on land use will be explored. In the second part of this chapter, the outcomes of the three sets of analyses will be compared at a regional level.

5.2 METHOD

5.2.1 CLOSING YIELD GAPS

To explore the land-use impact of closing the yield gaps described in Section 5.1.1, trajectories were prescribed in C-LLAMA to the maximum *attainable* yields for several major food crops, at each region in turn, for a total of twenty one scenarios (one for each region). Additionally, a scenario in which all regional yield gaps are closed simultaneously was produced. The attainable yields used were taken from the supplementary material of Mueller *et al.* (2012). The Global Yield Gap Atlas (GYGA) (yieldgap.org, 2021) is a more comprehensive data-set, with national yield gap estimates, as well as climate-zone aggregated data. The regional data from Mueller *et al.* (2012) is suitable given the exploratory nature of this work in C-LLAMA, however further work might involve a more in-depth analysis using the GYGA data in C-LLAMA. The values used in the scenarios are shown in Table 5.1.

	NA	LA/CA	WE	EE/CAs	ME/NAf	SSAf	SAs	EAs	SEAs/O
barley	3.51	3.88	5.26	4.38	3.02	3.31	3.11	4.01	2.67
cassava	–	18.18	–	–	–	16.25	27.01	19.53	18.11
maize	9.79	5.58	9.85	9.65	8.6	4.85	3.81	8.94	3.77
millet	1.98	1.98	2.0	1.99	1.38	1.1	1.3	1.99	1.46
oilpalm	–	19.38	–	–	–	17.97	–	19.94	20.52
potato	43.1	30.65	39.27	27.57	35.24	24.22	27.55	27.83	27.62
rapeseed	1.68	2.0	3.39	3.27	2.29	1.8	1.31	2.29	2.11
rice	7.43	5.89	9.29	9.37	7.87	5.24	4.84	7.72	5.09
sorghum	4.96	3.78	5.03	4.34	2.28	1.71	1.55	4.49	5.51
soybean	3.02	2.77	3.2	2.77	2.66	2.56	1.86	2.77	2.68
wheat	3.93	4.7	6.85	4.42	4.43	4.26	4.46	5.24	3.8

Table 5.1: Maximum attainable yield gap value for each region for several major crops (tonnes / ha / year), adapted from Mueller *et al.* (2012) supplementary material. NA = Northern America, LA/CA = Latin America and the Caribbean, WE = Western Europe, EE/CAs = Eastern Europe and Central Asia, ME/NAf = Middle East and Northern Africa, SSAf = Sub-Saharan Africa, SAs = South Asia, EAs = East Asia, SEAs/Oc = Southeast Asia and Oceania.

The prescribed trajectory begins with the 2021 yield of a given crop in the C-LLAMA anchor scenario, then moves linearly toward the maximum attainable yield for the region such that it reaches the value in 2050. The yield Y of a crop c in year n is then:

$$Y_c(n) = Y_c(2021) + \frac{n-2021}{2050-2021}(c_{\text{attainable}} - Y_c(2021)), \tag{5.1}$$

where $c_{\text{attainable}}$ is the regional attainable yield. In the case that the crop is not included in the attainable yield data the projection as produced by the anchor scenario continues as normal. Since the regions used in C-LLAMA are at a smaller spatial aggregations than the regions defined in Table 5.1, the C-LLAMA region uses data from the containing region in the table in the cases where they do not align. For example Latin America and the Caribbean (Table 5.1 region) contains all of South America, Central America, and the Caribbean (C-LLAMA regions).

5.3 RESULTS

5.3.1 CLOSING YIELD GAPS

The results of closing yield gaps in every region simultaneously are shown in Figure 5.1. Pasture area does not deviate from the anchor scenario at all, and reductions of approximately 100 Mha occur in both food and fodder crop areas, for a total of 200 Mha reduction. These numbers are of the same order as in the SSP1 scenario (just under 100 Mha reduction in rain-fed crop are by 2050) (Doelman *et al.*, 2018). Röös *et al.* (2017) found a total agricultural land use decrease of approximately 15% in a scenario in which diets are projected as normal but yield gaps were closed by 50%. However, many additional crop yield gap data were used in this scenario, essentially closing a greater number of yield gaps than in the C-LLAMA scenario. Unfortunately at the time of conducting the C-LLAMA scenario we were not aware of the data used to produce the Röös *et al.* (2017) scenario (this can be found in the supplementary material of Bajželj *et al.* (2014)): this is an avenue for more in depth exploration of the impacts of yield gaps on agricultural land in C-LLAMA.

The land use difference between the gap-closed scenario and the anchor scenario is very small when compared with the changes in land use achieved by reducing food waste or reducing animal product consumption as in previous chapters. In the C-LLAMA anchor scenario (see Section 2.4.1, yields are linearly projected forward using historical yield data. This results in relatively large yield increases over the 2021 - 2050

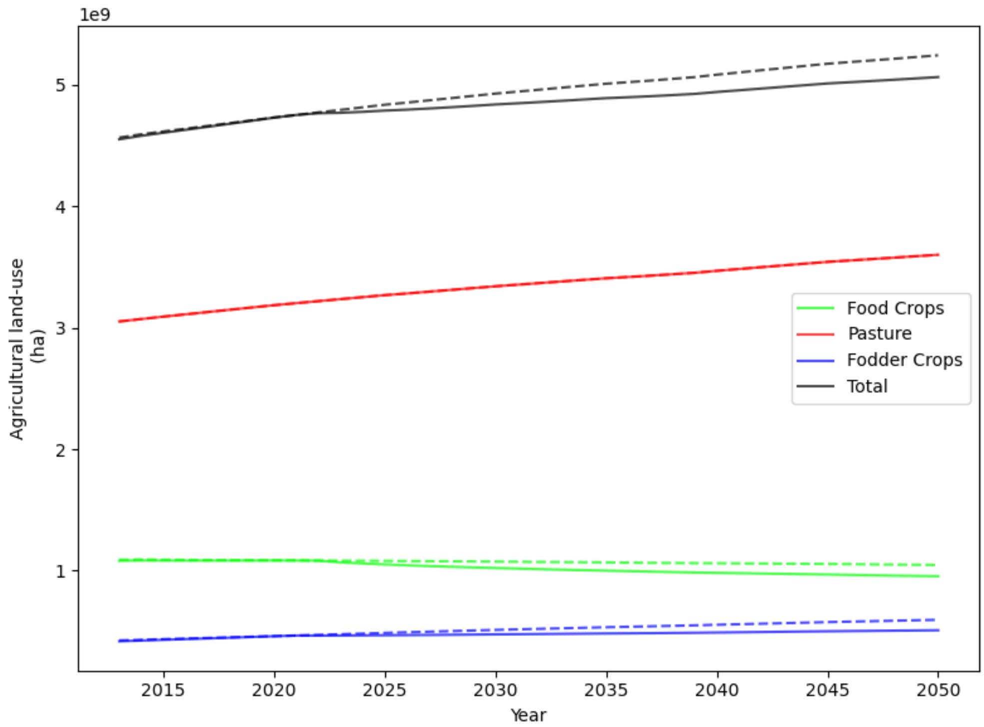

Figure 5.1: Global land-use trajectory when prescribing yield trajectories towards regional maximum attainable yields (shown in Table 5.1) and the C-LLAMA anchor scenario. Solid lines represent the yield-increase scenario, the dashed lines represent the anchor scenario.

time period in the anchor scenario, with many regions getting close to closing their yield gaps. Prescribing a trajectory toward closed yield gaps is less effective than other methods of 'efficiency increase', at least within the framework of C-LLAMA. In Section 2.4.2, disallowing crop yield projection in C-LLAMA leads to a 300 Mha increase in global agricultural land use in the year 2050 compared with the anchor. The scenario with closed yield gaps has approximately 500 Mha less land use in 2050 compared with the scenario with no changing yields (using present day yields). This is a 10% reduction; while a reduction in land-use is not directly comparable to an increase in production mass, Mueller *et al.* (2012) found a 30% increase in production mass for maize, wheat, and rice, globally by closing yield gaps.

Figure 5.2 represents 21 scenarios. In each, the yield gap was closed for that region only, while the yield in other regions was projected as normal in the C-LLAMA anchor scenario. In the simplistic world of C-LLAMA, changes in yield will only

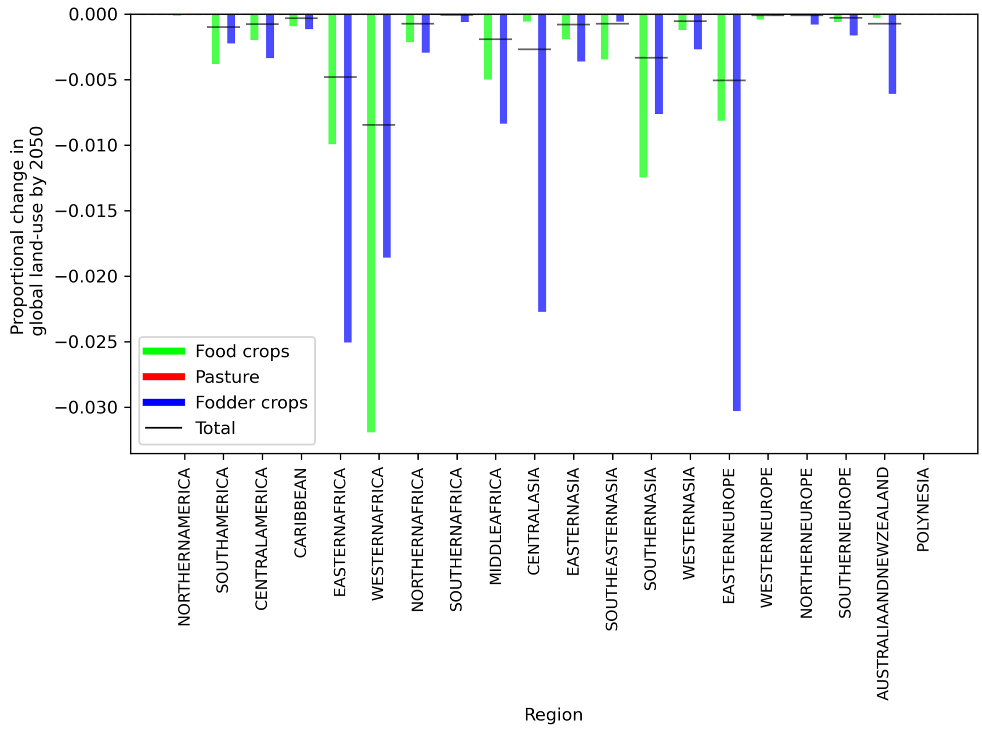

Figure 5.2: Proportional change in global land-use in 2050 compared to the anchor scenario when closing crop yield gaps in each of the twenty-one regions in C-LLAMA. Negative values represent a reduction in land-use compared to the anchor scenario (for example, -0.010 represents a 1% reduction in land use compared to the anchor scenario).

affect land use in the region in which the change occurs (there are no dynamic trade or economic mechanisms in the current version). There are no changes to pasture area since livestock intensification was not considered in these scenarios. In most regions, the changes in land use are comparable to those modelled in Chapter 4 (in the range 0-3%). In Northern America and Western, Northern, and Southern Europe, the reduction in land use compared to the anchor scenario is very small at less than 0.1%. This agrees with the findings of Mueller *et al.* (2012); each of those regions currently achieves nearly 100% of their respective attainable yields for the modelled crop groups, so closing their yield gaps will have only a small impact on land use. Eastern and Western Africa, Southern Asia, and Eastern Europe see the greatest decreases in land use (0.5, 0.8, 0.4, and 0.6% respectively change to the global total). Again these results are aligned with the general trends found by Mueller *et al.* (2012).

Much like waste and diet, the results here will be dependant on other factors within the model. In the case of crop yield analyses, the skew comes from production: regions with higher production quantities will inevitably see a better 'return on investment' by increasing yields in that region (land-use and yield are directly inversely proportional since there are no calculations that occur in between), similar to the influence of population when making efficiency improvements to diet and waste within C-LLAMA.

5.3.2 REGIONAL FOOD SYSTEM OPTIMISATION

The following analysis compares changes in yield (from the previous section), to changes in diet and food waste within C-LLAMA. The results in this section represent 63 scenarios; there are 21 regions in C-LLAMA, 3 scenarios were produced for each. In the first, a trajectory toward the EAT-Lancet planetary health diet was prescribed (see Section 3.2.1). In the second, trajectories toward values from the best performing countries in the food waste and loss index (FLI) were prescribed (see section 4.2.3). Thirdly, as discussed in the previous section, a trajectory toward the maximum attainable yield for certain crops in that region was prescribed (other crop yields were projected as normal in the C-LLAMA anchor scenario). In each of these scenarios, the normal linear projection of diet, waste values, and yields were used for regions outside the target region (see Section 2.3). Figure 5.3 shows the proportional change in *total global* agricultural land use (pasture and crops) from the anchor scenario in 2050 for each of these scenarios. The most obvious feature of Figure 5.3 is the 10% decrease in global land use when reducing waste in Southern Asia (the most populous country in which is India). For reference, the C-LLAMA anchor scenario sees a global agricultural land use of approximately 5300 Mha, so a 10% decrease equates to a reduction of 530 Mha. The efficacy of reducing waste in C-LLAMA is linked to both population (food demand), and food production quantity, both of which are high in Southern Asia. In 2017 Southern Asia produced 16% of the worlds cereal crops at 450 Mt: the third most globally, just behind Eastern Asia (including China) at 640 Mt and Northern America

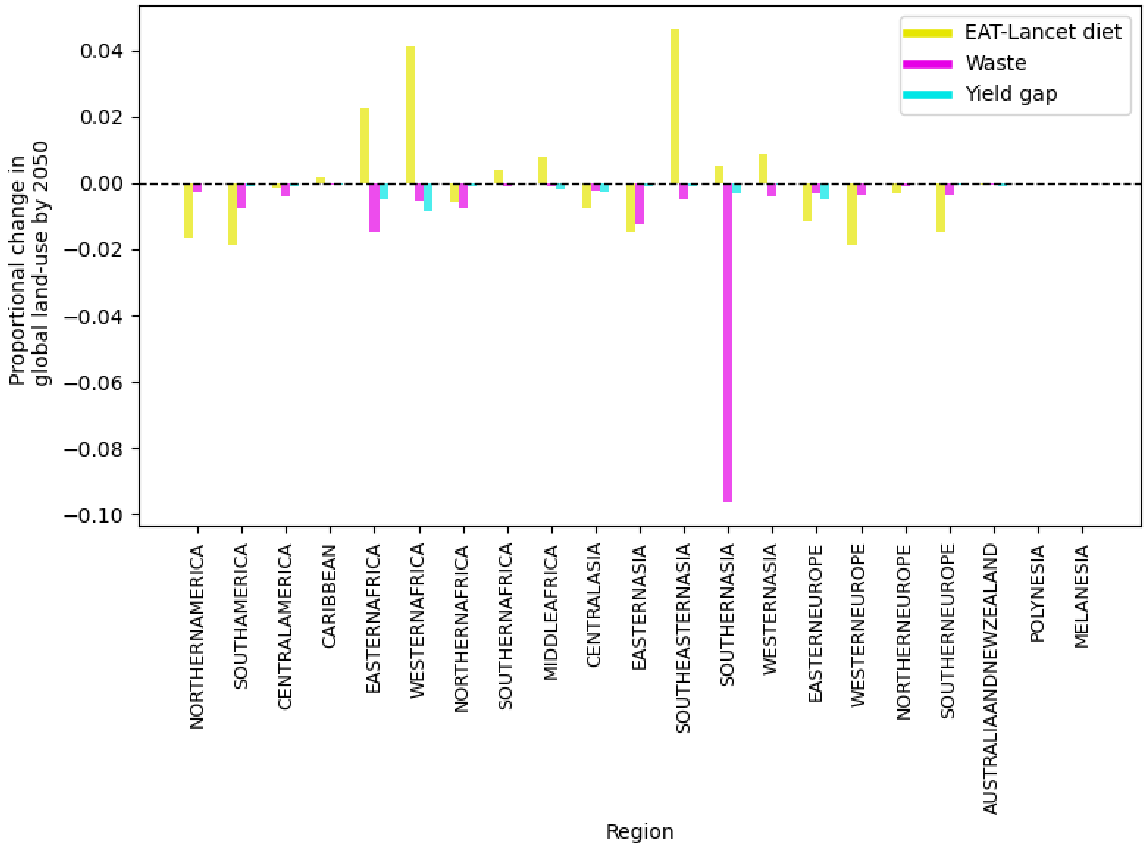

Figure 5.3: Proportional change in *global* land use compared to the C-LLAMA anchor scenario when prescribing one of three 'land use efficiency' options to the food system in a region.

at 500 Mt (FAO, 2022). In SSP2, the population of India grows by upward of 500 million people by 2050, whereas Northern America grows by only 100 million, and Eastern Asia actually sees a net decrease of 80 million people over the same time period (KC & Lutz, 2017).

In 14 of the 21 regions, the magnitude of land use impacts of transitioning to the EAT-Lancet diet are greater than the changes achieved through closing yield gap or reducing waste and losses. In fact, on the global stage, closing yield gaps appears to have very little impact on total agricultural land use at all; it only out 'performs' reducing waste in two regions: Western Africa and Eastern Europe. These two regions saw the largest proportional increases in cereal production (almost doubling in both cases) when closing yield gaps in Mueller *et al.* (2012).

From a global perspective, of the three options tested, the EAT-Lancet diet is the best option for improving land availability in mostly upper-middle and high income regions. Applying the diet in Northern America, and Western, Northern, and Southern Europe lead to global land use decreases of between 1-2%. This result aligns with the general trend of increased proportional consumption of less land efficient food products (animal products, and fruits and vegetables as opposed to cereals and starchy roots). It is also the best option in Eastern Asia, which has seen a rapidly rising consumption of beef in recent years and hence a projected continuation of this rise in C-LLAMA (Li *et al.*, 2018). In these regions, reducing waste has less impact than diet, surprising given the high levels of post-production waste in industrialised regions, which directly inflates food demand. However, the majority of countries in these regions have low levels of processing and distribution losses. This result highlights the importance of diet and the potential role of the consumer in achieving climate targets.

The EAT-Lancet diet causes relatively large increases in global agricultural land use (2-4%, or approximately 100-200 Mha) when prescribed in Eastern and Western Africa, and South-Eastern Asia. As discussed in Chapter 3, this does not mean that transitioning to such a diet in these regions should be avoided. The EAT-Lancet diet scenarios prescribe a trajectory toward a diet that is consistent with planetary boundaries, which may serve to improve environmental performance in these regions in aspects other than agricultural land use, in addition to improving diet quality and health (The Eat-Lancet Commission, 2019). However, since improving diet in these regions increases agricultural land use, decreasing agricultural land use through other means is likely to be more difficult in these regions if the goal of also providing a nutritionally sufficient diet is also to be met.

The results shown in Figure 5.3 are dependant on the total amount of food production and demands within the region compared with other regions. The general picture is altered when considering agricultural land use only within the region targeted by the changes to diet, waste, or yield, shown in Figure 5.4. Southern Asia once again sees

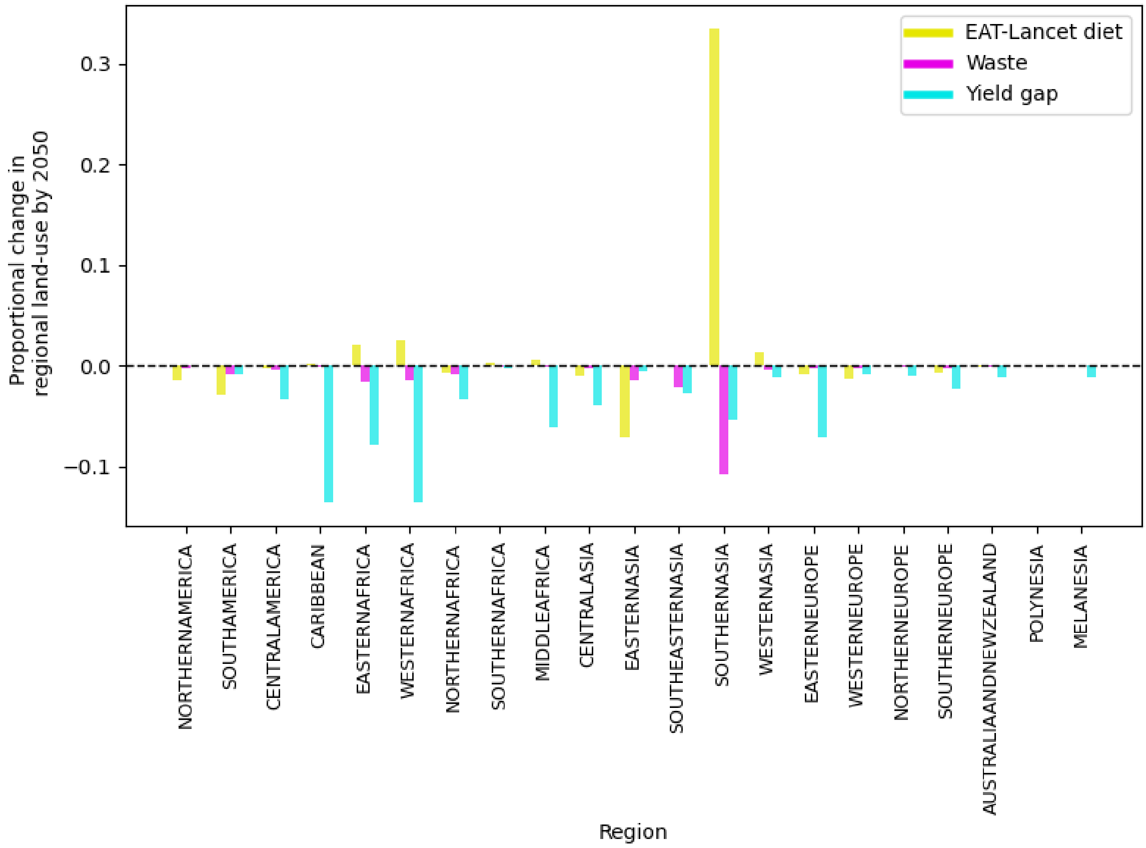

Figure 5.4: Proportional change in land use compared to the C-LLAMA anchor scenario for the target region when prescribing one of three 'land use efficiency' options to the food system.

the most dramatic land use change of any region with over a 30% increase, but this time in the diet scenario rather than the waste scenario. This result was discussed in Section 3.3.1, and is due to a combination of rapidly growing populations and initially high consumption of cereals and starchy roots, transitioning into higher quantities of fruits, vegetables, and pulses (which are more generally land extensive). With only four exceptions, prescribing any of the three changes to efficiency lead to a reduction in local agricultural land use within the region. In addition to diet in Southern Asia, the exceptions are all diet, in Eastern and Western Africa, and Western Asia. Like Southern Asia, diets in Western and Eastern Africa are heavy in cereals and starchy roots, especially cassava in Eastern and Western Africa (Tian & Yu, 2019). Western Asia (the largest producer and consumer in which is Turkey) sees a very marginal land use increase of 0.01% in the EAT-Lancet diet scenario.

In 16 of the 21 regions, closing the yield gap in that region leads to larger reductions in localised agricultural land use than reducing waste or prescribing the EAT-Lancet diet. As previously mentioned, increasing yield will decrease land use exclusively in the targeted region, whereas diet and waste will have impacts in both the targeted region and elsewhere, dependant on imports and exports. In the simple world of C-LLAMA, there is no dynamic trade or trade matrices; increases in a demand for a certain food product in a given region distribute the production globally based on historical production quantities (see Section 2.3.3). However, in reality, trade is much less universal. For example, Brazil is presently (as of 2019) the largest exporter of beef in the world, but the majority of it's exports are to a handful of regions rather than globally; almost 50% of it's exports go to China and Hong Kong, while these two countries do not account for 50% of global beef consumption (Zia *et al.*, 2019). Trade is complex, and typically the domain of economic equilibrium models, however it is probable that if beef consumption in a country were to increase, much of that demand would be met by countries from which it already imports. C-LLAMA currently fails to capture this, and hence fails to capture the fact that prescribing changes to food system efficiency in one region is likely to impact external regions in different ways.

5.4 CONCLUSION

In this chapter, the impact of closing yield gaps on agricultural land use (when compared with a projection of current yield growth) was modelled in C-LLAMA. These results were then compared with results from Chapters 3 and 4 to explore the 'best options' for improving land use efficiency at a regional level. Unsurprisingly, regions with large populations (or projected populations) were especially sensitive to changes particularly in diet (albeit sometimes leading to an increase in land use), since in C-LLAMA the food demand of a region is directly proportional to its population.

Food waste in C-LLAMA is divided into two components: post-production waste, and production (processing and distribution) losses. Post-production waste is tied directly to diet and hence population, whereas production losses occur in the region of production, so are linked more closely to total regional food production production. As a country industrialises and production wastes decrease, post-production waste tends to increase (see Section 4.1, Gustavsson *et al.* (2011)). In the scenarios analysed here, waste seemed to have the greatest impact in regions of generally lower and middle incomes (Southern America, Eastern, Western and Northern Africa, and Eastern and Southern Asia). In general, more food is wasted earlier in the supply chain than later at 48% and 35% respectively of the estimated global total (Lipinski *et al.*, 2013), so sensitivity is skewed toward less industrialised regions, since they are where higher levels of early-stage waste and losses occur. Additionally, in C-LLAMA the transition between the two 'states' of full subsistence and fully industrialised is linear. Each country in C-LLAMA sees waste at both stages; those that lie in the middle get 'medium' values for both waste and loss avenues. Given two inversely proportional linear trajectories, their product will always be maximised at the point where they intersect, so countries that lie somewhere in the middle will get the worst of both worlds and see higher levels of overall food waste. The real world is far more complex than C-LLAMA however, and this linear transition between the two cases may not be the case, and so the middle peak may never occur; exploration of this is an avenue for further research.

With the goal of producing biomass feedstock for energy generation and carbon capture and storage (BECCS), land made available in one region is not equivalent to another. As will be discussed in more detail in Chapter 6, productivity varies significantly between regions and even on a country level scale, in addition to the fact that many forecasts and bioenergy potentials assume that second generation energy crops (such as miscanthus x giganteus) are grown on less-productive marginal or degraded agricultural land (Wang *et al.*, 2021; Næss *et al.*, 2021). Indeed, many integrated assessment model scenarios favour tropical climates for energy crop production due to their productivity (see Chapter 6). Many of the regions most sensitive to the changes made in the C-LLAMA scenarios lie in the tropics (Eastern and Western Africa, South-Eastern Asia, and Southern Asia); and in three of these regions applying the EAT-Lancet diet led to a significant increase in global land use upward of 2% (100 Mha). Food insecurity and hunger are prevalent in these regions (Cooper *et al.*, 2021), so the sustainable production of energy crops may present additional challenges and competition for land use.

In almost all regions, the most effective change to the food system to improve land use was different depending on the consideration of total land footprint (global land use), or land use specifically within the region where the changes were applied. Unsurprisingly, yield was significantly more impactful than diet or waste at the local scale, since it only applies to local land use, whereas changes to diet or waste have impacts on land use in other regions due to trade. The lack of a dynamic trade module is highlighted as a key step in the future development of the C-LLAMA model. Currently, an increase in a food commodity demand in a region affects all regions independent of where the increase occurred (production an additional demand for 100 tonnes of wheat will be distributed the same if the demand comes from the Caribbean or Western Asia). Realistically, despite increasing globalisation, trade favours proximity more than the C-LLAMA mechanism would indicate (illustrated by Figure A.1).

6

Environmental governance quality and other factors may jeopardise delivery of bioenergy in mitigation scenarios

Abstract

Land based mitigation strategies play a crucial role in future scenarios consistent with Paris Agreement warming limits. Biomass energy is likely to require unprecedented land use change for energy generation and greenhouse gas removal. However, the risk of relying on countries with poor governance quality and other pressures on land-use is yet unquantified. In this chapter it is shown that a high proportion (approximately 35-70% by 2050 and 41-70% by 2100) of bioenergy production in mitigation scenarios with end-of-the-century radiative forcing values of 2.6 Wm^{-2}

and 1.9 Wm^{-2} consistently occurs in regions with historically poor environmental and general governance quality, with 4% having extremely poor environmental performance. Nearly half of cumulative energy crop production occurs in regions with a tropical climate before 2050 (36-37% by 2100), where land productivity and emissions due to land use change are high. Almost one third (57%) of production occurs in regions with a food demand growth of up to 30%, and 37-38% occurs in regions with food demand growth of between 30% and 60%, which are likely to experience increased pressures on land use from food demand, production, and growing populations. The efficacy of bioenergy as a carbon neutral energy source and BECCS as a greenhouse gas removal technology will be reduced in countries where these factors accumulate.

6.1 INTRODUCTION

Biomass is a prominent energy source in future low emission scenarios, used as both an energy source and, when coupled with carbon capture and storage (BECCS), a greenhouse gas removal (GGR) method. The integrated assessment models (IAMs) used to produce these scenarios rely heavily on the deployment of biomass energy due to it being potentially carbon neutral and versatile - usable for heat, electricity generation and transport fuel (Daioglou *et al.*, 2019). Biomass feedstock can come from dedicated energy crops as well as forestry and agricultural residues and food waste (Breunig *et al.*, 2017; Rogelj *et al.*, 2018b). In IMAGE scenarios approximately half of the total biomass energy is delivered by energy crops, with the remainder coming from residues (Vaughan *et al.*, 2018). Scenarios with lower end-of-the-century radiative forcing values have greater bioenergy use, with RCP1.9 scenarios ranging from below 50EJ yr^{-1} to upward of 500EJ yr^{-1}, with SSP1 and SSP2 scenarios making up the lower range of estimates, and SSP4 and SSP5 scenarios accounting for the higher end (Rogelj *et al.*, 2018b). There are a wide range of practical energy crop potential estimates from 130 EJ yr^{-1} to over 350 EJ yr^{-1} by 2050, with the former having tighter constraints on land selected for deployment (Fuss *et al.*, 2018).

For biomass to be effective as a carbon neutral energy feedstock or means of greenhouse gas removal, it is crucial that carbon removed from the atmosphere during photosynthesis is not offset by positive emissions elsewhere in the process. In addition to associated biodiversity impacts (Durán *et al.*, 2020), land use change is a potential source of significant greenhouse gas emissions in the production of biomass energy feedstock, as soil and vegetation carbon stocks are disrupted during land use change (Searchinger *et al.*, 2018). Land use change for crops and pasture are together the largest contributors to agricultural land emissions through expansion into forests and grasslands (Hong *et al.*, 2021). Between 20-25% of current cumulative greenhouse gas emissions are the result of land use change (Searchinger *et al.*, 2018). Carbon stocks and thus potential emissions due to land use change are dependent on several factors: climate, previous land-use (including other types of agriculture), and vegetation. Deforestation and poor forest management are major contributors to anthropogenic greenhouse gas emissions; the worlds forests are a major carbon sink and store, especially in tropical climates (Csillik *et al.*, 2019). In the pursuit of land intensive mitigation strategies forest removal is not likely to be beneficial, and should be avoided (Harper *et al.*, 2018).

Literature exploring the mechanisms to facilitate widespread bioenergy deployment highlight the importance of effective governance and policies at domestic and international scales (Dooley & Kartha, 2018; Hurlbert *et al.*, 2019; Kreuter & Lederer, 2021). Integrated assessment model projections infer some level of national action, but a 'high level of abstraction' is required to represent the non-economic factors (social and policy) surrounding the production of energy crops (Low & Schäfer, 2020). A significant portion of energy crop production in mitigation scenarios occurs in countries with historically poor environmental governance (Vaughan *et al.*, 2018). However, presently there are few attempts to quantify the risk of relying on countries of historically poor environmental or general governance quality to deliver sustainable biomass energy (Torvanger, 2019). Deforestation, land use change emissions, and food competition are likely to be key factors in the sustainable deployment of large-scale energy crop production, especially in developing regions, and those lacking effective governance frameworks (Humpenöder *et al.*, 2018; Haberzettl *et al.*, 2021). Reducing Emissions from Deforestation and forest Degradation, and the enhancement of forest carbon stocks (REDD+) is a framework for sustainable forest management and policy implementation (UNFCCC, 2022). REDD+ is a global initiative that typically operates at project scales, and has thus far been only moderately successful (Duchelle *et al.*, 2018). Similar frameworks are likely to play an essential role in the pursuit of bioenergy as a negative emissions technology (Kreuter & Lederer, 2021).

In this chapter we identify three sources of uncertainty surrounding the sustainable governance of bioenergy delivery and make an exploratory attempt to quantify them. First, tropical land is more productive than temperate land and thus generally favoured by IAMs for energy crop production. However, carbon stocks are also higher in tropical land, increasing the risk of emissions due to poor land management. Second, poor governance quality could incur some 'leakage', placing the sustainable delivery of biomass energy at risk if policy measures are not implemented properly. Finally, many counties projected to produce energy crops are also likely to see an increase in food demand, potentially introducing competition for land use between the food and energy crop agriculture.

6.2 METHODS

SCENARIO DATA

Scenario data in this chapter is used at two levels of regional disaggregation. The analysis contextualising the scenario space (Section 6.3.1) was conducted using publicly available data from the SSP scenario database (Rogelj *et al.*, 2018b; Gidden *et al.*, 2019; Riahi *et al.*, 2017). Energy crop production in 2020 was subtracted from the 2050 value, at the five-regional level, for all scenarios in the database. The five regions and constituent countries are listed in Table 6.1. Additionally SSP2 scenarios in the database compatible with end-of-the-century post-industrial global warming limits of 2.0°C and 1.5°C were analysed.

For analyses of governance, climate, and food demand (Sections 6.3.2 to 6.3.4), IMAGE scenario data for four SSP2 scenarios were used. The data for these four scenarios was kindly provided by collaborators Prof van Vuuren and Dr Daioglou at the PBL Netherlands Environment Agency. The four scenarios are: a reference scenario, and three scenarios following representative concentration pathways (RCP) with end-of-the-century radiative forcing values of 4.5, 2.6, and 1.9 Wm^{-2}, labelled as RCP4.5, RCP2.6, and RCP1.9 respectively. RCP2.6 and RCP1.9 are compatible with end-of-the-century post-industrial global warming limits of 2.0°C and 1.5°C respectively. Data in these scenarios is aggregated into 26 regions, with some regions containing only one country (for example Japan and Brazil are their own region). Regional definitions and constituent countries can be found in Table 6.2.

CLIMATE CLASSIFICATION

The quantity of energy crop produced and energy crop land cover in 5 different climates (tropical, arid, temperate, cold (continental), and polar) was calculated for the four IMAGE SSP2 scenarios. The portion of Köppen-Geiger climate classes making up each country was calculated as a percentage of the country's total land area (Beck *et al.*, 2018). The proportional climatic make-up of a given region was calculated using a weighted (by land-area) sum of the climate make-up of constituent

Asia	Latin America	Middle East and Africa	OECD countries	Reforming economies
Most Asian countries with the exception of former Soviet Union states, Japan, and the Middle East	*Includes Latin America and the Caribbean*	*As described*	*OECD90 and EU member states (and candidates)*	*Countries from the reforming economies of Eastern Europe and the former Soviet Union*
Afghanistan, Bangladesh, Bhutan, Brunei Darussalam, Cambodia, China (incl. Hong Kong and Macao, excl. Taiwan) Democratic People's Republic of Korea, Fiji, French Polynesia, India, Indonesia, Lao People's Democratic Republic, Malaysia, Maldives, Micronesia (Fed. States of), Mongolia, Myanmar, Nepal, New Caledonia, Pakistan, Papua New Guinea, Philippines, Republic of Korea, Samoa, Singapore, Solomon Islands, Sri Lanka, Taiwan, Thailand, Timor-Leste, Vanuatu, Viet Nam	Argentina, Aruba, Bahamas, Barbados, Belize, Bolivia (Plurinational State of), Brazil, Chile, Colombia, Costa Rica, Cuba, Dominican Republic, Ecuador, El Salvador, French Guiana, Grenada, Guadeloupe, Guatemala, Guyana, Haiti, Honduras, Jamaica, Martinique, Mexico, Nicaragua, Panama, Paraguay, Peru, Suriname, Trinidad and Tobago, United States Virgin Islands, Uruguay, Venezuela (Bolivarian Republic of)	Algeria, Angola, Bahrain, Benin, Botswana, Burkina Faso, Burundi, Cameroon, Cape Verde, Central African Republic, Chad, Comoros, Congo, Côte d`Ivoire, Democratic Republic of the Congo, Djibouti, Egypt, Equatorial Guinea, Eritrea, Ethiopia, Gabon, Gambia, Ghana, Guinea, Guinea-Bissau, Iran (Islamic Republic of), Iraq, Israel, Jordan, Kenya, Kuwait, Lebanon, Lesotho, Liberia, Libyan Arab Jamahiriya, Madagascar, Malawi, Mali, Mauritania, Mauritius, Mayotte, Morocco, Mozambique, Namibia, Niger, Nigeria, Occupied Palestinian Territory, Oman, Qatar, Rwanda, Réunion, Saudi Arabia, Senegal, Sierra Leone, Somalia, South Africa, South Sudan, Sudan, Swaziland, Syrian Arab Republic, Togo, Tunisia, Uganda, United Arab Emirates, United Republic of Tanzania, Western Sahara, Yemen, Zambia, Zimbabwe	Albania, Australia, Austria, Belgium, Bosnia and Herzegovina, Bulgaria, Canada, Croatia, Cyprus, Czech Republic, Denmark, Estonia, Finland, France, Germany, Greece, Guam, Hungary, Iceland, Ireland, Italy, Japan, Latvia, Lithuania, Luxembourg, Malta, Montenegro, Netherlands, New Zealand, Norway, Poland, Portugal, Puerto Rico, Romania, Serbia, Slovakia, Slovenia, Spain, Sweden, Switzerland, The former Yugoslav Republic of Macedonia, Turkey, United Kingdom, United States of America	Armenia, Azerbaijan, Belarus, Georgia, Kazakhstan, Kyrgyzstan, Republic of Moldova, Russian Federation, Tajikistan, Turkmenistan, Ukraine, Uzbekistan

Table 6.1: Region descriptions and constituent countries at the five-regional level in the SSP scenario database.

Region	Constituent countries
Canada	Canada
USA	St. Pierre and Miquelon, United States
Mexico	Mexico
Central America	Anguilla, Aruba, The Bahamas, Barbados, Belize, Bermuda, Cayman Islands, Costa Rica, Dominica, Dominican Republic, El Salvador, Grenada, Guadeloupe, Guatemala, Haiti, Honduras, Jamaica, Martinique, Montserrat, Netherlands Antilles, Nicaragua, Panama, Puerto Rico, St. Kitts and Nevis, St. Lucia, St. Vincent and the Grenadines, Trinidad and Tobago, Turks and Caicos Isl., Virgin Isl. (Br.), Virgin Islands (U.S.)
Brazil	Brazil
Rest of South America	Argentina, Bolivia, Chile, Colombia, Ecuador, Falklands Isl., French Guyana, Guyana, Paraguay, Peru, Suriname, Uruguay, Venezuela, RB
Northern Africa	Algeria, Egypt (Arab Rep.), Libya, Morocco, Tunisia, Western Sahara
Western Africa	Benin, Burkina Faso, Cameroon, Cape Verde, Central African Republic, Chad, Congo (Dem. Rep.), Congo (Rep.), Cote d'Ivoire, Equatorial Guinea, Gabon, Gambia, The, Ghana, Guinea, Guinea-Bissau, Liberia, Mali, Mauritania, Niger, Nigeria, Sao Tome and Principe, Senegal, Sierra Leone, St. Helena, Togo
Eastern Africa	Burundi, Comoros, Djibouti, Eritrea, Ethiopia, Kenya, Madagascar, Mauritius, Reunion, Rwanda, Seychelles, Somalia, Sudan, Uganda
South Africa	South Africa
Western Europe	Andorra, Austria, Belgium, Denmark, Faeroe Islands, Finland, France, Germany, Gibraltar, Greece, Iceland, Ireland, Italy, Liechtenstein, Luxembourg, Malta, Monaco, Netherlands, Norway, Portugal, San Marino, Spain, Sweden, Switzerland, United Kingdom, Vatican City State
Central Europe	Albania, Bosnia and Herzegovina, Bulgaria, Croatia, Cyprus, Czech Republic, Estonia, Hungary, Latvia, Lithuania, Macedonia (FYR), Poland, Romania, Serbia and Montenegro, Slovak Republic, Slovenia
Turkey	Turkey
Ukraine	Belarus, Moldova, Ukraine
Central Asia	Kazakhstan, Kyrgyz Republic, Tajikistan, Turkmenistan, Uzbekistan
Russia	Armenia, Azerbaijan, Georgia, Russian Federation
Middle East	Bahrain, Iran (Islamic Rep.), Iraq, Israel, Jordan, Kuwait, Lebanon, Oman, Qatar, Saudi Arabia, Syrian Arab Republic, United Arab Emirates, Yemen (Rep.)
India	India
Korea	Korea (Dem. Rep.), Korea (Rep.)
China	China, Hong Kong, China, Macao, China, Mongolia, Taiwan
South-Eastern Asia	Brunei, Cambodia, Lao PDR, Malaysia, Myanmar, Philippines, Singapore, Thailand, Vietnam
Indonesia	East Timor, Indonesia, Papua New Guinea
Japan	Japan
Oceania	American Samoa, Australia, Cook Isl., Fiji, French Polynesia, Kiribati, Marshall Islands, Micronesia (Fed. Sts.), Nauru, New Caledonia, New Zealand, Niue, Northern Mariana Islands, Palau, Pitcairn, Samoa, Solomon Islands, Tokelau, Tonga, Tuvalu, Vanuatu, Wallis and Futuna Island
Rest of South Asia	Afghanistan, Bangladesh, Bhutan, Maldives, Nepal, Pakistan, Sri Lanka
Rest of Southern Africa	Angola, Botswana, Lesotho, Malawi, Mozambique, Namibia, Swaziland, Tanzania, Zambia, Zimbabwe

Table 6.2: Region descriptions and constituent countries at the 26-regional level in four SSP2 scenarios produced in IMAGE (PBL Netherlands Environmental Assessment Agency, 2018).

countries. For example, the region containing the USA (only), is <1% tropical, 23% arid, 32% temperate, 36% cold, and 8% polar. Energy crop production in the four IMAGE SSP2 scenarios (reference, RCP4.5, RCP2.6, and RCP1.9) is then categorised by the climate of the region. This has the consequence of placing some production in polar climates (for example 8% of production in the USA), which in reality is unlikely given the lack of productivity in polar climates. However, in the absence of spatial energy crop production data, this method is sufficient for an exploratory quantification.

GOVERNANCE AND ENVIRONMENT INDICATORS

The Worldwide Governance indicators (WGI) are a set of six metrics which together are designed to capture the many aspects of governance quality (World Bank, 2019). Each country is assigned a score between -2.5 and +2.5 for each of the six metrics, which are: voice and accountability, political stability and absence of violence, government effectiveness, regulatory quality, rule of law and control of corruption. The metrics are highly inter-linked; it can be shown that the first component of a principle component analysis sufficiently describes 86% of the inter-metric variance (Langbein & Knack, 2010). We perform a principle component analysis of the 2019 values of the dataset to produce a combined score to represent the whole dataset. The Environmental Performance Index is an aggregate metric based on 32 individual indicators of environmental governance quality for 180 countries (Wendling *et al.*, 2020). Scores in 2021 for the metric range between 22.6 and 82.5, with the lowest score being Liberia and the highest being Denmark.

Energy crop production and energy crop land cover in regions of different WGI and EPI scores was calculated for the four IMAGE SSP2 scenarios. Both the first principle component of the WGI dataset and the EPI scores were divided into five bins of equal score range. Each nation was assigned two scores from 1 to 5 based to represent the ‘risk’ of failure to deliver sustainable bioenergy due to either general governance or environmental performance quality, with bin 1 containing nations of least concern and bin 5 containing nations of high concern. A third score of 'disagreement' was calculated: the difference in score between the two bins. Energy crop production for each 'bin' in the WGI and EPI is calculated.

FOOD SUPPLY

Energy crop production and energy crop land cover was calculated for regions of given proportional changes in food demand energy, for the four IMAGE SSP2 scenarios. C-LLAMA (Country-Level Land Availability Model for Agriculture) is an open-source, national-level statistical-empirical model of food demand and production based on UN FAOSTAT data (Ball *et al.*, 2022). C-LLAMA makes linear projections of diet and food supply for each country to the year 2050. The food supply trajectory takes post-production waste into account: it is the amount of food energy required to feed each person in the country for a given year assuming some of that food is wasted post-production (see Sections 2.3.2 and 4.1 for further detail). To calculate the growth in food energy demand for a given region, the projected food supply (per capita) was multiplied by the UN medium population scenario projection for countries within the region, then the sum of projected demands is calculated. Finally, the proportional growth between 2020 and 2050 is calculated. The range of values was split into 5 bins (from -30% to greater than 100% change in proportional food energy demand), and the energy crop production and land cover in regions of each bin calculated. The region containing only Japan, and the UKR region (Belarus, Moldova, and Ukraine) see reductions in food energy demand. The EAF region (Eastern Africa: including Burundi, Comoros, Djibouti, Eritrea, Ethiopia, Kenya, Madagascar, Mauritius, Reunion, Rwanda, Seychelles, Somalia, Sudan, and Uganda) is the only region that sees a food energy demand increase greater than 100% between 2020 and 2050 (between 100% and 130% increase).

6.3 RESULTS

6.3.1 SCENARIO CONTEXT

In this section, all instances of ‘energy crop production’ refer to the production of dedicated energy crops. This includes first generation crops such as sugarcane and maize, and second generation lignocelluosic crops such as miscanthus and switchgrass. Initial energy crop production varies significantly between scenarios, but more significantly between models: MESSAGE-GLOBIOM scenarios all have global energy crop production between 900 and 1400 Mt(DM) (million tonnes of dry matter) per year in 2020, and GCAM4 scenarios between 350 and 420 Mt(DM) yr^{-1}. Scenarios from IMAGE and REMIND-MAGPIE models range from 80 to 180 Mt(DM) yr^{-1} energy crop production mass in 2020, and AIM/GCE scenarios range from 19 to 24 Mt(DM) yr^{-1}. Only IMAGE and REMIND-MAGPIE have any energy crop production in 2010, so the increases between 2010 and 2020 are dramatic in many cases: from 0 to 1400 Mt(DM) yr^{-1} in one instance. However, the increases in production over the first half of the century (2020 to 2050) are more stable: most models see significant energy crop production increases in this time period.

Figure 6.1 shows the range of bioenergy crop production mass change from 2020 to 2050 in all modelled scenarios in the SSP database. Lower RCP scenarios rely heavily on energy crop production. The expansion of energy crop production from 2020 to 2050 is consistently lower as the end of century radiative forcing (RCP) value increases, with production increases greater than 2000 Mt(DM) yr^{-1} in RCP1.9, RCP2.6, and RCP4.5 scenarios, and increases of less than 1000 Mt(DM) yr^{-1} in all but one RCP 6.0 scenario. All scenarios see the least energy crop production increase in the reforming economies and a greater change in production in Asia, Latin America and OECD countries. In some RCP1.9 and RCP2.6 scenarios: Asia, Latin America, and OECD countries see production increases upward of 2000 Mt(DM) yr^{-1}

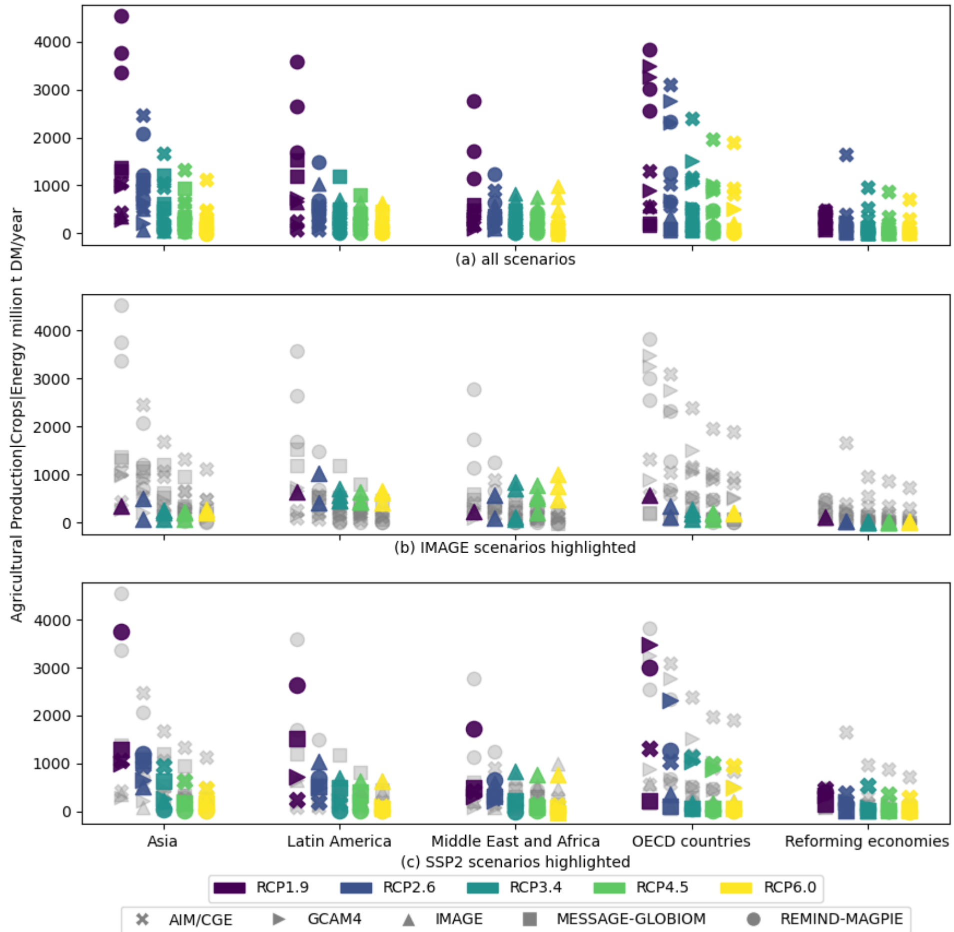

Figure 6.1: Change in energy crop production between years 2020 and 2050 in (a) all SSP-RCP database scenarios (n = 81), (b) IMAGE model scenarios (n = 14) and (c) SSP2 scenarios (n = 24). Representative concentration pathways 1.9, 2.6, 3.4, 4.5 and 6.0 are arranged into columns with 11, 13, 17, 17, and 12 scenarios respectively. REF to the SSP scenarios here – specifically the data.

between 2020 and 2050. In 2011 an estimated 1200 Mt of biomass feedstock was produced *globally*, of which only 17% was used for energy generation (Haberzettl *et al.*, 2021). Approximately 1% of global agricultural land use was dedicated to the production of biomass in the same year (Haberzettl *et al.*, 2021). Considering these historical estimates, future regional production quantities of thousands Mt(DM) yr^{-1} are unprecedented.

IMAGE is the most conservative model in the suite, with lower energy crop production than other models in the majority of scenarios (Figure 1(b)). In no IMAGE scenarios does production mass in any region significantly exceed 1000 Mt(DM) yr^{-1}. In all scenarios, IMAGE places relatively more of this energy crop production increase in the Middle East & Africa and Latin America regions than other models do, with increases between 200 and 1000 Mt(DM) yr^{-1}. Interestingly, the largest increases in energy crop production in the Middle East and Africa occur in higher RCP (3.4, 4.5, and 6.0) IMAGE scenarios. IMAGE places very little energy crop production in the reforming economies in all scenarios, with an SSP1-RCP1.9 scenario seeing the largest increase at just over 100 Mt(DM) yr^{-1} between 2020 and 2050. Since it typically makes the most conservative estimates for energy crop production in mitigation scenarios, results in this chapter will be focused around IMAGE scenarios. SSP2 scenarios are selected as the focus of this chapter, since SSP2 is the 'middle-of-the-road' shared-socioeconomic pathway, with medium challenges the adoption of mitigation strategies in addition to a 'medium' population scenario: many aspects of the SSP2 marker scenario reflect an extension of the historical experience (Fricko *et al.*, 2017).

Figure 6.2 shows the production of energy crops in a range of SSP2 scenarios with end-of-the-century radiative forcing values of 1.9 Wm^{-2} (RCP1.9) and 2.6 Wm^{-2} (RCP2.6), all consistent with pre-industrial warming targets of 1.5°C and 2.0°C. In the marker scenarios, rapid increases in energy crop production to 3000 Mt(DM) yr^{-1} occur throughout the century for Asia and Latin America, with slight slowing toward the latter half of the century. The lower boundary is higher for Asia (approximately 1000 Mt(DM) yr^{-1} by 2100) than Latin America (approximately 100 Mt(DM) yr^{-1} by 2100), and the upper limit is much greater at nearly 6000 Mt(DM) yr^{-1} by 2100 compared to approximately 3300 Mt(DM) yr^{-1} in Latin America. In the OECD countries, energy crop production in the marker scenarios is slightly over half of that in Asia and Latin America by 2100, but the upper boundaries for both RCP1.9 and RCP2.6 scenarios are both approximately 6000 Mt(DM) yr^{-1} by 2100, with faster production increases occurring before 2050. Relatively little energy crop production is allocated to the

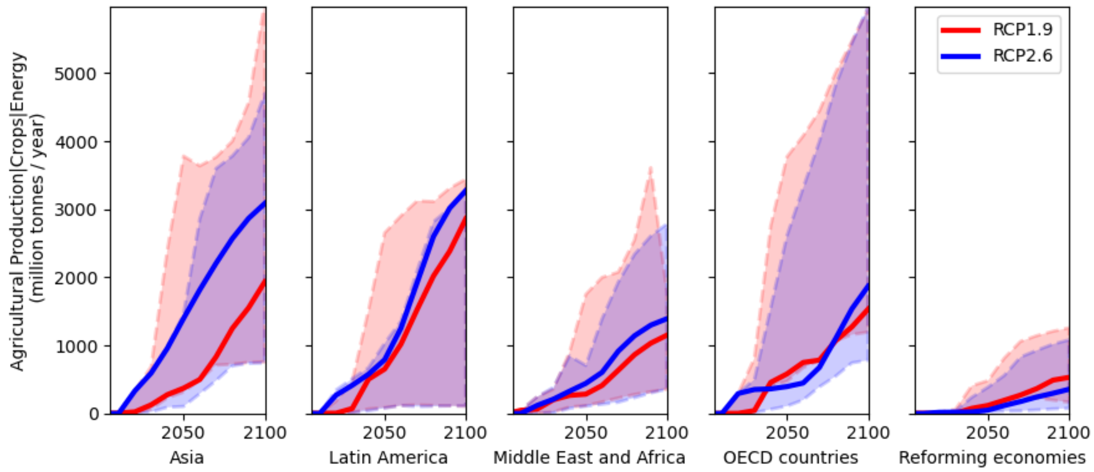

Figure 6.2: Regional energy crop production in SSP2 scenarios consistent with Paris Agreement warming targets to end of century. Solid lines represent the marker scenarios, shaded areas are the range of other scenarios.

reforming economies in all scenarios, with the RCP2.6 and RCP1.9 marker scenarios reaching 400 and 500 Mt(DM) yr^{-1} by 2100 respectively. The upper boundary for energy crop production in the reforming economies by 2050 is just under 500 Mt(DM) yr^{-1} in both RCP1.9 and RCP2.6 scenarios.

6.3.2 CLIMATE

In the four IMAGE SSP2 scenarios with end-of-the-century radiative forcing values of 4.5 Wm^{-2} (RCP4.5), 2.6 Wm^{-2} (RCP2.6), 1.9 Wm^{-2} (RCP1.9), and a reference scenario, increases in energy crop production are front-loaded to the first half of the century, with the rate of increase in production mass and land cover peaking at around 2070 (Figure 6.3). In the reference scenario and RCP4.5, energy crop production increases steadily for the first part of the century, reaching around 250 Mt(DM) yr^{-1} by 2030. The majority of this increase is in tropical regions for both scenarios, accounting for over 60% in both cases. From 2030 to around 2070, more rapid increases in production mass take place, reaching approximately 1000 Mt(DM) yr^{-1}, at which point the acceleration slows and production increases by an approximate further 100 Mt(DM) yr^{-1}. The tropical share of production is approximately half of the global

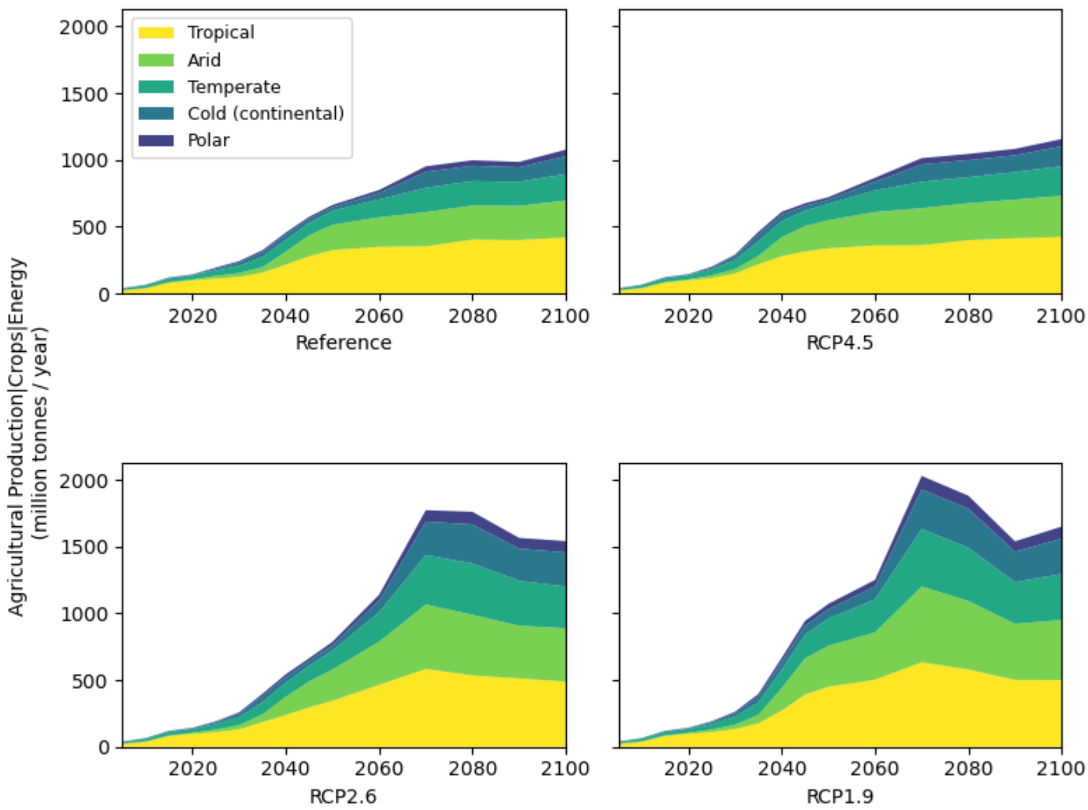

Figure 6.3: Energy crop production mass for regions of different Koppen climate classifications, in IMAGE SSP2 reference, RCP4.5, RCP2.6, and RCP1.9 scenarios. Each region was apportioned a percentage of each climate classification; leading to the result that a small amount of energy crop is produced in polar climates.

total by 2100 in both of these scenarios. Temperate regions have the second largest share in production, although production in arid and cold climates is comparable (approximately 30%, 20%, and 10% of total 2100 production for temperate, arid, and cold climates respectively). In the scenarios consistent with warming targets of 1.5°C and 2.0°C (RCP1.9 and RCP2.6), global energy crop production mass increases considerably from 2030 to 2070, from around 300 Mt(DM) yr^{-1} to 1750 Mt(DM) yr^{-1} in RCP2.6, and to 2000 Mt(DM) yr^{-1} in RCP1.9. Initially, much of this production increase occurs in the tropics, which produce almost half of all energy crops until around 2060 (48% and 45% for RCP2.6 and RCP1.9 respectively), at which point production in other climates beings to catch up, with the total yearly production in other climates overtaking that of the tropics around 2070. In RCP2.6, tropical regions account 38% of the total energy crop production over the course of the century, with arid, temperate, cold, and polar regions account for 25%, 20%, 12%, and 4% respectively. The pattern is similar in RCP1.9, with tropical regions producing 37% of the cumulative total; arid, temperate, cold, and polar regions account for 26%, 20%, 12%, and 4% respectively.

Comparing the energy crop production mass results of Figure 6.3 with the energy crop land-cover results of Figure 6.4, similar patterns emerge. All scenarios are characterised by an initially rapid rate of expansion before 2050, with the rate of expansion slowing by 2070. In all scenarios, energy crop land cover begins to shrink around the year 2080. Crop yields in these scenarios are assumed to increase throughout the century in many regions, albeit slowing before 2050, gradually increasing the land-use efficiency of energy crop production (van Zeist *et al.*, 2020). Additionally, the requirement for energy crop production decreases slightly toward the end of the century as cumulative carbon emissions are brought closer to pre-industrial levels, leaving only the requirement to offset gross emissions. All four scenarios have resurgences in expansion rate from 2060 to 2080, but this is more pronounced in mitigation scenarios RCP1.9 and RCP2.6. The fastest rate of initial expansion occurs in RCP1.9, from less than 10 Mha in 2020 to over 250 Mha in 2050, compared with a change from 10 to approximately 180 Mha over the same time period in the RCP2.6 scenario. As with production mass, the tropics host the majority of the pre-2050 energy crop land cover expansion (around 35-40% of global cover in 2050 in all four scenarios). In RCP2.6 and RCP1.9, energy crop land use also expands quickly in arid climates to around 40% of the total, then slowing around 2050. After around 2060 contribution to energy crop land cover from the tropics drops to 36% of the total (in 2080), and the total contributions from arid, temperate, and cold climates slightly overtake (approximately 20%, 25%, and 20% respectively). As discussed in Section 6.1, tropical climates are generally highly productive, thus placing energy crop production there may reduce the overall land footprint of climate change mitigation. However, production in these regions poses a greater risk of disrupting the initially high terrestrial carbon stocks, especially when forests are removed to facilitate energy

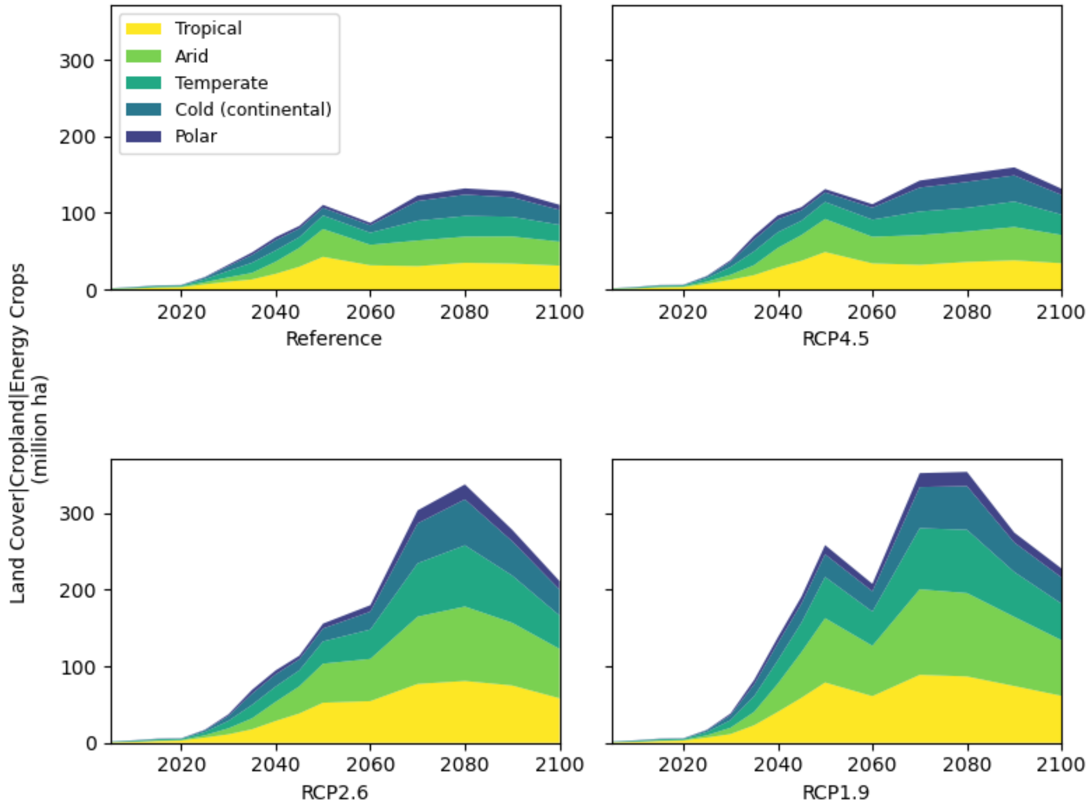

Figure 6.4: Energy crop land cover in regions of different climate classifications, in IMAGE SSP2 reference, RCP4.5, RCP2.6, and RCP1.9 scenarios.

crop production (Harper *et al.*, 2018).

6.3.3 GOVERNANCE

Country-level scores on the Worldwide Governance Indicators metric (WGI) and the Environmental Performance Indicators (EGI) metric are shown in Figure 6.5. At the continental scale, the two metrics generally agree with one another. Countries in highly industrialised regions such as Europe, Australia, Japan, South Korea, and North America have low scores of 1 and 2 on both metrics. Scores in South America are between 2 and 5 on both metrics. Most countries in Central and Southern Asia (including China and India) have WGI scores of 3, but EPI scores of 4 and 5. Illicit forestry practices and illegal deforestation are widespread issues in Southern Asia (including India) and South-Eastern Asia (including Indonesia), which is reflected in

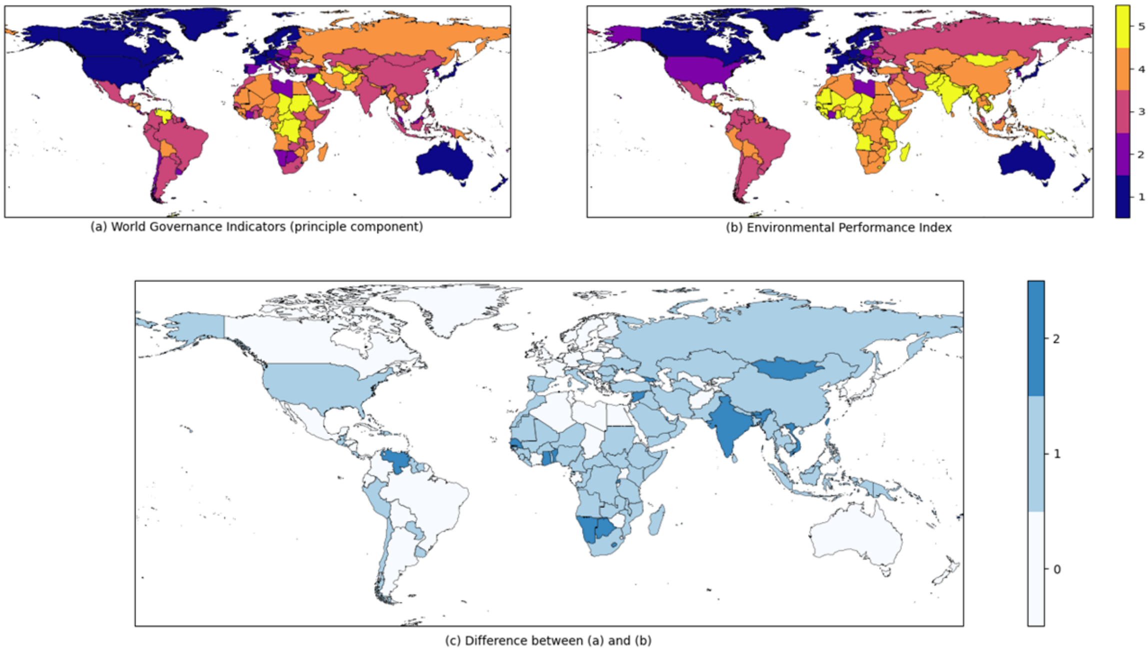

Figure 6.5: Country scores on the principle component of the Worldwide Governance Indicators (WGI) (a), the Environmental Performance Indicators (EGI) (b), and the magnitude of difference between the two (c). Values for (a) and (b) range from 1 to 5, where 1 represents a country of high quality governance according to the WGI, and good environmental performance according to the EPI. No countries have a score difference of 4 and only Fiji, Micronesia, and Cabo Verde have a score difference of 3 (omitted for visual clarity).

their moderate WGI scores but poor EPI scores (Kumari *et al.*, 2019; Tacconi *et al.*, 2019). The majority of the African continent scores 3 and 5 on the WGI metric, with the exceptions of Namibia, Botswana, Libya, and Côte d'Ivoire, which score 2. EPI scores across Africa are generally higher than the WGI scores, with most countries scoring 4 or 5. Russia scores 4 and 3 on the WGI and EPI metrics respectively.

Disagreement between the metrics (Figure 6.5(c)) is generally low in North and South America, Europe, North Africa, and Oceania. Disparities between the scores are larger in Sub-Saharan Africa and much of Asia. Based on the results shown in Figure 6.5, it appears that discrepancies between the scores are highest in lower-middle and middle-income countries. This is perhaps reflective of increased economic activity and hence environmental pressures, especially GHG emissions (the environmental Kutznet curve), while policy action to address environmental impacts lags behind (Dasgupta *et al.*, 2006).

Figures 6.6 and 6.7 show energy crop production four IMAGE SSP2 scenarios (reference, RCP4.5, RCP2.6, and RCP1.9), grouped by regional scores on the WGI (principle component) and EPI metrics. Regions with a WGI score of 3 (moderate overall governance quality) make up the majority share in pre-2050 production (66 - 70% of cumulative 2020 to 2050 production in all 4 scenarios). Production in regions with scores of 2 and 4 (good and poor governance quality respectively) begins around 2030. In these two brackets, production rate doesn't vary dramatically between scenarios but is slightly higher in the RCP2.6 and RCP1.9 scenarios, peaking at around 250 Mt(DM) yr^{-1} in both. Energy crop production in regions with a score of 1 (excellent governance quality) begins around 2050 in all scenarios. In RCP1.9 and RCP2.6, energy crop production in regions with a score of 1 is significantly higher than in the reference and RCP4.5 scenarios, with more than double the yearly production by around 2080. No regions were assigned a WGI score of 5, hence no production occurs in that bracket. Overall, 70% of cumulative energy crop production by 2050 occurs in regions with a WGI score of 3 or 4 in RCP2.6 and RCP1.9 (also approximately 70% by 2100). The distribution of production across the EPI scores is more even than that of the WGI metric, with less emphasis being placed on one particular score-bracket. As with the WGI metric, pre-2050 energy crop production initially favours regions with a score of 3. However around 2030, production increases quickly in regions with scores of 1 and 2, up to around 500 Mt(DM) yr^{-1} in the reference and RCP4.5 scenarios, and up to approximately 1000 Mt(DM) yr^{-1} in the RCP2.6 and RCP1.9 scenarios. Regions with scores 3, 4, and 5 increase production in the latter half of the century, especially in the RCP2.6 and RCP1.9 scenarios, where they produce just over 750 Mt(DM) yr^{-1}, or just under half of total production, at their peak (around 2070). Overall, 35% of cumulative energy crop production by 2050 occurs in regions with EPI scores of 3 or 4 in RCP2.6 and RCP1.9 (increasing approximately 41% by 2100). Around 4% of production throughout the century occurs in regions with a score of 5 (extremely poor environmental performance).

While these metrics are not analogous to sustainable energy crop production in a

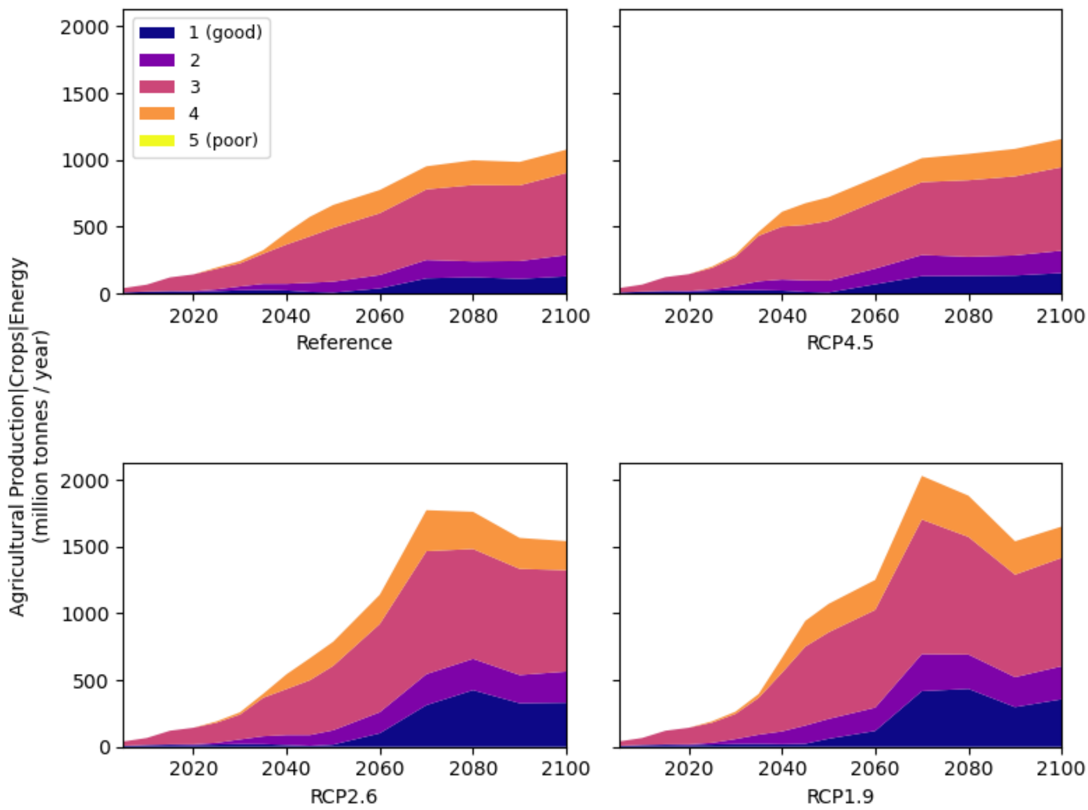

Figure 6.6: Energy crop production mass in IMAGE SSP2 reference, RCP4.5, RCP2.6, and RCP1.9 scenarios, categorised by regional scores on the Worldwide Governance Indicators (WGI) principle component metric. Colours correspond to Figure 6.5: scores of 1 and 5 correspond to high and low quality governance respectively. When aggregating countries into regions to align with scenario data, no regions have an aggregate score of 5.

given region, they represent the potential greater challenges to sustainability and increased risk of failure. Regions with a scores of 1 and 2 on either metric are likely to be at low risk of unsustainable energy crop production, since they have quality governance frameworks (WGI) and a history of good environmental performance (EPI) in place. On the other hand, regions with higher scores may represent a greater risk of unsustainable energy crop delivery through failure due to weaker governance structures (e.g. poor provision of monitoring and verification). The initial rapid ramp-up of energy crop production assigned to regions with a WGI score of 3, and the reliance on regions with EPI scores greater than 2 may be cause for concern. A significant portion of energy crop production occurs in these regions, a portion that may be at risk of diminished sustainability and therefore reduced efficacy as

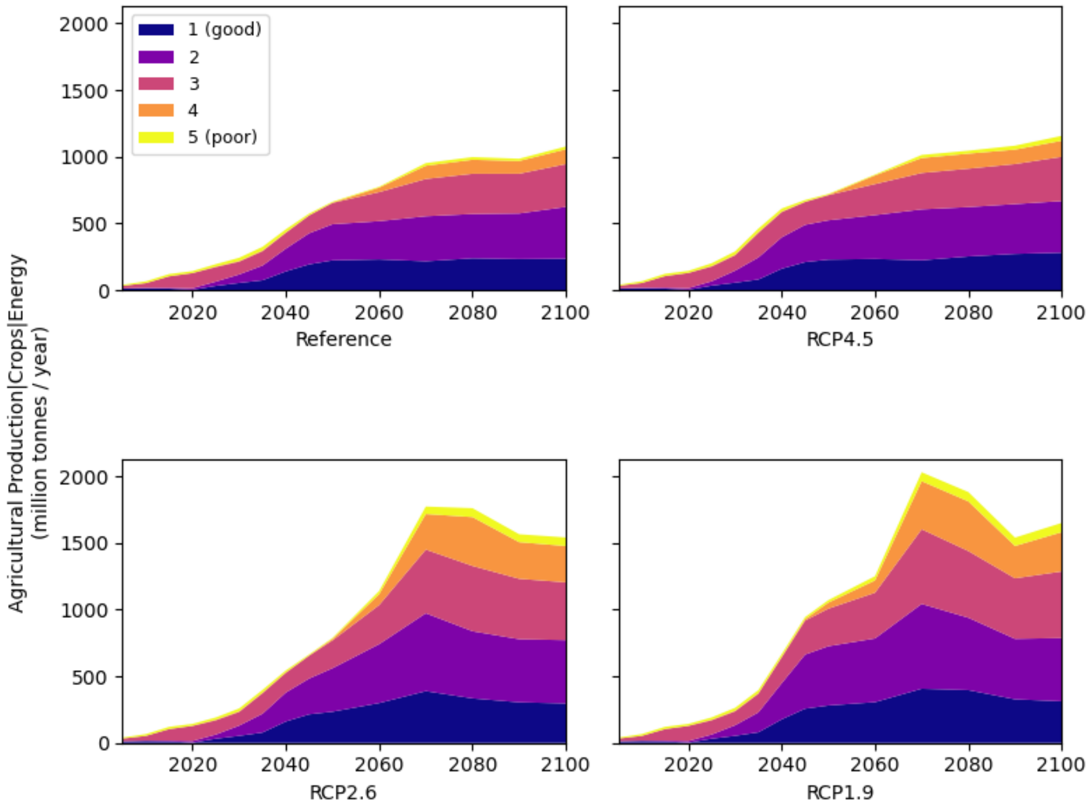

Figure 6.7: Energy crop production mass in IMAGE SSP2 reference, RCP4.5, RCP2.6, and RCP1.9 scenarios, categorised by regional scores on the Environmental Performance Index (EPI) metric. Colours correspond to Figure 6.5: scores of 1 and 5 correspond to good and poor environmental performance respectively.

a low carbon energy source or GHG removal strategy. However, it is important to note that the scores used in these results are snapshots of the present, so there is plenty of scope for change, especially post-2050. Additionally, global governance frameworks, guidance, and incentives (analogous to REDD+ in the forestry industry) may be able to aid the sustainability of biomass production in regions with historically lower governance quality (Torvanger, 2019).

6.3.4 FOOD DEMAND

An additional pressure on land available for for energy crop production in mitigation scenarios are the increasing food demands of many regions. There are a wide range of estimates for future bioenergy potentials, but few consider the already increasing global food energy demand, or ever prevalent aspirations to improve nutritional content and sustainability of diet in many regions (Dias *et al.*, 2021). In response to growing populations and increasing demand for less land-efficient food products, it is expected that agricultural production will need to approximately double by 2050 (Duro *et al.*, 2020), and cropland to expand by upward of 69 Mha (Bahar *et al.*, 2020). Along with the pressures increasing food demand will place on natural forests and ecosystems, it also adds an additional dimension of complexity for energy crop production.

C-LLAMA makes simple linear projections of food energy demand and dietary trajectories; it does not make any prescriptions regarding the nutritional content of projected diets (see Section 2.3.1). Despite this, C-LLAMA projects that food energy demand increases in almost all countries by 2050, along with increases in the portion of food energy provided by animal products (Figure 2.3). Note that these trajectories also take into account an estimate of post-production food waste and are reflective of the characteristic increase in food-waste quantity that accompanies increased food availability (Katt & Meixner, 2020). Taking into account changing populations, these food supply trajectories are used to calculated country-level yearly total demand for food.

Figures 6.8 and 6.9 show energy crop production mass and land cover in four IMAGE SSP2 scenarios, grouped by proportional, regional changes in food demand energy (from 2020 to 2050). In all scenarios, the vast majority of energy crop production and land expansion occurs in regions with an increased food demand by 2050. In all scenarios, less than 2% of the cumulative 2100 total energy crop is produced in regions with a reduction in total food demand energy. In the reference and RCP4.5 scenarios, 60% of all energy crops are produced in regions with up to a 30% increase in total food demand. In RCP2.6 and RCP1.9, 57% is produced in these regions. Cumulatively throughout the century, 34%, 33%, 37%, and 38% energy crop production occurs in regions with a 30% to 60% increase in total food demand, in the

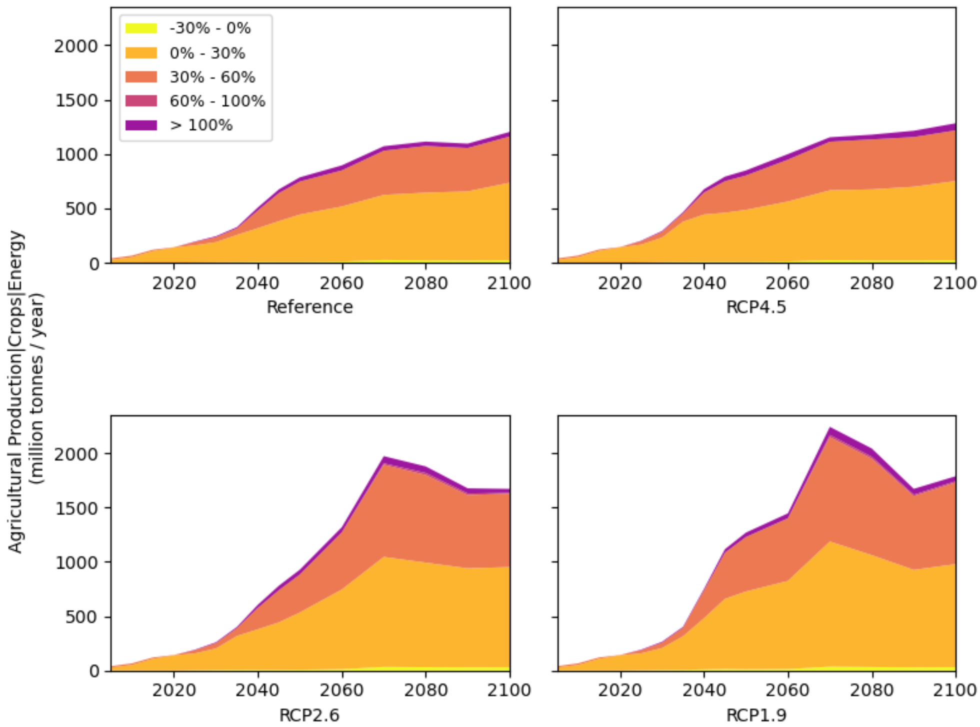

Figure 6.8: Energy crop production mass in IMAGE SSP2 reference, RCP4.5, RCP2.6, and RCP1.9 scenarios, categorised by proportional change in food supply quantity (total food supply calories multiplied by projected population) from 2020 to 2050 (C-LLAMA runs until 2050). Values between 0.7 and 1.0 indicates a net reduction in food supply from 2020 to 2050 of up to 30%. Values between 1.0 and 1.3 indicate a net growth of up to 30%.

reference, RCP4.5, RCP2.6, and RCP1.9 scenarios respectively. Regions with a food supply increase between 60% and 100% produce a very small quantity of energy crop (cumulatively less than 0.5% in all scenarios). However, the group of regions with food demand increases greater than 100% produce 3% of the cumulative total in the RCP2.6 and RCP1.9 scenarios.

In all scenarios, the initial deployment of energy crop production occurs in regions with up to 30% growth in food energy demand, until around 2040. Expansion in the 30% group continues after 2040, but is accompanied by additional expansion in the 30% to 60% growth bracket. This result is unsurprising given the rising requirement and demand for food, but highlights a further complication.

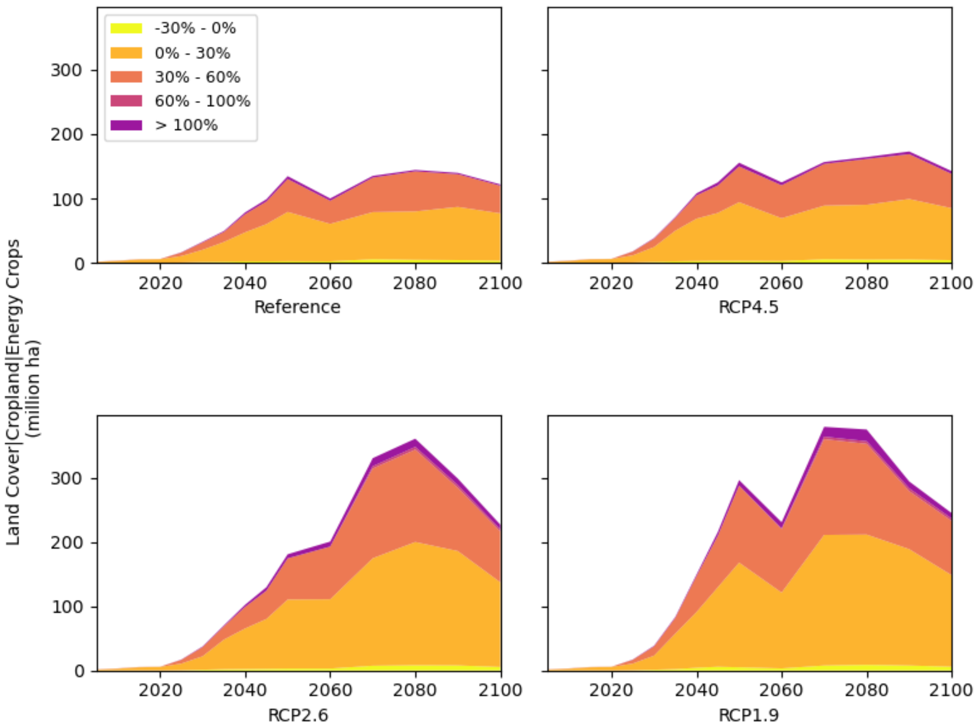

Figure 6.9: Energy crop land cover in IMAGE SSP2 reference, RCP4.5, RCP2.6, and RCP1.9 scenarios, categorised by proportional change in food supply quantity (total food supply calories multiplied by projected population) from 2020 to 2050.

6.4 CONCLUSION

Future projections made by IAMs are not certain, and there is a high level of uncertainty surrounding the quantity and land-use required to produce sufficient energy crops to meet climate targets in these scenarios. This is especially true in low emissions scenarios such as RCP1.9 and RCP2.6, where the production requirement to meet Paris temperature goals may be anywhere between 2500 Mt(DM) yr^{-1} to upward of 10000 Mt(DM) yr^{-1} by 2100 (Popp *et al.*, 2017). IMAGE scenarios were the focus of this chapter, and while the ramp-up in energy crop production pre-2050 may seem dramatic, IMAGE is also typically a conservative model in the suite.

In this chapter it was found that there may be significant complications to the deployment of energy crops. Tropical climates are preferred within IAMs for energy crop production due to their generally higher productivity and therefore yields; this is reflected in the four SSP2 scenarios analysed here, where nearly half of initial energy crop production (pre-2050) occurs in tropical climates. Additionally, between 35 and 70% of production occurs in regions which have had historical adversity surrounding governance quality and environmental performance. Many of these regions are also lower or middle income, so may face additional challenges during their ongoing development. These include rapidly growing populations and therefore food energy requirements, along with rising increase for less land efficient food commodities, especially animal products.

To ensure that bioenergy is carbon neutral, and that BECCS delivers on net atmospheric carbon removal, it is essential that emissions in the supply chain, especially land-use change emissions, are minimised (Harper *et al.*, 2018). Strong environmental governance is essential to minimise carbon 'leakage' during energy crop production and carbon storage (Lyngfelt *et al.*, 2019). This means complete aversion to deforestation (which comes with additional ecological benefits), since forests account for a significant portion of the terrestrial carbon pool, especially tropical forests which hold an estimated 306–324 Pg of carbon (Mackey *et al.*, 2020). Tropical forest deforestation (and deforestation in other climates) to make way for energy crop production is generally avoided in most IAM scenarios. However, in the real world this is not the case: over half of the world's remaining primary forest can be found in developing countries (Mackey *et al.*, 2015), where food demand and competition for land are increasing. Forest removal to facilitate agriculture (often illegal but poorly policed) is an ongoing problem (Tacconi *et al.*, 2019).

While the methods of analysis used in this chapter are crude compared to the incredible complexity of the real world, they provide an exploratory estimate of the magnitude of potential challenges to sustainable energy crop delivery. Meeting climate targets is likely to require unprecedented large-scale energy crop production, the governance frameworks for which are not yet in place (Martin *et al.*, 2020; Torvanger, 2019). Placing large portions of pre-2050 energy crop production in these regions, where deforestation, weak governance, and increasing food demand may accumulate may compound the risk, since there will be no previous examples of energy crop production on the required scale from which to learn.

7

Discussion and conclusion

This chapter will provide a summary and discussion of the work carried out in this thesis and the findings of the previous chapters. A large portion of the work in this thesis was the development of the Country-Level Land Availability Model for Agriculture (C-LLAMA). C-LLAMA is used in all subsequent chapters, so a discussion of the development process and sensitivity findings will follow, but additional reference to the model and it's strengths and weaknesses will be made as part of the discussion for other chapters.

Chapter 2 describes the development of the C-LLAMA model, along with the C-LLAMA anchor scenario, and sensitivity to changes in some of the key components of the model. This chapter was not framed around a specific research question as such, rather the purpose of C-LLAMA is to provide an open and transparent framework for modelling the land footprint of the agricultural system from a bottom up approach, beginning with food demand. In Chapter 1, three key drivers of agricultural land use were identified: diet, waste and losses, and yields of both crops and pasture. C-LLAMA include a representation of each of these drivers, and behaves as expected when manipulating them, both in the sensitivity analyses conducted in Chapter 2, but also in the general findings of Chapters 3, 4, and 5. In that sense, the development of C-LLAMA has been successful, the simplicity of the model allows it to be easily modified to construct scenarios surrounding any of those drivers.

The C-LLAMA anchor scenario is a baseline scenario in which all dynamic factors in the model, such as diets, yields, waste streams, and efficiency parameters are projected linearly to 2050 from their historical data, or calculated historical values. It acts as a business as usual scenario from which to compare the results of other modelled scenarios. The global land use trajectory in the anchor scenario is comparable to that of FALAFEL (Powell, 2015), starting at around 4.7 Gha in 2017, then growing to approximately 5.2 Gha in 2050, with pasture and fodder crop areas growing, and food crops seeing a slight decrease of around 50 Mha over the time period. Each continent sees a continuation of it's historical trend in land use, with the exception of Europe, that has a slight increase where historically it was decreasing; this is down to Russia having extensive production of crops and livestock, which in C-LLAMA leads to it being allocated a high portion of production as demand grows. C-LLAMA doesn't aim to make explicit predictions about future land use, but rather to represent the food system in an internally consistent way. So by comparing modelled scenarios to the anchor scenario, the sensitivity of the food system to the drivers of agricultural land use can be inferred.

While C-LLAMA is a solid initial framework for food system modelling, there are a number of avenues for development of the model that would improve it's representation of the food system and it's nuances. The first is the land use aspect of the model; the current version of C-LLAMA simply calculates the land necessary to meet the food production demand each year. However, in reality agricultural land use is far more complex: land use is not 'on or off', agricultural land may be abandoned due to reduced productivity (sometimes indefinitely) or lack of local necessity, driving agriculture into natural grasslands or forest, or sometimes in a rotation around previously used crop and pasture land (Subedi *et al.*, 2021; Munroe *et al.*, 2013). The abandonment and reutilisation process is not linear (as the structure of C-LLAMA might imply), and is also highly dependant on the ecology, climate, industrialisation, and policy of the area (Subedi *et al.*, 2021). A next step in the development of C-LLAMA would be to implement a dynamic land use system, with a country-level bin for each land type (including natural biomes), then a set of rules to govern the transition of land between each category, driven by the food production demand. Such a system would also facilitate the inclusion of a simple land use change carbon emissions and uptake model, and perhaps an exploration of the 'carbon opportunity costs' described by Hayek *et al.* (2021) and Searchinger *et al.* (2018).

There are other food system models with a similar simplistic structure as that of C-LLAMA. Bijl *et al.* (2017) present a food demand model, in which the demand for food commodities (equivalent to the diet section of C-LLAMA) are modelled based on projections of income and expenditure. However, the structure of the rest of the model is similar, although it terminates at 'crop-use' for food and animal feed, and 'grass-use' for animal feed. Another model that takes a similar approach is the Biomass Balance Model (BioBaM). BioBaM attempts to balance the supply and demand of 14 biomass streams (and corresponding food commodities) for 11 regions of the world (Kalt *et al.*, 2021). The BioBaM model doesn't have a land use allocation component, rather asking *is it possible to produce the required biomass on the land that is available?*, then discarding scenarios in which supply and demand are incompatible. Both of these models forego the inclusion of any kind of trade implications (by either stopping before, or using the balancing method in BioBaM). While the representation of trade in C-LLAMA is coarse, it is at least a first-pass attempt at constructing such a model with an inferred trade mechanism.

The functionality of C-LLAMA is currently somewhat limited to exploring trends in global land use and the land footprints of regions without an improved trade mechanism, but the model provides a reasonable foundation upon which a trade mechanism can be built. Arguably, BioBaM provides the same foundation, since functionally the models are very similar, but C-LLAMA operates at a country-level and for a greater range of food commodities. Perhaps the reason there exist no comparable models of the food system in the spirit of BioBaM or C-LLAMA with a trade system, is that implementing one is impossible without surrendering the traceability of the model to an agent-based or economic equilibrium approach. This would be an unsatisfying outcome, so high on the agenda for further development of C-LLAMA is to attempt an improvement of the trade mechanism in a transparent way, perhaps by projecting trade matrices. In the event that a trade matrix for specific food commodities is not available, general 'food products' matrices could be used, and projected forward in time to 2050. This would allow C-LLAMA to explore scenarios with high levels of growth in regions that are currently less productive. Doing so would have been preferable in this iteration of C-LLAMA, but unfortunately the inconsistency and data complexity placed this outside the scope of this work.

In Chapter 3 the impacts of transitioning from projected dietary trends toward the EAT-Lancet planetary health diet (Willett *et al.*, 2019) were explored using C-LLAMA. The resulting global land use trajectory was actually very similar to that of the C-LLAMA anchor scenario, although the composition changed, with food crop area increasing by around 700 Mha, and pasture and fodder crop area decreasing by around 300 Mha and 250 Mha respectively, leading a slight overall increase in land use of approximately 150 Mha. Higher income regions and those with higher beef consumption saw overall decreases in land footprint as a result of prescribing the diet there. It also became clear that regions of larger population (or with higher projected population growth) were the most sensitive to changes toward the EAT-Lancet diet, with dramatic impacts when applying it in Central, Eastern, and especially Southern Asia which lead to a 40% increase in global crop area.

Population changes are the single most impactful driver of agricultural land use in a 'food first' modelling framework and in the context of the sustainable development goals. Throughout this thesis, the population trajectories used have been kept constant, but the UN medium population trajectory is just one scenario, and the reality may be very different. The findings of Chapter 3 indicate that while it may help to address ongoing global hunger and malnourishment, transitioning to a sustainable diet is likely to increase pressure on land use, meaning that improving land use efficiency in other areas (such as waste and yields) is all the more important.

Chapter 4 investigated the potential for increasing land availability through reductions in food waste and losses. Halving post-production food waste (globally) by 2030, a target set out by SDG 12.3, lead to a modest global agricultural land use decrease of 700 Mha compared with the anchor scenario in 2050, with the majority of that decrease (500 Mha) occurring in pasture. A similar pattern but slightly smaller decrease in land use of around 430 Mha was achieved when halving processing and distribution losses by 2030, again with the largest decrease occurring in pasture. All waste and loss streams in C-LLAMA (with the exception of harvest losses, which are not included here) are applied equally to all food products, so the change in land use for each of food crops, fodder crops, and pasture in these scenarios was proportional to their initial value. In reality, certain commodities are wasted or lost in higher quantities than others, for example roots and tubers are wasted the most (63% of global production energy), and oilseeds and pulses the least (10% of global production energy) (Lipinski *et al.*, 2013).

The availability of data for waste and losses was a source of frustration during the development of C-LLAMA. There are data available: for example the FAOSTAT food balance sheets have estimates of loss (FAO, 2021a), the Food Loss Index (also from the FAO (Koester & Galaktionova, 2021)), and the Food Waste Index (United Nations, 2021a) all have estimates for portions of commodities lost and wasted, but all suffer significant gaps in their data, especially for developing countries and less-traded commodities. It may be possible to take an accounting-based approach to estimating the portion of each commodity lost or waste, based on production, consumption, and import and export values. To do this for every country and commodity in C-LLAMA was outside the scope of the work in this thesis, but is an inviting avenue for development of the model; it would significantly improve the robustness of the model framework.

The first part Chapter 5 was an investigation of crop yields and the global land use implication of closing regional 'yield gaps' for several major food crops in C-LLAMA. Closing all yield gaps at once resulted in only a 100 Mha reduction in land use when compared with the C-LLAMA anchor scenario. In the regional analysis of closing yield gaps, the general expected trends of a greater land use impact in lower income countries, and those with a high portion of global cereal production were generally observed. Only a minimal reduction in land use compared to the anchor of up to 1% was observed when closing yield gaps in upper-middle and high income regions such as North America, Europe (excluding Eastern Europe), and Oceania.

The results of these analyses were less impactful than perhaps expected, especially given the disparity between currently achieved and attainable yields across many regions of the world (yieldgap.org, 2021). The C-LLAMA anchor scenario linearly projects yields forward to 2050; the relatively minor reduction in land use when closing yield gaps globally highlights the fact that perhaps continuously increasing yields every year leads to an overestimation of future crop yields, especially over periods of several decades. However, this is exactly the approach that many IAMs take, at least in the production of key scenarios surrounding Paris warming targets. For example, IMAGE assumes a universal increase in yield 0.75% per year in the RCP2.6 baseline scenario, an assumption based on historical yield increases (van Vuuren *et al.*, 2011). While 0.75% appears to be fairly conservative, it translates to an 82% yield increase over a period of 80 years (e.g. 2020 to 2100, or a 25% increase in the 10 years between 2020 and 2030). Note that it is unclear if this is a compound effect, but in the case that it is linear, the increase is still 60% over the same time period.

The second part of Chapter 5 was a comparison of the previous results in the chapter with the results of Chapter 3 and Chapter 4. In this part of Chapter 5, an attempt was made to assess the most effective changes for reducing the land use footprint of food demand within a given region. A clear result of these results was that in high income regions and those with high levels of animal product consumption, transitioning to the EAT-Lancet planetary health diet lead to the greatest reduction in land footprint (up to 2% decrease in global land use when applied in North and South America, and much of Europe). Of the three 'options' (diet, waste, and yield), changing diet lead to the largest change in land use footprint in 15 out of the 21 regions, although in three of those the change in land use was a positive one (Eastern and Western Africa, and South-Eastern Asia). Reducing waste was significantly more effective in regions with large populations (Eastern and Southern Asia) or those with high projected population growth (Eastern and Western Africa). The impact of reducing waste in Southern Asia was the largest effect of any option in any region, with a reduction in global agricultural land use of 10%.

The results of this section highlight the significant benefits of efficiency improvements in the global food system, not only for making land available for land based mitigation options, but also for ensuring the sustainable provision of food for future generations, and the provision of food to those currently suffering the effects of limited food availability and malnutrition. The EAT-Lancet diet is alone in the set of options in that it provides a direct benefit; even in high income regions where the availability of food is not a concern to most, the goal of the EAT-Lancet diet is to improve public health, which also applies to highly developed countries where overconsumption is a problem (Willett *et al.*, 2019; Schmidt & Matthies, 2018). In this sense, it is worth considering the case where the EAT-Lancet diet is prescribed everywhere. In this case, the improvements to land availability that come from reducing waste and improving crop yields become all the more important in light of the projected land demands of afforestation and BECCS, which are only likely to compound competition from the growing demands of the food system.

Chapter 6 explored the use of bioenergy in the whole scenario-space for scenarios in the SSP database. The scale of expansion (between 2020 and 2050) of bioenergy production varied dramatically between scenarios, from less than 500 Mt(DM) yr^{-1} to upward of 4000 Mt(DM) yr^{-1} within one region in RCP1.9 scenarios. The initial expansion of production was the least in IMAGE scenarios, with increases in the 2020 to 2050 time period of less than 1000 Mt(DM) yr^{-1} in all regions for all IMAGE scenarios. Asia and Latin America were identified as the regions allocated the most energy crop production in SSP2 scenarios. Both of these regions have countries across a range of economic development.

An exploratory attempt was made to quantify some of the risks posed to the sustainable delivery of energy crops for energy provision and BECCS in four SSP2 scenarios (a reference scenario, RCP4.5, RCP2.6, and RCP1.9). In the first half of the century all scenarios saw rapid expansion of energy crop production up to around 2050. In low emissions scenarios (RCP2.6 and RCP1.9, consistent with 2 °C and 1.5 °C respectively) the rate of expansion is greater, and continues well into the latter half of the century.

In the four IMAGE scenarios, but particularly the low emission scenarios, tropical regions bore a large portion of the pre-2050 ramp up of energy crop production (approximately one-third). Tropical regions are favoured due to their (typically) higher productivity. However, the high carbon stocks of tropical forests, and the historical propensity of some tropical regions to unsustainable forest management and deforestation raises questions surrounding the risk of leakage occurring during energy crop production in these regions. The quantity of energy crop production occurring in regions of varying general and environmental governance quality was then assessed for the four IMAGE scenarios. The metrics used for governance were the principle component of the Worldwide Governance Indicators (WGI) and the Environmental Governance Index (EPI). Both metrics were partitioned in 5 bins, from excellent (1) to poor (5). The results for the WGI metric showed that the majority of energy crop production in the scenarios (especially pre-2050) occurred in regions of moderate (3) governance, while regions with excellent (1) and good (2) governance quality only saw energy crop production beginning in earnest in the latter half of the century. The story was slightly more encouraging for the EPI metric; just over half of production occurred in regions of excellent (1) and good (2) environmental performance throughout the scenarios.

The method employed for this set of analyses was coarse: placing regions into bins of governance and historical environmental performance is a dramatic simplification of a complex system. Every country is different, and realistically, governing the production of energy crops for bioenergy and BECCS at national and international levels will require a careful approach on likely a case by case basis. Nevertheless, when considering both the WGI and EPI metrics, more than half of energy crop production occurs in regions where there might be an increased risk of leakage. The actual risk of relying on these regions unquantified (perhaps even unquantifiable), but there is little doubt that the risk is increased when compared with regions of high quality governance and environmental performance. Energy crops produced in these areas may have a larger carbon footprint than anticipated, obstructing the path to achieving climate targets. An avenue for further work might be to assess the historical carbon leakage in these regions, to estimate the level of leakage that might be incurred, and re-considering the governance and magnitude of energy crop production accordingly (Kreuter & Lederer, 2021).

The final part of Chapter 6 was a look into the projected food demand increases for regions producing energy crops in the four IMAGE SSP2 scenarios. The first few stages of C-LLAMA were used to estimate the growth in total food supply energy for each region, then each region was placed into a bin by proportional growth in food demand by 2050. In the C-LLAMA anchor scenario and hence this analysis, almost all regions undergo an increase in food demand by 2050. In the scenarios consistent with 2.0 °C and 1.5 °C warming targets, approximately 60% of energy crop production occurred in regions with a projected food demand growth up to 30%, and around 35% in regions with a growth up to 60%. A tiny portion (<4%) was produced in regions with a reduction in food demand or regions with a doubling of food demand. This is a simple result, but it highlights the importance of considering the production of food for growing populations and wealth, and the potential for increased competition for land use with energy crop production in these regions.

7.0.1 OUTLOOK

Those practicing the least destructive behaviours, contributing the smallest burdens on the planet, are likely to be the first affected by the repercussions of anthropogenic climate change. How we arrived at this circumstance is a certainty, and while the same cannot be said for the future, the efforts of climate science have provided us with pathways to mitigate the impending damage. Bioenergy, BECCS, and afforestation are the champions of integrated assessment modelling scenarios, and although they are subject to contested authority and controversial assumptions, directing our efforts there currently appears to be our best option. To achieve 1.5 °C by 2100 with BECCS and afforestation as keystone technologies will be a challenge in of itself, but even more so whilst upholding the tenets of sustainable development. The goal of this thesis has been to explore global land use prospects for mitigation in the context of one aspect of sustainable development: the provision of food. C-LLAMA takes a very simple approach to modelling the global food system, but in it's simplicity also lies it's strength: it has allowed each lever of the drivers of agricultural land use to be pulled in turn.

The recurring theme in the results of this thesis is that there is no single answer; short of eradicating animal product consumption overnight, not one of the drivers alone can alleviate the growing land use pressure for food production to facilitate the deployment of BECCS and afforestation. However, another recurring theme has been that the people and governments of income regions not only have the least sustainable food consumption and waste habits, but also the economic means and accessible solutions to improve them, for themselves and for others. To achieve 1.5 °C within the boundaries of equity for both nature and people, it is essential that the those that have the means to act now begin to do so on the behalf of those that cannot.

A

APPENDICES

Counter-intuitive behaviour arises when setting the proportion of animals fed through fodder and residues (fed without forage - FWF) to extreme values. Decreasing the FWF factor (more animals are fed through pasture) leads to an increase in land-use by 2050. This is expected, as pasture is typically far less land-efficient than housed animals fed through fodder and residues (Pikaar *et al.*, 2018). However, this trend does not continue when the FWF is increased, instead an increased land-use is observed. The behaviour of the FWF prompted further investigation; the factor was scaled by a range of values between 0.5 and 1.5 to observe the behaviour around the default values (a scaling of 1.0), the global agricultural land-use values for which are shown in Figure A.4.

Inspection of the land-use for pasture, fodder and food crops revealed that food crop land-use was constant as expected since only animal product production methods are being varied. Fodder crop land-use also behaved as expected – increasing with FWF, as more fodder crops must be produced to meet the feed demand of animals not produced on pasture. However, pasture did not behave as expected, instead following

Model Section	Description of processes within the section	Relevant modules
Diet and food supply	Projections of the contribution of each food commodity toward the national diet. Projection of national calorie supply per capita. Calculation of a global demand for each food commodity.	food_demand_and_waste_production diet_makeup
Food-system efficiency	Projection of losses and efficiencies that are used at various stages of the model. A food system efficiency parameter is developed to inform these values.	industrialisation_metric industrialisation_metric_calculations food_waste_gen harvest_residues
Crop production	Losses are used to calculate total production requirement for each food commodity, a portion of which is then allocated to each country. Crop yields are projected for each food and fodder crop in the model.	crop_yield_and_production_hist crop_yield_and_production_params crop_yield_projects crop_and_livestock_production crop_production_ratios
Livestock	The global production requirement for livestock is calculated and allocated to each country. Livestock consume a mix of feed and foraged food, the proportion coming from each varies by livestock type and country.	livestock_feed_demand fodder_crops
Land use	Production requirement energy is converted to mass and combined with yield to produce a land area requirement for both food and fodder crops. An 'effective livestock yield' is developed and used to calculate pasture land requirements.	crop_land_calculations pasture_land_calculations land_use_calculation

Table A.1: Five main sections within C-LLAMA, each comprised of a handful of model-process modules. There are sixteen model-process modules in total. There is some overlap between model-processes; the sections and model-process modules listed here are not necessarily in the order that they appear in C-LLAMA, some sections are re-visited at later stages of the model. The first section of the model produces a food supply at a national level, disaggregated into calories and commodities.

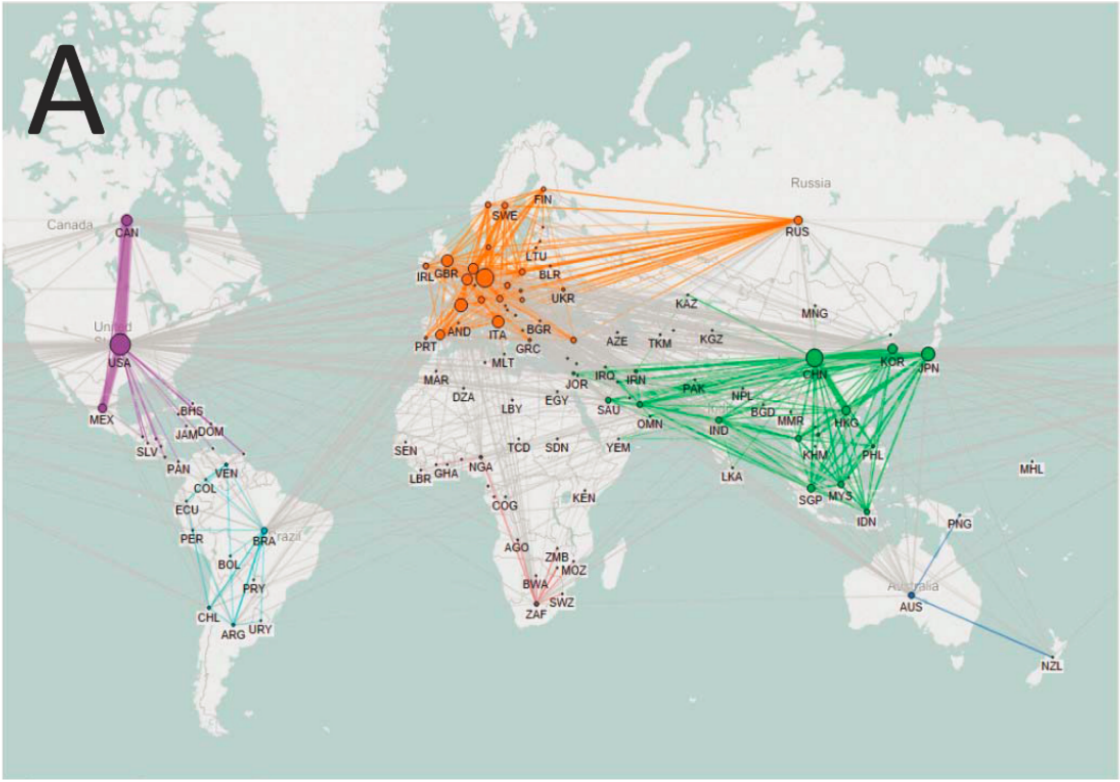

Figure A.1: Flow of international food trade between countries in 2018, taken from Konar *et al.* (2018). The size of the points are proportional to the flux of food (imports and exports) through the country.

the same trend as the global land-use, with an increased land-use when varying the FWF factor in either direction. The cause of this behaviour has been identified as the scaling method applied to pasture land area. When the scaling is turned off, variations in the FWF factor lead to expected behaviour: global land use decreases as FWF increases. The effective pasture yield is calculated using the projected 2017 land-use value before any scaling is applied. When FWF is increased the quantity of animal products produced on pasture decreases, including the 2017 value, however the historical pasture area remains unchanged. The result is an artificial decrease in effective pasture yield as FWF increases when the scaling is applied, as shown in Figure A.5.

To resolve this and any similar anomalies arising from scaling methods, the effective pasture yield is now scaled based on the projected pasture area in the anchor scenario, regardless of the scenario parameters. This can introduce minor discrepancies in the

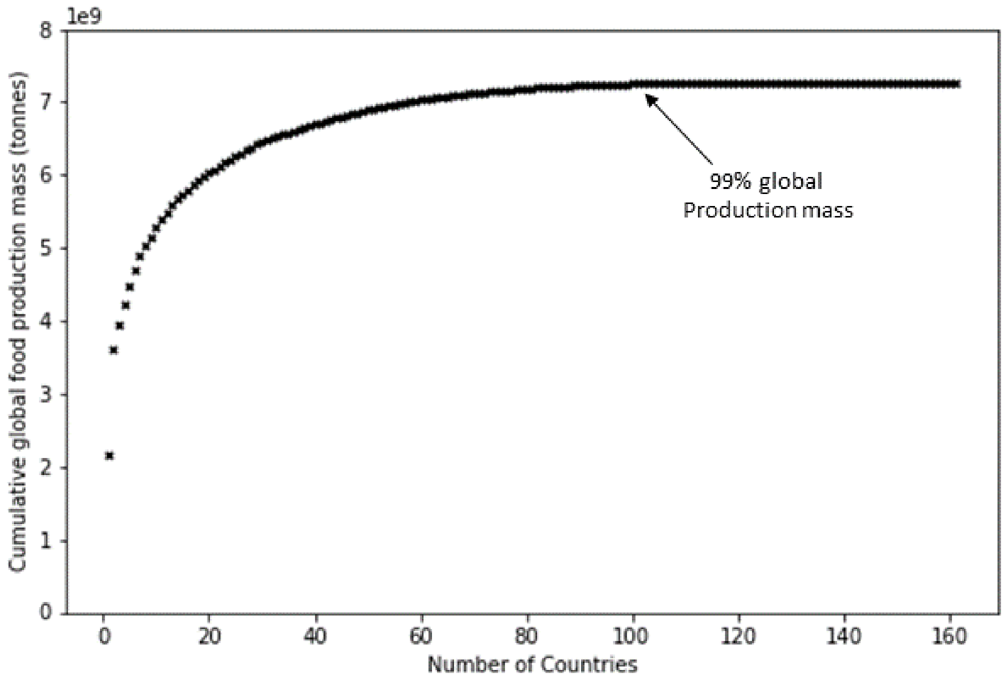

Figure A.2: Cumulative food production mass for the year 2017 of all current countries in the FAOSTAT database, dissolved states are not included.

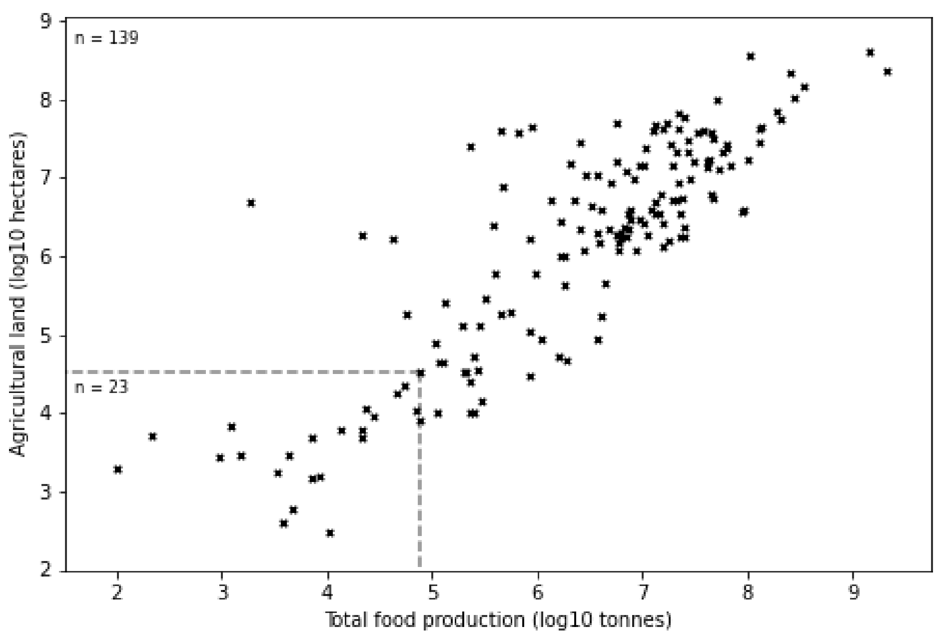

Figure A.3: Log of agricultural land area against total food production mass for the year 2017 for all countries in the FAOSTAT database, dissolved states are not included. Countries contained in the small dotted-line box are not included in model processes (n = 23), while the remaining countries are included (n = 139).

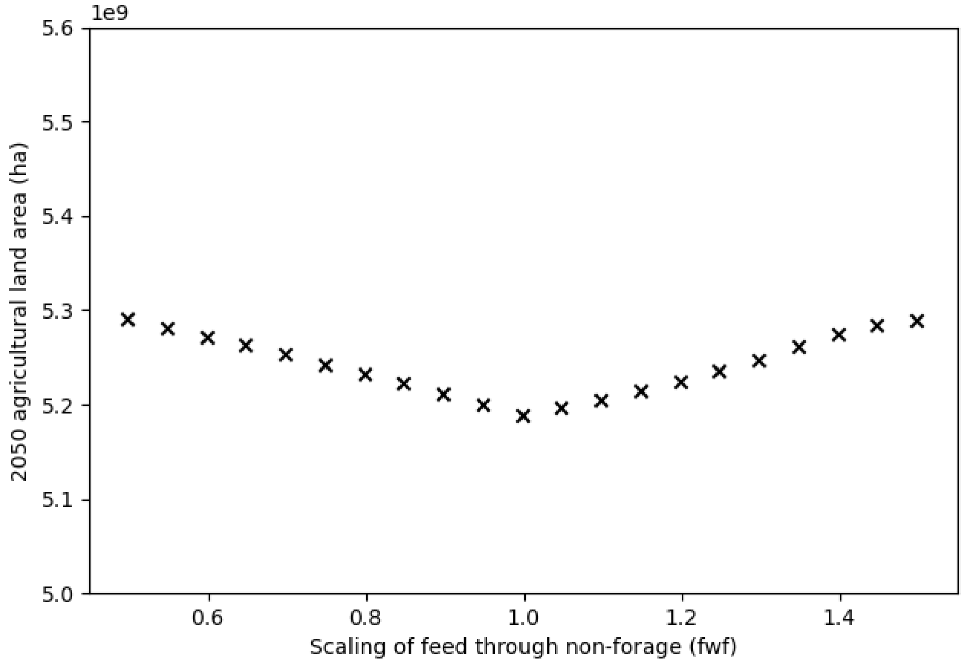

Figure A.4: Change in global agricultural land-use when varying the proportion of livestock feed from non-forage (FWF)

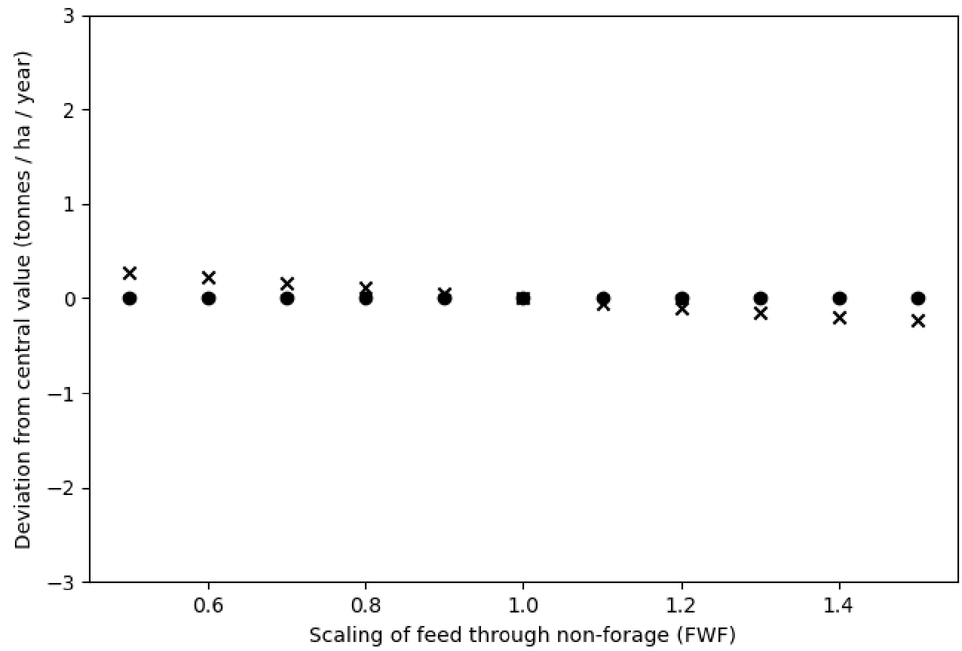

Figure A.5: Magnitude of change in pre and post global mean scaled effective pasture yield for forced scaling of livestock feed through non forage (FWF).

early years of the projection when setting factors to a fixed value, but this is not the normal mode of operation for the model. This sensitivity test varied the FWF factor for the entire projection, including the starting values, where in normal model operation any changes to this factor would be applied as a gradual deviation from the normal value. For example, the scaling might vary from 1.0 in 2017 to 1.5 in 2050, as opposed to being 1.5 from the start as in this sensitivity analysis.

Individual products	Grouped products
Wheat	Cereals
Rice	Fruits
Maize	Vegetables
Palm Oil	Pulses
Rape and mustard seed	Starchy roots
Soyabeans	Oil crops
Sunflower seed	Spices
Potatoes	Sugar crops
Cassava	Luxuries
Nuts and products	Other vegetal products

Table A.2: Vegetal products and grouped vegetal products. Grouped products do not contain any products represented as staple products. The luxury group consists of tea, coffee and cocoa

Individual products	Grouped products
Bovine meat	Other meat
Poultry meat	Dairy products
Pigmeat	
Mutton and goat meat	
Eggs	

Table A.3: Animal products and groups. In the case of these animal products, the 'individual' animal products represent a small group of products but are dominated by a single product. For example, while bovine meat includes derivative products and buffalo, the majority of the bovine meat supply and consumption is formed of cattle meat. There are only two sets of grouped animal products: dairy and 'other meat'. Dairy is a significant contributor to global food supply and demand, but meat products not listed individually do not. Dairy includes milk, butter, ghee and cream. Products such as cheese and yoghurt are also included in the data for milk.

	Sub-Saharan Africa	North Africa and West Asia	Europe	Central and Southern Asia	East and South-East Asia	Oceania	North America	Latin America
Wheat	2.3	1.5	1.3	1.7	1.5	1.2	1.2	1.5
Maize	3.5	3	1.6	3.5	3	1.2	1.2	3
Rice	1.5	1.2	1.2	1.5	1	1.2	1.2	1.2
Soyabeans	1.5	1.5	1.4	1.5	1.2	1.2	1.2	1.5
Potatoes	1	1	1	1	1	1	1	1
Nuts	1.5	1.5	1.2	1.5	1.2	1.2	1.2	1.5
Cassava	0.8	0.8	0.8	0.8	0.8	0.8	0.8	0.8
Rape and mustard seed	2.3	2.3	1.9	2.3	2.3	1.9	1.9	2.3
Palm oil	1.9	1.9	1.9	1.9	1.5	1.9	1.9	1.9
Sunflower seed	2.3	2.3	1.9	2.3	2.3	1.9	1.9	2.3
Cereals	2.3	1.5	1.25	1.7	1.5	1.2	1.2	1.5
Oil crops	2.3	2.3	1.9	2.3	2.3	1.9	1.9	2.3
Pulses	0.4	0.4	1	0.4	0.4	1	1	0.4
Starchy roots	1	1	1	1	1	1	1	1
Sugar crops	0.7	0.7	0.5	0.7	0.7	0.7	0.5	0.7
Fruits	2.5	2.5	2.5	2.5	2.5	2.5	2.5	2.5
Vegetables	1.9	1.5	1.2	1.6	1.5	1.3	1.3	1.6
Spices	1.1	1.1	1.1	1.1	1.1	1.1	1.1	1.1
Luxuries	0.5	0.5	0.5	0.5	0.5	0.5	0.5	0.5
Other vegetal products	1.9	1.5	1.3	1.6	1.5	1.3	1.3	1.5

Table A.4: Vegetal product harvest factors – the ratio of the mass of useful product to above ground biomass. Values in this table are adapted from Krausmann *et al.* (2008). Where a direct mapping was impossible, the average value of other products was used (for example – vegetables). Fruits are assumed to be permanent crops.

	Sub-Saharan Africa	North Africa and West Asia	East Europe	West Europe	Central and South-East Asia	East Asia	North America and Oceania	Latin America
Cassava and products	0.8	0.8	0.3	0.0	0.8	0.8	0.0	0.8
Cereals - Excluding Beer	0.9	0.8	0.8	0.7	0.9	0.8	0.7	0.8
Fruits - Excluding Wine	0.8	0.7	0.6	0.4	0.8	0.7	0.4	0.7
Luxuries (excluding Alcohol)	0.8	0.7	0.6	0.4	0.8	0.7	0.4	0.7
Maize and products	0.9	0.8	0.8	0.7	0.9	0.8	0.7	0.8
Oilcrops	0.9	0.8	0.8	0.7	0.9	0.8	0.7	0.8
Other	0.8	0.7	0.6	0.4	0.8	0.7	0.4	0.7
Palm Oil	0.9	0.9	0.9	0.9	0.9	0.9	0.9	0.9
Potatoes and products	0.8	0.8	0.3	0.0	0.8	0.8	0.0	0.8
Nuts and products	0.9	0.8	0.8	0.7	0.9	0.8	0.7	0.8
Pulses	0.5	0.5	0.5	0.0	0.5	0.5	0.0	0.5
Rape and Mustard seed	0.7	0.7	0.7	0.7	0.7	0.7	0.7	0.7
Rice (Milled Equivalent)	0.9	0.8	0.8	0.7	0.9	0.8	0.7	0.8
Soyabeans	0.5	0.5	0.5	0.0	0.5	0.5	0.0	0.5
Spices	0.8	0.7	0.6	0.4	0.8	0.7	0.4	0.7
Starchy Roots	0.8	0.8	0.3	0.0	0.8	0.8	0.0	0.8
Sugar Crops	0.8	0.8	0.3	0.0	0.8	0.8	0.0	0.8
Sugar cane	0.9	0.9	0.9	0.9	0.9	0.9	0.9	0.9
Sunflower seed	0.5	0.5	0.5	0.5	0.5	0.5	0.5	0.5
Vegetable Oils	0.8	0.7	0.6	0.4	0.8	0.7	0.4	0.7
Vegetables	0.8	0.7	0.6	0.4	0.8	0.7	0.4	0.7
Wheat and products	0.9	0.8	0.8	0.7	0.9	0.8	0.7	0.8

Table A.5: Vegetable product residue recovery factors – the recovered proportion of potential harvest residues. As with Table A.4, this table is also adapted from Krausmann *et al.* (2008).

Livestock Product	Harvest residues	Processing waste	Post-production waste
Dairy	25%	5%	0%
Bovine Meat	25%	5%	0%
Eggs	0%	11%	0%
Poultry Meat	0%	11%	0%
Pigmeat	5%	15%	45%
Mutton & Goat Meat	20%	11%	0%
Other Meat	20%	5%	0%

Table A.6: Maximum portion (z) of livestock feed that can be derived from each residue source. These values are taken from FALAFEL (Powell & Lenton, 2012).

Input		Value or data		Source
Population		SSP2 population trajectory		Fricko et al., 2017.
Idealised food supply target calories		3200 (kcal/capita/day)		Kearney, 2010; Alexander et al., 2017; Parfitt et al., 2010
Idealised food supply target year		2100		Aligns with Paris agreement temperature goals.
Overall efficiency improvement		0.0		There is no enforced change to overall agricultural efficiency in the anchor scenario.
Change to vegetal diet		0.0		No enforced change to portion of food energy from vegetal products in the anchor scenario.
Change to dairy diet		0.0		No enforced change to portion of food energy from dairy products in the anchor scenario.
Waste factor limits		*Subsistence*	*Industrial*	Refer to section 4.2 and Table 2.
	Post production	0.07	0.3	
	Processing	0.10	0.06	
	Distribution	0.5	0.05	
Post-production waste to feed		0.40	0.05	(Powell, 2015)
Other waste to feed		0.15	0.40	

Table A.7: Inputs, values and data used to produce the anchor scenario in C-LLAMA.

Region	Item	2020	2030	2040	2050
NORTHERNAMERICA	Food Crops	1.44E+08	1.48E+08	1.52E+08	1.55E+08
	Pasture	2.78E+08	2.83E+08	2.88E+08	2.9E+08
	Fodder Crops	59102644	67120616	74375777	80618936
SOUTHAMERICA	Food Crops	92609372	93982867	95152719	96217646
	Pasture	4.53E+08	4.77E+08	4.98E+08	5.19E+08
	Fodder Crops	41950885	47980106	53268586	57606791
CENTRALAMERICA	Food Crops	24486324	24883564	25113116	25144180
	Pasture	90549873	89083781	87279927	84992096
	Fodder Crops	10298992	10854346	11290526	11608143
CARIBBEAN	Food Crops	5701552	5814101	5898041	5947747
	Pasture	4735629	4983965	5261775	5484907
	Fodder Crops	768887.3	867706.7	962794.9	1046271
EASTERNAFRICA	Food Crops	44627557	44787338	44348960	43227455
	Pasture	1.96E+08	2.12E+08	2.26E+08	2.37E+08
	Fodder Crops	27711651	30686740	33367389	35708687
WESTERNAFRICA	Food Crops	70371563	70589754	69519405	66931695
	Pasture	1.87E+08	1.95E+08	2E+08	2.01E+08
	Fodder Crops	33461679	34978667	36429016	37396721
NORTHERNAFRICA	Food Crops	33026116	33370613	33414347	33119937
	Pasture	60159833	64754843	68517651	72314640
	Fodder Crops	13791410	14023182	14217248	14445584
SOUTHERNAFRICA	Food Crops	9524790	9679176	9798009	9876671
	Pasture	1.52E+08	1.6E+08	1.66E+08	1.7E+08
	Fodder Crops	4506502	4753946	4954572	5111965
MIDDLEAFRICA	Food Crops	13486305	13360842	12961523	12276739
	Pasture	1.22E+08	1.29E+08	1.34E+08	1.37E+08
	Fodder Crops	7890880	8567387	9229300	9799051
CENTRALASIA	Food Crops	20611646	20265557	19786873	19078910
	Pasture	2.62E+08	2.91E+08	3.16E+08	3.37E+08
	Fodder Crops	18174812	20534064	22860266	25172668
EASTERNASIA	Food Crops	1.09E+08	1.1E+08	1.1E+08	1.09E+08
	Pasture	5.15E+08	5.44E+08	5.64E+08	5.98E+08
	Fodder Crops	37005906	39669148	41686753	43263691
SOUTHEASTERNASIA	Food Crops	1.09E+08	1.11E+08	1.12E+08	1.12E+08
	Pasture	17297852	18576964	19557564	20315505
	Fodder Crops	14473651	15505407	16259165	16769792

SOUTHERNASIA	Food Crops	1.97E+08	1.96E+08	1.93E+08	1.87E+08
	Pasture	79168805	84059651	88382231	91860597
	Fodder Crops	43910757	47504797	50725443	53662898
WESTERNASIA	Food Crops	27309881	27202184	26859498	26261145
	Pasture	2.2E+08	2.21E+08	2.21E+08	2.18E+08
	Fodder Crops	11275983	11807883	12254763	12668759
EASTERNEUROPE	Food Crops	1.47E+08	1.45E+08	1.43E+08	1.39E+08
	Pasture	1.22E+08	1.35E+08	1.48E+08	1.59E+08
	Fodder Crops	51319529	56769933	62024203	67294659
WESTERNEUROPE	Food Crops	26417618	26343260	26198250	25928975
	Pasture	25054210	27539612	29787514	31851160
	Fodder Crops	8910851	9151293	9307426	9462245
NORTHERNEUROPE	Food Crops	7865396	7719001	7647723	7594364
	Pasture	24317404	28344686	32765160	35600568
	Fodder Crops	10971461	11199462	11375065	11577335
SOUTHERNEUROPE	Food Crops	30710974	30774176	30477722	29798789
	Pasture	25655657	28352163	30802283	32903614
	Fodder Crops	6694103	7164839	7548375	7914750
AUSTRALIAANDNEWZEALAND	Food Crops	18777577	18029310	16918547	15466293
	Pasture	3.5E+08	3.44E+08	3.37E+08	3.27E+08
	Fodder Crops	13146533	14248087	15188036	16059053
POLYNESIA	Food Crops	22455.07	23645.13	24856.15	26018.59
	Pasture	25840.88	28426.17	30704.33	32588.92
	Fodder Crops	33490.12	34066.78	34799.68	36579.62
MELANESIA	Food Crops	538313.8	549717.5	560089.8	568835.8
	Pasture	405376.9	420432.4	431176.1	437022.8
	Fodder Crops	20676.97	21164.86	21608.33	22026.5

Table A.8: Table of aggregated land-use areas at a regional level in the C-LLAMA anchor scenario. Values are in hectares.

Bibliography

Aleksandrowicz, L. et al. 2016. The impacts of dietary change on greenhouse gas emissions, land use, water use, and health: A systematic review. *PLoS ONE*, **11**(11), 1–16.

Alexander, P. et al. 2016. Human appropriation of land for food: The role of diet. *Global Environmental Change*, **41**, 88 – 98.

Alexander, P. et al. 2017. Losses, inefficiencies and waste in the global food system. *Agricultural Systems*, **153**, 190–200.

Ali, A. et al. 2021. Analysis of determinants to mitigate food losses and waste in the developing countries: empirical evidence from Egypt. *Mitigation and Adaptation Strategies for Global Change*, **26**(6), 1–26.

Arneth, A. et al. 2019. Chapter 1: Framing and context. *Special report on land use and climate change*, 46–54.

Asseng, S. et al. 2020. Wheat yield potential in controlled-environment vertical farms. *Proceedings of the National Academy of Sciences of the United States of America*, **117**(32), 19131–19135.

Babji, A.S. and Ghassem, M. 2010. Updates in meat science technology. *Proceedings of the World Halal Research Conference, HDC, Kuala Lumpur Convention Centre, Malaysia*, 173.

Baccini, A. et al. 2012. Estimated carbon dioxide emissions from tropical deforestation improved by carbon-density maps. *Nature climate change*, **2**(3), 182.

Bahar, N.H. et al. 2020. Meeting the food security challenge for nine billion people in 2050: What impact on forests? *Global Environmental Change*, **62**(December 2019), 102056.

Bajželj, B. et al. 2014. Importance of food-demand management for climate mitigation. *Nature Climate Change*, **4**(10), 924–929.

Ball, T.S. et al. 2022. C-LLAMA 1.0: a traceable model for food, agriculture, and land use. *Geoscientific Model Development*, **15**(2), 929–949.

Battisti, R. et al. 2018. Soybean Yield Gap in the Areas of Yield Contest in Brazil. *International Journal of Plant Production*, **12**(3), 159–168.

Bazzano, L.A. et al. 2005. Dietary intake of whole and refined grain breakfast cereals and weight gain in men. *Obesity Research*, **13**(11), 1952–1960.

Beck, H.E. et al. 2018. Present and future köppen-geiger climate classification maps at 1-km resolution. *Scientific Data*, **5**, 1–12.

Beerling, D.J. et al. 2020. Potential for large-scale CO2 removal via enhanced rock weathering with croplands. *Nature*, **583**(7815), 242–248.

Bell, A.W. et al. 2011. The Australasian beef industries- Challenges and opportunities in the 21st century. *Animal Frontiers*, **1**(2), 10–19.

Belton, P.S. and Taylor, J.R. 2004. Sorghum and millets: Protein sources for Africa. *Trends in Food Science and Technology*, **15**(2), 94–98.

Benke, K. and Tomkins, B. 2017. Future food-production systems: Vertical farming and controlled-environment agriculture. *Sustainability: Science, Practice, and Policy*, **13**(1), 13–26.

Berndes, G. and Cowie, A. 2021. Land sector impacts of early climate action. *Nature Sustainability*, **4**(12), 1021–1022.

Bhattacharya, A. 2019. Global climate change and its impact on agriculture. *Changing climate and resource use efficiency in plants*, 1–50.

Bijl, D.L. et al. 2017. A physically-based model of long-term food demand. *Global Environmental Change*, **45**(September 2016), 47–62.

Bodirsky, B.L. et al. 2020. The ongoing nutrition transition thwarts long-term targets for food security, public health and environmental protection. *Scientific Reports*, **10**(1), 1–14.

Boogaard, B.K. et al. 2011. Socio-cultural sustainability of pig production: Citizen perceptions in the Netherlands and Denmark. *Livestock Science*, **140**(1-3), 189–200.

Bordonal, R.d.O. et al. 2018. Sustainability of sugarcane production in Brazil. A review. *Agronomy for Sustainable Development*, **38**(2).

Brack, D. and King, R. 2021. Managing Land-based CDR: BECCS, Forests and Carbon Sequestration. *Global Policy*, **12**(S1), 45–56.

Bradford, K.J. et al. 2018. The dry chain: Reducing postharvest losses and improving food safety in humid climates. *Trends in Food Science and Technology*, **71**(November 2017), 84–93.

Breunig, H.M. et al. 2017. Bioenergy Potential from Food Waste in California. *Environmental Science and Technology*, **51**(3), 1120–1128.

Bui, M. et al. 2018. Carbon capture and storage (CCS): The way forward. *Energy and Environmental Science*, **11**(5), 1062–1176.

Burns, W. and Nicholson, S. 2017. Bioenergy and carbon capture with storage (BECCS): the prospects and challenges of an emerging climate policy response. *Journal of Environmental Studies and Sciences*, **7**(4), 527–534.

Byerly, T. 1967. Efficiency of feed conversion. *Science*, **157**(3791), 890–895.

Calvin, K. et al. 2013. Implications of simultaneously mitigating and adapting to climate change: initial experiments using GCAM. *Climatic Change*, **117**(3), 545–560.

Cattaneo, A., Federighi, G. and Vaz, S. 2021. The environmental impact of reducing food loss and waste: A critical assessment. *Food Policy*, **98**, 101890.

Chapin, F.S. et al. 1987. Plant Responses to Multiple Environmental Factors. *BioScience*, **37**(1), 49–57.

Cicatiello, C. and Franco, S. 2018. Food waste due to over-nutrition in the Italians' dietary habits. *Rivista di Studi sulla Sostenibilita*, 159–180.

Clark, D.B. et al. 2011. The Joint UK Land Environment Simulator (JULES), model description - Part 2: Carbon fluxes and vegetation dynamics. *Geoscientific Model Development*, **4**(3), 701–722.

Clark, M. and Tilman, D. 2017. Comparative analysis of environmental impacts of agricultural production systems, agricultural input efficiency, and food choice. *Environmental Research Letters*, **12**(6).

Consoli, C.P. and Wildgust, N. 2017. Current Status of Global Storage Resources. *Energy Procedia*, **114**, 4623 – 4628. 13th International Conference on Greenhouse Gas Control Technologies, GHGT-13, 14-18 November 2016, Lausanne, Switzerland.

Cook-Patton, S.C. et al. 2020. Mapping carbon accumulation potential from global natural forest regrowth. *Nature*, **585**(7826), 545–550.

Cooper, M. et al. 2021. Monitoring and projecting global hunger: Are we on track? *Global Food Security*, **30**(March), 100568.

Creutzig, F. et al. 2019. The mutual dependence of negative emission technologies and energy systems. *Energy and Environmental Science*, **12**(6), 1805–1817.

Csillik, O. et al. 2019. Monitoring tropical forest carbon stocks and emissions using Planet satellite data. *Scientific Reports*, **9**(1), 1–12.

Culliford, A. and Bradbury, J. 2020. A cross-sectional survey of the readiness of consumers to adopt an environmentally sustainable diet. *Nutrition Journal*, **19**(1), 1–13.

Daioglou, V. et al. 2019. Integrated assessment of biomass supply and demand in climate change mitigation scenarios. *Global Environmental Change*, **54**(December 2018), 88–101.

Dasgupta, S. et al. 2006. Environment During growth: Accounting for governance and vulnerability. *World Development*, **34**(9), 1597–1611.

Davis, K.F. and D'Odorico, P. 2015. Livestock intensification and the influence of dietary change: A calorie-based assessment of competition for crop production. *Science of the Total Environment*, **538**, 817–823.

De Miranda, E.E. and Fonseca, M.F. 2019. *Sugarcane: Food production, energy, and environment*. Elsevier Inc.

de Moraes, C.C. et al. 2020. Retail food waste: mapping causes and reduction practices. *Journal of Cleaner Production*, **256**, 1–16.

De Oliveira Silva, R., Barioni, L.G. and Moran, D. 2021. Fire, deforestation, and livestock: When the smoke clears. *Land Use Policy*, **100**(July 2020), 104949.

Dhir, A. et al. 2020. Food waste in hospitality and food services: A systematic literature review and framework development approach. *Journal of Cleaner Production*, **270**, 122861.

Dias, T.A.d.C. et al. 2021. Global potential assessment of available land for bioenergy projects in 2050 within food security limits. *Land Use Policy*, **105**(April 2020).

Dobon, A. et al. 2011. The sustainability of communicative packaging concepts in the food supply chain. A case study: Part 2. Life cycle costing and sustainability assessment. *International Journal of Life Cycle Assessment*, **16**(6), 537–547.

Dodson, J.C. et al. 2020. Population growth and climate change: Addressing the overlooked threat multiplier. *Science of the Total Environment*, **748**, 141346.

Doelman, J.C. et al. 2018. Exploring SSP land-use dynamics using the IMAGE model: Regional and gridded scenarios of land-use change and land-based climate change mitigation. *Global Environmental Change*, **48**, 119–135.

Dooley, K. and Kartha, S. 2018. Land-based negative emissions: Risks for climate mitigation and impacts on sustainable development. *International Environmental Agreements: Politics, Law and Economics*, **18**(1), 79–98.

Dora, M. et al. 2020. Importance of sustainable operations in food loss: evidence from the Belgian food processing industry. *Annals of Operations Research*, **290**(1-2), 47–72.

Duchelle, A.E. et al. 2018. What is REDD+ achieving on the ground? *Current Opinion in Environmental Sustainability*, **32**, 134–140.

Durán, A.P. et al. 2020. A practical approach to measuring the biodiversity impacts of land conversion. *Methods in Ecology and Evolution*, **11**(8), 910–921.

Duro, J.A. et al. 2020. Global inequalities in food consumption, cropland demand and land-use efficiency: A decomposition analysis. *Global Environmental Change*, **64**(February), 102124.

Eitelberg, D.A., van Vliet, J. and Verburg, P.H. 2015. A review of global potentially available cropland estimates and their consequences for model-based assessments. *Global Change Biology*, **21**(3), 1236–1248.

Elliott, J. et al. 2014. Constraints and potentials of future irrigation water availability on agricultural production under climate change. *Proceedings of the National Academy of Sciences*, **111**(9), 3239–3244.

Elsen, P.R. et al. 2020. Keeping pace with climate change in global terrestrial protected areas. *Science Advances*, **6**(25).

Erb, K.H. et al. 2017. Land management: data availability and process understanding for global change studies. *Global Change Biology*, **23**(2).

Eshel, G. et al. 2016. Environmentally Optimal, Nutritionally Aware Beef Replacement Plant-Based Diets. *Environmental Science and Technology*, **50**(15), 8164–8168.

FAO. 2011. Energy-smart food for people and climate. Issue Paper. *Food and Agriculture Organization of the United Nations.*, 66.

FAO. 2021a. *FAOSTAT - Data.* https://www.fao.org/faostat/en/#data[Accessed: 2021-11-11].

FAO. 2021b. *Production notes.* www.fao.org/waicent/faostat/agricult/prod-e.htm[Accessed: 2021-12-07].

FAO. 2022. *FAOSTAT - Crops and livestock products.* www.fao.org/faostat/en/#data/QCL[Accessed: 2022-03-18].

Forster, J. et al. 2020. Mapping feasibilities of greenhouse gas removal: Key issues, gaps and opening up assessments. *Global Environmental Change*, **63**(November 2019), 102073.

Fricko, O. et al. 2017. The marker quantification of the Shared Socioeconomic Pathway 2: A middle-of-the-road scenario for the 21st century. *Global Environmental Change*, **42**, 251–267.

Friedlingstein, P. et al. 2020. Global Carbon Budget 2020. *Earth System Science Data*, **12**(4), 3269–3340.

Frieler, K. et al. 2017. Understanding the weather signal in national crop-yield variability. *Earth's Future*, **5**(6), 605–616.

Fritz, S. et al. 2015. Mapping global cropland and field size. *Global Change Biology*, **21**(5), 1980–1992.

Fujimori, S., Masui, T. and Yuzuru, M. 2012. AIM/CGE [basic] manual. *Center for Social and Environmental Systems Research, NIES - Discussion Paper Series*, 02.

Fuss, S. et al. 2018. Negative emissions - Part 2: Costs, potentials and side effects. *Environmental Research Letters*, **13**(6).

Garg, A. 2014. Recent Trends in Agriculture: Vertical Farming and Organic Farming. *Advances in Plants & Agriculture Research*, **1**(4).

Gidden, M.J. et al. 2019. Global emissions pathways under different socioeconomic scenarios for use in CMIP6: A dataset of harmonized emissions trajectories through the end of the century. *Geoscientific Model Development*, **12**(4), 1443–1475.

Godfray, H.C.J. et al. 2010. Food Security: The Challenge of Feeding 9 Billion People. *Science*, **327**(5967), 812–818.

Godfray, H.C.J. et al. 2018. Meat consumption, health, and the environment. *Science (New York, N.Y.)*, **361**(6399).

Gough, C. et al. 2018. Challenges to the use of BECCS as a keystone technology in pursuit of 1 . 5 o C. *Global Sustainability*, 1–9.

Grassini, P. et al. 2015. How good is good enough? Data requirements for reliable crop yield simulations and yield-gap analysis. *Field Crops Research*, **177**, 49–63.

Grumezescu, A.M. and Holban, A.M. 2018. *Food processing for increased quality and consumption*. Vol. 18. Academic Press.

Gustavsson, J., Cederberg, C. and Sonesson, U. 2011. Global Food Losses and Food Waste. *Save Food at Interpack Düsseldorf, Germany*, 01.

Haberzettl, J., Hilgert, P. and von Cossel, M. 2021. A critical review on lignocellulosic biomass yield modeling and the bioenergy potential from marginal land. *Agronomy*, **11**(12).

Hansson, A. et al. 2021. Boundary Work and Interpretations in the IPCC Review Process of the Role of Bioenergy With Carbon Capture and Storage (BECCS) in Limiting Global Warming to 1.5°C. *Frontiers in Climate*, **3**(April), 1–14.

Harper, A.B. et al. 2018. Land-use emissions play a critical role in land-based mitigation for Paris climate targets. *Nature communications*, **9**(1), 1–13.

Haszeldine, R.S. 2009. Carbon Capture and Storage: How Green Can Black Be? *Science*, **325**(5948), 1647–1652.

Hatfield, J.L. and Prueger, J.H. 2015. Temperature extremes: Effect on plant growth and development. *Weather and Climate Extremes*, **10**, 4–10.

Havlık, P. et al. 2014. Climate change mitigation through livestock system transitions. *Proceedings of the National Academy of Sciences*, **111**(10), 3709–3714.

Hayek, M.N. et al. 2021. The carbon opportunity cost of animal-sourced food production on land. *Nature Sustainability*, **4**(1), 21–24.

He, P. et al. 2018. The environmental impacts of rapidly changing diets and their nutritional quality in China. *Nature Sustainability*, **1**(3), 122–127.

Hemler, E.C. and Hu, F.B. 2019. Plant-Based Diets for Personal, Population, and Planetary Health. *Advances in Nutrition*, **10**(6), S275–S283.

Henderson, B. et al. 2021. Policy strategies and challenges for climate change mitigation in the Agriculture, Forestry and Other Land Use (AFOLU) sector. *OECD Publishing, OECD Food, Agriculture and Fisheries Papers*, **149**(149).

Herrero, M. et al. 2016. Greenhouse gas mitigation potentials in the livestock sector. *Nature Climate Change*, **6**(5), 452–461.

Hirvonen, K. et al. 2020. Affordability of the EAT–Lancet reference diet: a global analysis. *The Lancet Global Health*, **8**(1), e59–e66.

Hitzmann, B. and Ahmad, M.H. 2017. *Measurement, modeling and automation in advanced food processing*. Vol. 161. Springer.

Holman, B.W. and Malau-Aduli, A.E. 2013. Spirulina as a livestock supplement and animal feed. *Journal of Animal Physiology and Animal Nutrition*, **97**(4), 615–623.

Hong, C. et al. 2021. Global and regional drivers of land-use emissions in 1961–2017. *Nature*, **589**(7843), 554–561.

Humpenöder, F. et al. 2018. Large-scale bioenergy production: How to resolve sustainability trade-offs? *Environmental Research Letters*, **13**(2).

Hurlbert, M. et al. 2019. Chapter 7: Risk Management and Decision making in Relation to Sustainable Development. *Special report on land use and climate change*, 673–800.

Hurtt, G.C. et al. 2011. Harmonization of land-use scenarios for the period 1500 – 2100: 600 years of global gridded annual land-use transitions, wood harvest, and resulting secondary lands. *Climatic Change*, **109**, 117–161.

Huynh, T.T.T. et al. 2007. Pig Production in Cambodia, Laos, Philippines, and Vietnam: A Review. *Asian Journal of Agriculture and Development*, **4**(1), 70–90.

Iizumi, T. et al. 2017. Responses of crop yield growth to global temperature and socioeconomic changes. *Scientific Reports*, **7**(1), 1–10.

IPCC. 2022. Summary for Policymakers. *Climate Change 2022: Mitigation of Climate Change. Contribution of Working Group III to the Sixth Assessment Report of the Intergovernmental Panel on Climate Change.*

Jeswani, H.K., Figueroa-Torres, G. and Azapagic, A. 2021. The extent of food waste generation in the UK and its environmental impacts. *Sustainable Production and Consumption*, **26**, 532–547.

Jia, G. et al. 2019. Chapter 2: Land–climate interaction. *Special report on land use and climate change*, 131–149.

Jose, S. and Dollinger, J. 2019. Silvopasture: a sustainable livestock production system. *Agroforestry Systems*, **93**(1), 1–9.

Joseph, S. et al. 2021. How biochar works, and when it doesn't: A review of mechanisms controlling soil and plant responses to biochar. *GCB Bioenergy*, **13**(11), 1731–1764.

Kahn, L. and Cottle, D. 2014. *Beef cattle production and trade*. Csiro Publishing.

Kalt, G. et al. 2020. Greenhouse gas implications of mobilizing agricultural biomass for energy: a reassessment of global potentials in 2050 under different food-system pathways. *Environmental Research Letters*, **15**(3).

Kalt, G. et al. 2021. Exploring the option space for land system futures at regional to global scales: The diagnostic agro-food, land use and greenhouse gas emission model BioBaM-GHG 2.0. *Ecological Modelling*, **459**.

Katt, F. and Meixner, O. 2020. Food waste prevention behavior in the context of hedonic and utilitarian shopping value. *Journal of Cleaner Production*, **273**, 122878.

Kavanaugh, M. and Quinlan, J.J. 2020. Consumer knowledge and behaviors regarding food date labels and food waste. *Food Control*, **115**(January), 107285.

KC, S. and Lutz, W. 2017. The human core of the shared socioeconomic pathways: Population scenarios by age, sex and level of education for all countries to 2100. *Global Environmental Change*, **42**(jan), 181–192.

Keller, D.P. et al. 2018. The Carbon Dioxide Removal Model Intercomparison Project (CDRMIP): rationale and experimental protocol for CMIP6. *Geoscientific Model Development*, **11**, 1133–1160.

Khobragade, A. et al. 2021. Indoor Farming Hydroponic Plant Grow Chamber. *International Journal of Scientific Research & Engineering Trends*, **7**(3), 2050–2052.

Kindermann, G. et al. 2008. Global cost estimates of reducing carbon emissions through avoided deforestation. *Proceedings of the National Academy of Sciences*, **105**(30), 10302–10307.

Kitinoja, L. 2013. Use of cold chains for reducing food losses in developing countries. *PEF White Paper*, **6**(13), 1–16.

Koester, U. and Galaktionova, E. 2021. FAO food loss index methodology and policy implications. *Studies in Agricultural Economics*, **123**(1), 1–7.

Konar, M. et al. 2018. Scaling properties of food flow networks. *PLOS ONE*, **13**(07), e0199498.

Kottek, M. et al. 2006. World map of the Köppen-Geiger climate classification updated. *Meteorologische Zeitschrift*, **15**(3), 259–263.

Krausmann, F. et al. 2008. Global patterns of socioeconomic biomass flows in the year 2000: A comprehensive assessment of supply, consumption and constraints. *Ecological Economics*, **65**(3), 471–487.

Kreidenweis, U. et al. 2018. Pasture intensification is insufficient to relieve pressure on conservation priority areas in open agricultural markets. *Global Change Biology*, **24**(7), 3199–3213.

Kreuter, J. and Lederer, M. 2021. The geopolitics of negative emissions technologies: Learning lessons from REDD+ and renewable energy for afforestation, BECCS, and direct air capture. *Global Sustainability*, **4**.

Kukal, M.S. and Irmak, S. 2018. Climate-Driven Crop Yield and Yield Variability and Climate Change Impacts on the U.S. Great Plains Agricultural Production. *Scientific Reports*, **8**(1), 1–18.

Kumar, D. and Kalita, P. 2017. Reducing postharvest losses during storage of grain crops to strengthen food security in developing countries. *Foods*, **6**(1), 1–22.

Kumari, R. et al. 2019. Deforestation in India: consequences and sustainable solutions. *Forest degradation around the world*, 1–18.

Kummu, M. et al. 2012. Lost food, wasted resources: Global food supply chain losses and their impacts on freshwater, cropland, and fertiliser use. *Science of the Total Environment*, **438**, 477–489.

Lakhiar, I.A. et al. 2018. Modern plant cultivation technologies in agriculture under controlled environment: A review on aeroponics. *Journal of Plant Interactions*, **13**(1), 338–352.

Lambin, E.F. and Meyfroidt, P. 2011. Global land use change, economic globalization, and the looming land scarcity. *Proceedings of the National Academy of Sciences*, **108**(9), 3465–3472.

Lambin, E.F., Geist, H.J. and Lepers, E. 2003. Dynamics of land-use and land-cover change in tropical regions. *Annual Review of Environment and Resources*, **28**, 205–241.

Langbein, L. and Knack, S. 2010. The worldwide governance indicators: Six, one, or none? *Journal of Development Studies*, **46**(2), 350–370.

Laquale, K.M. 2009. Nutritional needs of the recreational athlete. *Athletic Therapy Today*, **14**(1), 12–15.

Lenton, T.M. et al. 2019. Climate tipping points — too risky to bet against. *Nature*, **575**, 592–595.

Li, X., Yan, C. and Zan, L. 2018. Current situation and future prospects for beef production in China — A review. *Asian-Australas J Anim Sci*, **31**(7), 984–991.

Licker, R. et al. 2010. Mind the gap: How do climate and agricultural management explain the 'yield gap' of croplands around the world? *Global Ecology and Biogeography*, **19**(6), 769–782.

Liew, N.M. 2020. *Nutrient Composition of Cereal, Pseudo-Cereals and Legumes Flours: an Overview of Literature Data*. Ph.D. thesis, Tunku Abdul Rahman University College.

Lipinski, B. et al. 2013. Reducing food loss and waste. *World Resource Institute - Creating a Sustainable Food Future*, **2**, 1–40.

Liu, C. et al. 2016. Food waste in Japan: Trends, current practices and key challenges. *Journal of Cleaner Production*, **133**(2016), 557–564.

Liu, X., Cai, Z. and Yuan, Z. 2021. Environmental burdens of small-scale intensive pig production in China. *Science of the Total Environment*, **770**, 144720.

Lobell, D.B. and Field, C.B. 2007. Global scale climate-crop yield relationships and the impacts of recent warming. *Environmental Research Letters*, **2**(1).

Low, S. and Schäfer, S. 2020. Is bio-energy carbon capture and storage (BECCS) feasible? The contested authority of integrated assessment modeling. *Energy Research and Social Science*, **60**(May 2019), 101326.

Lyngfelt, A., Johansson, D.J. and Lindeberg, E. 2019. Negative CO2 emissions - An analysis of the retention times required with respect to possible carbon leakage. *International Journal of Greenhouse Gas Control*, **87**(May), 27–33.

Mace, M.J. et al. 2021. Large-Scale Carbon Dioxide Removal to Meet the 1.5°C Limit: Key Governance Gaps, Challenges and Priority Responses. *Global Policy*, **12**(S1), 67–81.

Mackey, B. et al. 2015. Policy Options for the World's Primary Forests in Multilateral Environmental Agreements. *Conservation Letters*, **8**(2), 139–147.

Mackey, B. et al. 2020. Understanding the importance of primary tropical forest protection as a mitigation strategy. *Mitigation and Adaptation Strategies for Global Change*, **25**(5), 763–787.

Madhukar, A., Kumar, V. and Dashora, K. 2020. Spatial and Temporal Trends in the Yields of Three Major Crops: Wheat, Rice and Maize in India. *International Journal of Plant Production*, **14**(2), 187–207.

Malhi, Y. et al. 2020. *Climate change and ecosystems: Threats, opportunities and solutions.*

Mankin, J.S. et al. 2019. Mid-latitude freshwater availability reduced by projected vegetation responses to climate change. *Nature Geoscience*, **12**(12), 983–988.

Martin, A. et al. 2020. Environmental Justice and Transformations to Sustainability. *Environment*, **62**(6), 19–30.

Mengis, N. and Matthews, H.D. 2020. Non-CO2 forcing changes will likely decrease the remaining carbon budget for 1.5 °C. *npj Climate and Atmospheric Science*, **3**(1), 1–7.

Milford, A.B. et al. 2019. Drivers of meat consumption. *Appetite*, **141**(June), 104313.

Millar, R.J. et al. 2017. Emission budgets and pathways consistent with limiting warming to 1.5 ^{o}c. *Nature Geoscience*, **10**(10), 741–747.

Mohanty, S.K. and Swain, M.R. 2019. *Bioethanol Production From Corn and Wheat: Food, Fuel, and Future.* Elsevier Inc.

Mueller, N.D. et al. 2012. Closing yield gaps through nutrient and water management. *Nature*, **490**(7419), 254.

Munroe, D.K. et al. 2013. Alternative trajectories of land abandonment: causes, consequences and research challenges. *Current Opinion in Environmental Sustainability*, **5**(5), 471 – 476. Human settlements and industrial systems.

Næss, J.S., Cavalett, O. and Cherubini, F. 2021. The land–energy–water nexus of global bioenergy potentials from abandoned cropland. *Nature Sustainability*, **4**(6), 525–536.

Nicholson, S., Jinnah, S. and Gillespie, A. 2018. Solar radiation management: a proposal for immediate polycentric governance. *Climate Policy*, **18**(3), 322–334.

Nweke, F.I., Spencer, D.S.C. and Lynam, J.K. 2002. *The cassava transformation: Africa's best kept secret*. Michigan State University Press.

Oerke, E.C. and Dehne, H.W. 2004. Safeguarding production - Losses in major crops and the role of crop protection. *Crop Protection*, **23**(4), 275–285.

Oliveira Vieira, E. et al. 2015. Production, Conservation and Health Assessment of Acid Silage Vicera of Freshwater Fish as a Component of Animal Feed. *International Journal of Agriculture and Forestry*, **5**(3), 177–181.

O'Neill, B.C. et al. 2014. A new scenario framework for climate change research: the concept of shared socioeconomic pathways. *Climatic change*, **122**(3), 387–400.

Palm, H.W. et al. 2018. Towards commercial aquaponics: a review of systems, designs, scales and nomenclature. *Aquaculture International*, **26**(3), 813–842.

Pan, Y. et al. 2011. A Large and Persistent Carbon Sink in the World's Forests. *Science*, **333**(6045), 988–993.

Parfitt, J., Barthel, M. and Macnaughton, S. 2010. Food waste within food supply chains: quantification and potential for change to 2050. *Philosophical transactions of the royal society B: biological sciences*, **365**(1554), 3065–3081.

PBL Netherlands Environmental Assessment Agency. 2018. *IMAGE Region classification map*. models.pbl.nl/image/index.php/Region_classification_map[Accessed: 2022-02-25].

Pendrill, F. et al. 2019. Agricultural and forestry trade drives large share of tropical deforestation emissions. *Global Environmental Change*, **56**(March), 1–10.

Pexas, G. et al. 2020. Environmental impacts of housing conditions and manure management in European pig production systems through a life cycle perspective: A case study in Denmark. *Journal of Cleaner Production*, **253**, 120005.

Pietrosemoli, S. and Tang, C. 2020. Animal welfare and production challenges associated with pasture pig systems: A review. *Agriculture (Switzerland)*, **10**(6), 1–34.

Pikaar, I. et al. 2018. Decoupling Livestock from Land Use through Industrial Feed Production Pathways. *Environmental Science & Technology*, **52**(13), 7351–7359.

Poore, J. and Nemecek, T. 2018. Reducing food's environmental impacts through producers and consumers. *Science*, **360**(6392), 987–992.

Popp, A. et al. 2014. Land-use transition for bioenergy and climate stabilization: model comparison of drivers, impacts and interactions with other land use based mitigation options. *Climatic Change*, **123**(3), 495–509.

Popp, A. et al. 2017. Land-use futures in the shared socio-economic pathways. *Global Environmental Change*, **42**, 331–345.

Porat, R. et al. 2018. Postharvest losses of fruit and vegetables during retail and in consumers' homes: Quantifications, causes, and means of prevention. *Postharvest Biology and Technology*, **139**(November 2017), 135–149.

Porter, S.D. et al. 2018. Avoidable food losses and associated production-phase greenhouse gas emissions arising from application of cosmetic standards to fresh fruit and vegetables in Europe and the UK. *Journal of Cleaner Production*, **201**, 869–878.

Powell, T.W. 2015. *Closing loops to rebalance the global carbon cycle: Biomass flows modelling of global agricultural carbon fluxes.* PhD Thesis, University of Exeter, Exeter.

Powell, T.W.R. and Lenton, T.M. 2012. Future carbon dioxide removal via biomass energy constrained by agricultural efficiency and dietary trends. *Energy & Environmental Science*, **5**, 8116.

Pradhan, B.B., Chaichaloempreecha, A. and Limmeechokchai, B. 2019. GHG mitigation in Agriculture, Forestry and Other Land Use (AFOLU) sector in Thailand. *Carbon Balance and Management*, **14**(1), 1–17.

R. J. Nicholls, Z. et al. 2020. Reduced Complexity Model Intercomparison Project Phase 1: Introduction and evaluation of global-mean temperature response. *Geoscientific Model Development*, **13**(11), 5175–5190.

Radunsky, K. 2018. *The Politics and Governance of Negative Emissions Technologies.* Cham: Springer International Publishing. Pages 87–104.

Ramankutty, N. et al. 2018. Trends in global agricultural land use: implications for environmental health and food security. *Annual review of plant biology*, **69**, 789–815.

Ray, D.K. et al. 2012. Recent patterns of crop yield growth and stagnation. *Nature communications*, **3**, 1293.

Ray, D.K. et al. 2015. Climate variation explains a third of global crop yield variability. *Nature Communications*, **6**, 1–9.

Ray, D.K. et al. 2019. Climate change has likely already affected global food production. *PLoS ONE*, **14**(5), 1–18.

Riahi, K. et al. 2017. The Shared Socioeconomic Pathways and their energy, land use, and greenhouse gas emissions implications: An overview. *Global Environmental Change*, **42**, 153–162.

Roe, S. et al. 2019. Contribution of the land sector to a 1 . 5 ° C world. *Nature Climate Change*, **9**(November).

Rogelj, J. et al. 2018a. Chapter 2 - Mitigation Pathways Compatible with 1.5°C in the Context of Sustainable Development. *Global Warming of 1.5°C. An IPCC Special Report on the impacts of global warming of 1.5°C above pre-industrial levels and related global greenhouse gas emission pathways, in the context of strengthening the global response to the threat of climate change, sustainable development, and efforts to eradicate poverty.*

Rogelj, J. et al. 2018b. Scenarios towards limiting global mean temperature increase below 1.5 °c. *Nature Climate Change*, **8**(4), 325–332.

Ro'I, Y. and Wainer, A. 2009. Muslim identity and Islamic practice in post-Soviet Central Asia. *Central Asian Survey*, **28**(3), 303–322.

Roodhuyzen, D.M. et al. 2017. Putting together the puzzle of consumer food waste: Towards an integral perspective. *Trends in Food Science and Technology*, **68**, 37–50.

Röös, E. et al. 2017. Greedy or needy? Land use and climate impacts of food in 2050 under different livestock futures. *Global Environmental Change*, **47**(September), 1–12.

Sarofim, M.C. et al. 2021. Improving reduced complexity model assessment and usability. *Nature Climate Change*, **11**(1), 9–11.

Savary, S. et al. 2012. Crop losses due to diseases and their implications for global food production losses and food security. *Food Security*, **4**(4), 519–537.

Savary, S. et al. 2019. The global burden of pathogens and pests on major food crops. *Nature Ecology and Evolution*, **3**(3), 430–439.

Schanes, K., Dobernig, K. and Gözet, B. 2018. Food waste matters - A systematic review of household food waste practices and their policy implications. *Journal of Cleaner Production*, **182**, 978–991.

Schlenker, W., Hanemann, W.M. and Fisher, A.C. 2006. The impact of global warming on U.S. agriculture: An econometric analysis of optimal growing conditions. *Review of Economics and Statistics*, **88**(1), 113–125.

Schmidt, K. and Matthies, E. 2018. Where to start fighting the food waste problem? Identifying most promising entry points for intervention programs to reduce household food waste and overconsumption of food. *Resources, Conservation and Recycling*, **139**(July), 1–14.

Searchinger, T.D. et al. 2018. Assessing the efficiency of changes in land use for mitigating climate change. *Nature*, **564**(7735), 249.

Sesana, E. et al. 2021. Climate change impacts on cultural heritage: A literature review. *WIREs Climate Change*, **12**(4), e710.

Sha, L. and Xiong, Y.L. 2020. Plant protein-based alternatives of reconstructed meat: Science, technology, and challenges. *Trends in Food Science and Technology*, **102**(February), 51–61.

Sharma, M. et al. 2020. A comparison of the Indian diet with the EAT-Lancet reference diet. *BMC Public Health*, **20**(1), 1–13.

Sharma, N. et al. 2018. Hydroponics as an advanced technique for vegetable production: An overview. *Journal of Soil and Water Conservation*, **17**(4), 364.

Shepon, A. et al. 2016. Energy and protein feed-to-food conversion efficiencies in the US and potential food security gains from dietary changes. *Environmental Research Letters*, **11**(105002).

Singh, I.D. and Stoskopf, N.C. 1971. Harvest Index in Cereals1. *Agronomy Journal*, **63**(2), 224–226.

Sitch, S. et al. 2003. Evaluation of ecosystem dynamics, plant geography and terrestrial carbon cycling in the LPJ dynamic global vegetation model. *Global Change Biology*, **9**(2), 161–185.

Specht, K. et al. 2019. How will we eat and produce in the cities of the future? From edible insects to vertical farming-A study on the perception and acceptability of new approaches. *Sustainability (Switzerland)*, **11**(16), 1–22.

Spigarelli, C. et al. 2020. Welfare assessment on pasture: A review on animal-based measures for ruminants. *Animals*, **10**(4), 1–20.

Springmann, M. et al. 2018. Options for keeping the food system within environmental limits. *Nature*, **562**(7728), 519.

Stancu, V., Haugaard, P. and Lähteenmäki, L. 2016. Determinants of consumer food waste behaviour: Two routes to food waste. *Appetite*, **96**, 7–17.

Steenson, S. and Buttriss, J.L. 2020. The challenges of defining a healthy and 'sustainable' diet. *Nutrition Bulletin*, **45**(2), 206–222.

Strefler, J. et al. 2018. Potential and costs of carbon dioxide removal by enhanced weathering of rocks. *Environmental Research Letters*, **13**(3).

Subedi, Y.R., Kristiansen, P. and Cacho, O. 2021. Drivers and consequences of agricultural land abandonment and its reutilisation pathways: A systematic review. *Environmental Development*, **42**(December 2020), 100681.

Swain, M. et al. 2018. Reducing the environmental impact of global diets. *Science of the Total Environment*, **610-611**, 1207–1209.

Tacconi, L., Rodrigues, R.J. and Maryudi, A. 2019. Law enforcement and deforestation: Lessons for Indonesia from Brazil. *Forest Policy and Economics*, **108**(May), 101943.

Tang, A. and Kemp, L. 2021. A Fate Worse Than Warming? Stratospheric Aerosol Injection and Global Catastrophic Risk. *Frontiers in Climate*, **3**(November), 1–17.

Temme, E.H. et al. 2020. Demand-Side Food Policies for Public and Planetary Health. *Sustainability (Switzerland)*, **12**(15).

Teufel, N. et al. 2010. Livestock Production Systems in South Asia and the Greater Mekong Sub-Region. A Quantitative Description of Livestock Production in Bangladesh, Cambodia, India, Lao PDR, Nepal, Pakistan, Sri Lanka, Thailand, and Viet Nam. *PPLPI Working Paper*, **48**(48), 105.

The Eat-Lancet Commission. 2019. Healthy Diets From Planet; Food Planet Health. *The Lancet*, 32.

The Economist Intelligence Unit. 2021. *Food Sustainability Index 2021 (G20 Phase 1)*. foodsustainability.eiu.com[Accessed: 2021-12-13].

The World Bank. 2020. *Worldwide Governance Indicators*. info.worldbank.org/governance/wgi/[Accessed 2020-07-01].

The World Bank. 2021. *DataBank - Population estimates and projections*.

Thornton, P.K. 2010. Livestock production: Recent trends, future prospects. *Philosophical Transactions of the Royal Society B: Biological Sciences*, **365**(1554), 2853–2867.

Tian, X. and Yu, X. 2019. Crop yield gap and yield convergence in African countries. *Food Security*, **11**(6), 1305–1319.

Tilman, D. and Clark, M. 2014. Global diets link environmental sustainability and human health. *Nature*, **515**(7528), 518.

Tilman, D. et al. 2011. Global food demand and the sustainable intensification of agriculture. *Proceedings of the National Academy of Sciences*, **108**(50), 20260–20264.

Toma, L., Costa Font, M. and Thompson, B. 2020. Impact of consumers' understanding of date labelling on food waste behaviour. *Operational Research*, **20**(2), 543–560.

Torvanger, A. 2019. Governance of bioenergy with carbon capture and storage (BECCS): accounting , rewarding , and the Paris agreement. *Climate Policy*, **3062**.

Tsugane, S. and Sawada, N. 2014. The JPHC study: Design and some findings on the typical Japanese diet. *Japanese Journal of Clinical Oncology*, **44**(9), 777–782.

Tufarelli, V., Ragni, M. and Laudadio, V. 2018. Feeding forage in poultry: A promising alternative for the future of production systems. *Agriculture (Switzerland)*, **8**(6), 1–10.

Turner, M.G. et al. 2020. Climate change, ecosystems and abrupt change: science priorities. *Philosophical Transactions of the Royal Society B*, **375**(1794), 20190105.

UN Department of Economic and Social Affairs. 2021. *Zero Hunger - End hunger, achieve food security and improved nutrition and promote sustainable agriculture.* unstats.un.org/sdgs/report/2021/goal-02/[Accessed: 2022-02-03].

UN Environment World Conservation Monitoring Centre. 2018. 2018 United Nations List of Protected Areas. *UNEP-WCMC: Cambridge, UK*, 11.

UNFCCC. 2022. *What is REDD+?* unfccc.int/topics/land-use/workstreams/redd/what-is-redd[Accessed: 2022-03-08].

United Nations. 2019a. The sustainable development goals report 2019. *United Nations publication issued by the Department of Economic and Social Affairs*, 64.

United Nations. 2019b. World Population Prospects 2019. *Department of Economic and Social Affairs - Population Dynamics.* population.un.org/wpp[Accessed: 2021-06-07].

United Nations. 2021a. *Food Waste Index Report 2021.* United Nations Environment Programme.

United Nations. 2021b. *Goal 12: Ensure sustainable consumption and production patterns.* www.un.org/sustainabledevelopment/sustainable-consumption-production/[Accessed: 2021-12-11].

United Nations. 2021c. *Tier Classification for Global SDG Indicators*. unstats.un.org/sdgs/iaeg-sdgs/tier-classification[Accessed: 2021-01-10].

United Nations Treaty Series. 2015. *United Nations Framework Convention on Climate Change Paris Agreement*. XXVII, no. 54113.

van Diemen, R. et al. 2019. Annex 1: Glossary. *Special report on land use and climate change*, 803–830.

Van Dyk, J.S. et al. 2013. Food processing waste: Problems, current management and prospects for utilisation of the lignocellulose component through enzyme synergistic degradation. *Renewable and Sustainable Energy Reviews*, **26**, 521–531.

Van Rossum, G. and Drake Jr, F.L. 1995. *Python reference manual*. Centrum voor Wiskunde en Informatica Amsterdam.

van Sluisveld, M.A. et al. 2021. A race to zero - Assessing the position of heavy industry in a global net-zero CO2 emissions context. *Energy and Climate Change*, **2**(December 2020), 100051.

van Vuuren, D.P. et al. 2011. RCP2.6: exploring the possibility to keep global mean temperature increase below 2^o C. *Climatic Change*, **109**(95), 95–116.

van Vuuren, D.P. et al. 2011. The representative concentration pathways: an overview. *Climatic Change*, **109**(1), 5.

Van Zanten, H.H. et al. 2018. Defining a land boundary for sustainable livestock consumption. *Global Change Biology*, **24**(9), 4185–4194.

van Zeist, W.J. et al. 2020. Are scenario projections overly optimistic about future yield progress? *Global Environmental Change*, **64**(July 2019), 102120.

Vaughan, N.E. et al. 2018. Evaluating the use of biomass energy with carbon capture and storage in low emission scenarios. *Environmental Research Letters*, **13**(4).

Waller, L., Rayner, T. and Chilvers, J. 2021. Searching for a Public in Controversies over Carbon Dioxide Removal: An Issue Mapping Study on BECCS and Afforestation. *Science Technology and Human Values*, 1–34.

Wang, C. et al. 2021. Miscanthus: A fast-growing crop for environmental remediation and biofuel production. *GCB Bioenergy*, **13**(1), 58–69.

Weindl, I. et al. 2017. Livestock and human use of land : Productivity trends and dietary choices as drivers of future land and carbon dynamics. *Global and Planetary Change*, **159**(August), 1–10.

Wendling, Z.A. et al. 2020. *2020 Environmental Performance Index*. New Haven, CT: Yale Center for Environmental Law & Policy. epi.yale.edu[Accessed: 2020-06-09].

Wennersten, R., Sun, Q. and Li, H. 2015. The future potential for Carbon Capture and Storage in climate change mitigation - An overview from perspectives of technology, economy and risk. *Journal of Cleaner Production*, **103**, 724–736.

Willett, W. et al. 2019. Food in the Anthropocene: the EAT–Lancet Commission on healthy diets from sustainable food systems. *The Lancet*, **393**(10170), 447–492.

Winkler, K. et al. 2021. Global land use changes are four times greater than previously estimated. *Nature Communications*, **12**(1), 1–10.

Wirsenius, S., Azar, C. and Berndes, G. 2010. How much land is needed for global food production under scenarios of dietary changes and livestock productivity increases in 2030 ? *Agricultural Systems*, **103**(9), 621–638.

World Health Organization. 2019. *Healthy diet*. Tech. rept. World Health Organization. Regional Office for the Eastern Mediterranean. apps.who.int/iris/handle/10665/325828[Accessed: 2021-05-08].

yieldgap.org. 2021. *The Global Yield Gap and Water Productivity Atlas*. yieldgap.org[Accessed: 2021-01-10].

Zia, M. et al. 2019. Brazil Once Again Becomes the World's Largest Beef Exporter. *Amber Waves:The Economics of Food, Farming, Natural Resources, and Rural America*, **2019**(6), 2019–2021.